SSSU 86
ISSN 0140 3818

RESISTANCE EXPERIMENTS ON A SERIES OF HIGH SPEED DISPLACEMENT CATAMARAN FORMS: VARIATION OF PRISMATIC COEFFICIENT

A.F. Molland and A.R. Lee

Ship Science Report 86

February 1995

RESISTANCE EXPERIMENTS ON A SERIES OF HIGH SPEED DISPLACEMENT CATAMARAN FORMS: VARIATION OF PRISMATIC COEFFICIENT

A.F. Molland and Adrian R. Lee

Ship Science Report No.86

University of Southampton

February 1995

CONTENTS

NOMENCLATURE

The nomenclature follows the terms given by the 'ITTC Dictionary of Ship Hydrodynamics' [1], except for some additional terms which are as follows;

"CATAMARAN" refers to any ship with two hulls, side by side and joined to each other by means of a bridge structure above the free surface.

A "DEMIHULL" is one of the hulls which make up the catamaran vessel.

"SEPARATION", (S), is the distance between the centrelines of the demihulls of a catamaran.

C_T	: Total Resistance Coefficient	
C_F	: Frictional Resistance Coefficient	
C_{FO}	: Form Resistance Coefficient	: KC_F
C_V	: Viscous Resistance Coefficient	: $(1+K)C_F$
C_{WT}	: Wake Traverse Resistance Coefficient	
C_R	: Residuary Resistance Coefficient	: C_T-C_F
C_W	: Wave Resistance Coefficient	:C_T-C_V
C_{WP}	: Wave Pattern Resistance Coefficient	
C_I	: Induced Drag Coefficient	
C_{Wthe}	: Theoretical Wave Resistance Coefficient	
C_{TS}	: Transom Stern Resistance Coefficient	
$(1+K)$	: Form Factor	:C_V/C_F
$(1+K_{WP})$	: Form Factor	:$(C_T-C_{WP})/C_F$
L, LWL	: Length on Waterline	
LOA	: Length Overall	
B	: Beam	
T	: Draught	
D	: Depth	
S	: Separation distance between the centrelines of the demihulls of a catamaran.	
W	: Width of a Catamaran	
C_B	: Block Coefficient	
C_P	: Prismatic Coefficient	
C_W	: Waterline Coefficient	
C_M	: Midship Section Coefficient	
∇	: Displacement Volume	
V	: Ship Speed	
Fn	: Froude Number	
Re	: Reynolds Number	
Ω	: Residuary Resistance Interference Factor	
β	: Form Resistance Interference Factor	
τ	: Wave Resistance Interference Factor	

1 INTRODUCTION

The commercial applications of high speed displacement catamarans has increased significantly over the past few years. Little information is, however, available for carrying out powering estimates for such vessels, particularly in the high speed range.

Work on the resistance of high speed displacement catamarans has been ongoing over a number of years at the University of Southampton [2,3,4] in an effort to improve the understanding of their resistance components and to provide design data.

This report describes a series of model tests on catamarans in calm water. The experimental programme is a development of earlier work [2,3]. The current work has extended the parametric investigation to cover changes in prismatic coefficient. As in the earlier work, an approach comprising total resistance measurements together with wave pattern analysis was utilised. A wide range of hull separations was tested and, overall, the experiments covered 20 model configurations, each over a speed range up to a Froude Number of unity.

The information collected and presented in this report contributes to a further understanding of the resistance components of catamarans and provides resistance data for practical use at the preliminary design stage.

The work described forms part of a wider research programme which includes the development of theoretical methods for the prediction of the wave resistance of catamarans. The theoretical work relating to Prismatic coefficient is the subject of a separate report [5].

2 DESCRIPTION OF MODELS

The range of models used in the overall investigation are shown in Table 1. The models were computer generated on a hull fairing package. These were then cut from high density polyurethane foam on a computer controlled cutter and hand finished. The hulls were derived from the NPL series [6], are of round bilge form with transom sterns and symmetrical about the centre line. Models 3b, 4b and 5b had already been tested some four years earlier and their results published [3] where they are designated C3, C4 and C5. The base vessel used for this particular study was model 5b with a prismatic coefficient of 0.693. From this parent hull two hulls were derived, model 5d with a C_p of 0.653 and 5e with a C_p 0f 0.733 (Figure 1). Details of these hull forms are given in Table 2. Experiments were performed on these demihulls in isolation and in catamaran form with hull separations of S/L 0.2, 0.3, 0.4 and 0.5.

Model 5b was retested to provide the basis data for comparison with the new models 5d and 5e. The results were also used as further validation, as this model had been tested by both Insel [3] and Molland [4]. This model was tested as a monohull and with S/L of 0.2, 0.3 and 0.5.

Model 4b was also studied in its original condition and for a lower displacement. The lower displacement case coincided with the 5 series and produced a C_P close to model 5d.

All the models were tested in the free to trim and sink condition, but were constrained in surge, sway, yaw and roll. The model towing force was in the horizontal direction. The towing point was situated at the longitudinal centre of gravity, except for model 4b in the light displacement condition, and at an effective height one third of the draught above the keel. The models were fitted with turbulence stimulation comprising trip studs of 3.2mm diameter and 2.5mm height at a spacing of 25mm. The studs were situated 37.5mm aft of the stem. No underwater appendages were attached to the models. For some of the smaller displacement models it was necessary to apply a counter balance.

2.1 Prismatic Coefficient

The Prismatic coefficient is the ratio of the volume of displacement of the hull to the volume of a channel defined by the midships area and the water line length of the craft. It can also be defined as the block

coefficient divided by the midship coefficient. It is a measure of the longitudinal distribution of volume in a hull. A vessel with a high Prismatic coefficient will have more volume in the ends of the craft than one with a low C_P.

Changing the C_P of a hull will change the pressure distribution and therefore the flow around the hull. It affects the wave resistance and the form resistance. The importance of C_P on residuary resistance has been long recognised. Taylor [7] demonstrated that there was an optimum Prismatic for a given Froude number to minimise the residuary resistance and that residuary resistance is more sensitive to C_P at displacement speeds than at higher speeds.

Since catamaran resistance is concerned with the interaction of flow around the demihulls it was apparent that C_P would be a useful coefficient to study. There also appeared to be no systematic study of Prismatic coefficient for high speed transom sterned catamarans.

2.2 Hull Variables

To study the effect of Prismatic coefficient on the resistance of catamarans it was realised that the changes in this value would have to be significant to ensure a measurable difference, however, not so large as to make the values unrealistic.

The previous hulls described in [2,3] were designed to a Prismatic coefficient of 0.693 and one of these models 5b was to be used as the basis craft. A change of Prismatic coefficient of $\pm$ 0.04 was finally decided upon with model 5d having a C_P of 0.653 and model 5e a C_p of 0.733. This was for the following reasons: Taylor's work [7] had shown that there was a measurable change in residuary resistance dependant on length displacement ratio for C_p 0.65 to C_p 0.7. Although for any given displacement length ratio the change in residuary resistance with Prismatic coefficient of this order was relatively small. From the authors design experience it was known that the majority of semi-displacement craft were designed within this Prismatic range. In the event that catamarans did not conform to monohull predictions it was thought reasonable to study higher than normal Prismatic coefficients as well.

Previous work at Southampton had considered the systematic variation in length to breadth ratio and breadth to draft ratio. The various hulls could be produced by the scaling of the offsets in the X, Y and Z axis thus still maintaining the basic hull coefficients. This would not be possible with a change in C_P.

To isolate any changes in wave making resistance as being caused by C_P it was necessary to maintain as many coefficients and variables at constant values. Because of the relationship between Prismatic coefficient, midship area, displacement length ratio, and block coefficient it was impossible to vary Prismatic and hold all the others constant. Therefore an order of priority had to be established to see which could be allowed to change.

To achieve a systematic series it was necessary to maintain length beam ratio and beam draft ratio as these are the subject of other research on the series.

To establish that any changes in resistance were due to Prismatic and not block coefficient it was necessary to minimise changes in C_B. Equally, length displacement ratio had to be fixed as Bailey [Ref 6] has shown that this has a major effect on residuary resistance and the testing of model 4b in the light condition (discussed later) emphasised this point. It was also considered sensible to maintain the same value of L.C.B.

The profile line was maintained to help in the model making process, to control the number of possible permutations and reduce problems with the theoretical wave resistance program which is the subject of a separate Ship Science report [Ref 5].

Having fixed all of the above variables, the remaining variable, midship area, would be used as a means of varying C_P, noting that this would be likely to change the hull interaction. It was also realised that transom area to midship area ratio would also have to change to produce a sensible hull form with a sectional area

curve of similar nature to the parent hull. Because of all the other restraints waterplane area would have to change. This, however, is considered to be the most likely way a Naval Architect would choose to vary a hull form and therefore the most relevant for design data.

To maintain fixed draft and to fix the beam on the waterline through the majority of the length of the craft there would have to be a system of proportionate scaling of waterlines with maximum change occurring at mid draft.

The constraints on the hull design mean that these hulls should not be thought of as truly part of a systematic series.

2.3 Systematic Variation of Prismatic Coefficient

There are several well documented methods to systematically change Prismatic. The introduction of parallel middle body is not feasible on these hull forms nor considered desirable. Other methods of modifying the sectional area curve only work when the first and last ordinate have zero area. No systematic method of varying the S.A.C. is available for an immersed transom.

By first considering the sectional area curve in two separate halves the method described by Lackenby [8] was used to modify the forebody. For the afterbody it was considered that for a change in C_P a realistic approach would be to change the transom area to maximum area ratio. No reference regarding changing the transom area to maximum area ratio when modifying the Prismatic had been found and there appeared to be no straight forward way of establishing the change in ratio with change in C_P.

With respect to this problem an intuitive approach was taken. The basis sectional area curve was drawn on a CAD package and the forebody for the two new Prismatics established using the method mentioned above. The after portion of the curve was then copied, moved and rotated so that the displacement remained constant and thus establishing the new transom areas. The curve was then refaired and checked for LCB, C_P, and displacement (Figure 1).

The hull sections below the water line were then modified by the function $x(1-x)$. Using such a function ensured a systematic change in shape. The topsides were also modified slightly to maintain the character of the master curves. A minor refairing process was finally required to achieve fair lines and the correct hydrostatics.

The final models could be easily identified as having different Prismatic coefficients, 5d having noticeably finer bow and stern with firmer turn of bilge to the midship sections (Figure 1).

It should be noted that the models that are cut from high density polyurethane foam are not totally stable and that some hogging did occur. All the models tended to move in the same direction and the movement was of the order of one to two millimeters over 1.7 metres.

3 FACILITIES AND TESTS

The model experiments were performed in the towing tank at Southampton Institute, the dimensions of which are as follows:

Length : 60.0 m
Width : 3.658 m
Depth : 1.819 m
Max Speed : 4.6 m/s

The tank is of constant rectangular section with beaches at one end and along one side. The side beaches were lifted out of the water for all tests to improve the wave reflection for the wave pattern experiment.

The tank is equipped with a manned carriage and a two component dynamometer. The test distance is 15.24m long with sufficient distance before this to achieve a steady speed of up to 4.2 m/s.

The total resistance and sideforce measurements were made using the dynamometer which is fully described in [9]. Sideforce was constantly monitored to check the model alignment and total resistance was measured to an accuracy of $\pm$ 0.02 N. It is noted that with the low drag measurements at low speeds below Fn 0.1 the error can be significant.

A wave pattern analysis based on multiple longitudinal cuts was applied to all the models. The analysis system was fully automated and consisted of four resistance wave probes, a microcomputer based data acquisition system and data analysis which enabled wave pattern analysis and resistance determination during standard resistance tests.

All wave probes were located at an optimum longitudinal position for longest possible wave traces, whilst transverse position was chosen to obtain a suitable cosine term in the wave series for every harmonic. This had an important effect on the stability of the analysis which enabled the results to be effectively independent of the transverse positioning of the probes. The analysis method was based on a combined matrix solution of four longitudinal wave traces. The method accounted for short wave traces without truncation errors. A full description of the apparatus and analysis is given by Insel [2].

The running trim of the models was measured by one potentiometer mounted on the port hull tow fitting. The accuracy of the potentiometer was in the range $\pm$ 0.05 degree. Trim was measured positive for bow up in degrees.

The sinkage of the model was measured by a linear displacement potentiometer mounted on the tow post bearing unit and connected to the tow post guide arm ensuring a vertical movement. The accuracy was found to be $\pm$ 0.1mm. Sinkage, vertical motion downwards was taken as positive and nondimensionalised by dividing by the draught of the model.

The two microcomputer controlled data acquisition systems which were used in the experiments are described in [2]. The first was mounted on the carriage to acquire signals from the dynamometer, the sinkage potentiometer and the trim potentiometer. The second was positioned at the side of the tank to acquire data from the four wave probes to calculate wave pattern resistance. A full description of the apparatus and analysis method is given by Insel [2].

4 DATA REDUCTION AND CORRECTION

4.1 Temperature Correction

The experiments were conducted over a fourteen month period with a water temperature range of 15.8-19.1 celsius. The total resistance measurements were corrected to the standard temperature of 15 celsius using the ITTC correlation line.

4.2 Resistance due to Turbulence Studs

Turbulence studs were fitted to the hulls as described in Section 2. Resistance due to the studs is relatively small and no corrections were made.

4.3 Wetted Surface Area

The static wetted surface area of the hulls was used to calculate the resistance coefficients. This method was chosen rather than using the free running wetted surface area. The reason for this was that although a nominal running wetted surface area could be calculated for any combination of sinkage and trim it would not take into account the effect of the wave profile modifying the wetted surface area in the dynamic state. The wave profile was seen to substantially modify the wetted surface area. This could be estimated from photographs for the outboard side but it was difficult to obtain similar information for the modified flow between the demihulls.

Comparisons of the results for models 5d and 5e were carried out using static wetted area. A limited comparison was also carried out using a standardised wetted surface area (the wetted surface area of model 5b), Since the three hulls had different wetted surface areas (Table 2).

4.4 Tank Blockage and Shallow Water Effects

No corrections were used for viscous blockage or shallow water effects. However, for speeds in excess of Froude number 1 there is a small shallow water effect on the wave resistance.

5 PRESENTATION OF DATA

The basic presentation of data follows the same approach as that in the earlier work [2,3,4] and is summarised as follows:

$$C_{Tcat} = (1+\beta K)C_F + \tau C_W$$

Noting that for the demihull in isolation:

$$\beta = 1 \text{ and } \tau = 1$$

The measured experimental data are presented in Figures 2 to 39. Figures 2 to 21 give the total and wave pattern resistance data for the demihulls. In these diagrams the wave pattern resistance C_{WP} is plotted downwards from the total resistance C_T in the form (C_T-C_{wp}). The estimates of $(1+k)$ or $(1+\beta K)$ are also shown in the diagrams, these lines being set to the lower envelope of the (C_T-C_{wp}) curves when they settle at an approximately constant level above the ITTC ship correlation line at higher Froude numbers.

Results of trim and sinkage measurements are presented in Figures 22 to 39.

From a practical view point it is not necessary to confine the user to the particular values of $(1+K)$ or $(1+\beta K)$ derived in this work. Following the earlier work, for example, some concern was expressed over their magnitudes and application (see discussion to [3]). For this reason, residuary resistance coefficients C_R

(derived from C_T-$C_{F(ITTC)}$) have been calculated from the experimental data and are presented in Figures 40 to 51. These curves provide the data in a form suitable for practical powering applications and an overall comparison of the residuary components for the different hull configurations. The user is able to choose a suitable (1+k) or (1+ βK) from this work or other sources. For an estimate of the ship total resistance coefficient it can be shown that, for the monohulls:

$$C_{T(SHIP)} = C_{F(SHIP)} + C_{R(MODEL)} - k(C_{F(MODEL)} - C_{F(SHIP)})$$

and for catamarans:

$$C_{T(SHIP)} = C_{F(SHIP)} + C_{R(MODEL)} - \beta K(C_{F(MODEL)} - C_{F(SHIP)})$$

Use of these equations requires a knowledge of model C_F. Based on the model length of 1.6m and a kinematic viscosity for fresh water of 1.139×10^{-6} it can be shown that:

$$C_{F(MODEL)} = 0.075/(\log10[Fn \times 5.56 \times 10^6]-2)^2$$

Residuary resistance interference factors, used later in comparing the performance of the various hull configurations, are presented in Figures 52 to 61. The coefficients of wave pattern resistance are presented in Figures 62 to 73, whilst the curves of coefficient of wave resistance are presented in Figures 74 to 85.

The experimental data for C_T, C_{WP}, trim and sinkage for models 5d and 5e for all configurations over a range of speeds, together with derived residuary resistance coefficients C_R derived from these data, are tabulated at the back of the report.

6 DISCUSSION OF RESULTS

6.1 Correlation with earlier tests

To check the experimental procedure and validate new results models 4b and 5b were retested. Model 4b had been tested by Insel [3] and 5b by both Insel [3] and Molland [4] as there were some doubts about the original experimental results for the monohull.

The total resistance results for models 4b and 5b were in general marginally higher (2-3%) than previous tests (Figures 2,3,4). The total resistance results for 5b in monohull form produced higher values than obtained by Insel but were in better agreement with Molland. The results were, however, considered to be in close enough agreement to validate the experimental procedure.The new beta value for model 5b although smaller still supports the original theory [Reference 3].

Previous tests had shown that for some configurations there was an increase in C_T in the region of Fn 0.9 - 1.0. This occasional upward jump in the resistance curve is likely to be associated with the onset of shallow water effects but why this would affect some results and not all is not clear. Certainly for model 4b at normal displacement the wetting of the trimming weight and crossbeam may be causing the higher resistance at Fn 0.9 and above.

6.2 Total Resistance and Wave Pattern Resistance

By visual inspection alone it was difficult to identify any noticeable difference between models 5d and 5e which were tested in quick succession. Photographs were taken for various hulls and demihull separations. The results were disappointing as the wave patterns were difficult to identify clearly on the photographs. The bow wave and the transom wave were observed to break at certain speeds as they were shed from the hull.

6.2.1 Results for Monohulls

In monohull form model 5d (with the lower C_P) has the lower total resistance at low speed but this is reversed at higher speeds with model 5e (with the higher C_P) having the lower resistance. The differences in resistance are greater at lower Froude numbers (Figures 5,10,14).

As with the other components of resistance, model 5e displays a higher wave pattern resistance than 5d at lower speed (Figure 66). The Prismatic hump is more noticeable for 5e. At higher Froude numbers the wave pattern resistance for the two models is similar.

6.2.2 Results for Catamarans

In catamaran form the rooster tails generated by the transoms when clear of the water were modified by the reflected bow waves causing them to become asymmetric and possibly becoming steeper. At some speeds these two transom waves would combine on the centre line to form a third rooster tail. The two bow waves could also combine to form a rooster tail. These rooster tails contain spray and breaking waves and, depending on speed and demihull separation, a model can exhibit none, two, three or four rooster tails.

In catamaran form the differences in total resistance between 5d and 5e at lower speeds increase with reduction in hull separation. However, at higher speeds the resistance curves come closer together, with model 5e having the higher resistance at the narrower hull separations (Figures 6-9,15-18).

The humps and hollows in the C_T curve are more pronounced for model 5e than for 5d

The wave pattern resistance for the catamarans shows a higher Prismatic hump for 5e than 5d which increases with reduction in hull separation (Figures 67-70). The main hump is higher for 5d but there is no obvious trend with hull separation except that the Froude number at which the hump occurs moves with hull separation. The differences between the two hull forms at higher speeds decrease with reduction in hull separation.

The wave pattern results for models 5d and 5e in monohull and 5d for S/L 0.5 produced high values for Froude numbers in the region of 0.5 (see Figures 5,9,14). These were noted during the experiments and some additional runs were performed to verify their existence. These high values, which had not been seen for model 5b, may be due to the fact that there was less wave breaking and the probes were measuring more of the total wave energy.

Wave resistance C_w (based on $C_T-\{1+K_{wp}\}C_F$)

The results for the monohulls (Figure 78) shows 5d has a lower wave resistance than that for 5e at lower speeds and virtually identical at higher speeds. Moving through the catamaran results from wide hull separation to low hull separation (Figures 79-82) it can be seen that at low speed the same is true but there is little change in the magnitude. At higher speeds there is clearly a lower wave resistance for 5e. The cross over point in the curves appears to alter, with hull separation, but with no obvious trend.

6.3 Running Trim and Sinkage

As a monohull, model 5d trimmed more than model 5e through all the speed range (Figure 25). This difference in trim was increased for a hull separation of S/L 0.5. Reducing the hull separation increased the trim at the hump speed and reduced the difference in trim between the models. The hump positions is seen to move with demihull separation (Figure 31-33). The demi hull separation of 0.2 showed a strong hump speed effect for model 5d compared to 5e but after this the two curves start to converge. This difference in trim is most likely to be affected by the different transom areas. All graphs show a slight hollow in the curve after the main hump.

Hump speed sinkage increases with reduction in hull separation with 5e showing marginally less sinkage (Figures 34-38). Both hulls exhibit lift at higher speeds for S/L 0.2.

6.4 Residuary Resistance

6.4.1 Results for Monohulls

Model 5e with the higher C_p has a significantly higher residuary resistance at low speed with a high Prismatic hump (Figure 44). The curves cross over just before hump speed and 5e then has a consistently lower resistance.

6.4.2 Results for Catamarans

The residuary resistance shows the same trends as the total resistance (Figures 44-48) but what can be more clearly seen is that the crossover in the resistance curves for 5d and 5e occurs at a higher Froude number when going from monohull to catamaran S/L 0.5. The smaller S/L values produce small differences in resistance with 5d, the lower C_P, having the lower resistance.

There are greater differences in residuary resistance at lower speeds and, as hull separation decreases, there is a trend for the higher Prismatic hull 5e to increase its resistance relative to the low Prismatic, thus indicating a greater interference.

6.4.3 Residuary Resistance Interference Factors

The results show clearly that the model with the higher Prismatic coefficient has a higher interference factor above a Froude Number of 0.4 for all hull separations. Below this the results are the same except for the widest hull separation (Figures 56-59).

Considering hull separation it can be seen that the smaller the hull separations the greater the interference at hump speed (Figures 52-54). This interference decreases with speed so that above a Froude number of 0.6 for the low C_p and 0.7 for the high C_p there is little difference with hull separation. The fact that the interference factors converge at a higher Froude number for the higher C_p also indicates that there is a stronger interference with high C_P. It is interesting to note that the nature of the interference factor curve for S/L 0.2 for both models is different to that for the other hull separations. There also appears to be a phase shift between model 5d and 5e.

6.5 Viscous Resistance and Form Factors

The results in Table 3 show the form factors for 5b and 5d to be similar in monohull configuration. Model

5e produced a lower form factor for the monohull (1.21) and higher factors for the catamaran. There would appear to be a trend of increasing form factor with increasing C_P in catamaran form. This indicates a greater interaction between the hulls which is illustrated by the viscous interference factors, Table 4.

As mentioned earlier the wave pattern results for 5d and 5e in monohull and 5d for S/L 0.5 produced high values for Froude numbers in the region of 0.5 (Figures 5,9,14). These were noted during the experiments and some additional runs were performed to check there were no mistakes. These high values, which had not been seen for 5b, may be due to the fact that there was less wave breaking and the probes were measuring more of the total wave energy.

If one assumes this to be true and using these values to obtain the form factor the following are obtained.

5d monohull $(1+k)$ = 1.09
5d S/L 0.5 $(1+\beta k)$ = 1.15
5e monohull $(1+k)$ = 1.08

To determine a form factor from one point on a graph is not a procedure to be recommended but it may be an indication that the 'missing' energy required to produce the expected lower form factors is accounted for in breaking waves. The form factors quoted above are, however, still higher than those suggested by Cordier and Dumez [10].

When comparing all three hulls 5b, 5d, 5e it is seen (Figures 78-82) that model 5b compares more closely with 5e than 5d at lower Froude numbers. This may be due to model 5b having been manufactured some 5 years earlier. At higher speeds the difference between the three hulls is measurable but small. Out of interest, the hydrostatics for the free sinkage and trim cases at each Froude number were calculated for each of the hulls and it was observed that, for the larger trim angles, the Prismatic coefficients of the three hulls converged to virtually the same value.

The results were also analysed using a standardised wetted surface area (WSA of model 5b). This made minor alterations to the actual results but had no effect on the overall conclusions.

6.6 Comparison with other data

The above results have been compared with those of known monohull results. To do this a reanalysis of the Taylor series [7] was performed for a B/H=2.25 and $\nabla/(L/100)^3 = 45$ which are close to the values for the models 5b, 5d, 5e. The analysis showed that the higher Prismatic coefficient produced the higher resistance. This data only covered the speed range up to Fn = 0.64. It must also be remembered that the Taylor series was for hull forms without a submerged transom. Taylor's variation in Prismatic was achieved by moving section areas along the waterline thus changing ∇, C_W, C_B and half angle of entrance whilst maintaining C_M.

A second source of data was Nordstrom [11]. Although these data do not represent a systematic change in Prismatic, two hulls from this work were found to approximately fit the requirements (Table 5). The hulls considered were of slightly different forms with varying transom immersion and deadrise. Skegs were also fitted. The results are plotted in a non-dimensional form of total resistance. The speed range tested was only up to a Froude number of 0.66. However, the results show that the higher C_P hull had the lower resistance above a Fn of approximately 0.45, Indicating agreement with the current work.

Wigley's work [12] on the variation of Prismatic coefficient and the independent variation of angle of entrance is not strictly relevant. This was due to the fact that when Prismatic was varied, so was block coefficient, displacement, and half angle of entrance. The parameters that were fixed were length, beam, draft, and midship coefficient. Thus being the reverse of the parameters varied in this work. Doctors [13] theoretical variation on a Wigley hull used parallel middle body and therefore also varied block Coefficient. The results from both of these pieces of work was that the higher the Prismatic the higher the resistance.

6.7 Model 4b Light Displacement

A series of tests were conducted on 4b to determine the effect of significantly changing the length to displacement ratio. These tests were performed for a monohull and two catamaran hull separations, S/L 0.3 and 0.5.

Model 4b at the lower displacement had a nearly identical Prismatic to that of 5d and similar length displacement ratio, though many of the other parameters differed.

Although model 4b light can not be thought of as part of a systematic series the hull coefficients and ratios of the hull lie within the range tested in the series. For this reason it was thought that some useful data and conclusions may be obtained.

6.7.1 Experimental Results model 4b light displacement

The experimental results for 4b (light displacement) suffer from a lack of data points for S/L 0.3 due to technical problems during the testing. Some of the sinkage results for S/L 0.5 appear to have a zero shift probably caused by re-zeroing during the test runs.

All the results for 4b light are closer to those of the 5 series than model 4b demonstrating how overriding the importance of length/displacement ratio is to the residuary resistance.

Results for Monohull

The comparison of total resistance, residuary resistance and wave pattern resistance for the 4b light monohull shows a better comparison with model 5b rather than 5d (Figures 19,50,71).

The total resistance and residuary resistance are slightly lower than 5b at higher Froude numbers. Graphs of total resistance upon displacement and residuary resistance upon displacement have been plotted for the monohull and these show very little difference between 5b and 4b light.

The wave pattern resistance is close to that of 5b (Figure 71). For the monohulls the wave resistance of 4b (light displacement) is lower than for 5d and 5b once the transom is clear,but this is reversed at the lower hull speeds (Figure 83). There is also a lower than predicted form factor of approximately 1.25.

Results for Catamarans

Comparing results for 4b light for different hull spacings there is the typical relationships with the narrow hull spacing showing greater trim and wave resistance at hump speed which reduces with increasing Froude number (Figures 30, 84, 85).

For a demihull spacing of S/L 0.5 the wave pattern resistance curves (Figure 73) are all fairly similar at the lower speeds but there is a better comparison between model 4b light and model 5b.

For S/L 0.3 (Figure 72) there is little to choose between the C_{WP} curves at the higher speeds and the lack of results for 4b light at lower speeds make it hard to analyse.

The coefficient of residuary resistance for S/L 0.5 shows a large decrease in resistance compared to the 5 series hulls especially at lower Froude numbers (Figure 51).

Reducing the hull separation produces a greater influence on the wave pattern resistance for 4b light than 5b in the Froude number range 0.4-0.65 (Figures 63-65).

The reduction in C_W for 4b light compared to 5b for an S/L of 0.5 (Figure 85) is not as pronounced as for

C_R due to the change in value of the form factor based on C_{WP} and the value for β (1.6).

From the graphs of resistance components for 4b (light displacement) it can be seen that a form factor value for catamarans of 1.40 fits the C_{WP} curves (Figures 20,21). This is a lower than predicted although the change in value for S/L 0.5 could be within the range of experimental error.

The wave resistance interference factor shows again values closer to model 5b than 4b although it is noticeable that the plot has a different character with lower values at lower Froude number and higher values at higher Froude numbers than 5b with a cross over at about Fn 0.5.

Residuary resistance interference factors are not as easy to interpretate but again it is noticeable that below Fn 0.5 model 4b light has lower values than the other two hulls (Figure 60,61).

Using the form factors already quoted and therefore assuming they do not vary with hull spacing a viscous interference factor beta of 1.6 was calculated. This is marginally higher than for 4b at the normal displacement. This fits Insel's theory [3] as the length beam ratio for the light displacement is marginally higher, although other variables have also been changed.

6.7.2 Effects of changes in Prismatic Coefficient

By analysing other available data an attempt was made to investigate and estimate the effect that changing the various parameters would have on the resistance of the model.

Changing the length displacement ratio on 4b altered the following hull data (Table 2):

L/B	B/T
C_P	C_B
C_M	C_W
WSA	LCB
Transom area/Midship area	

Effect of change in L.C.B. from 6.4% aft to 4.5% aft.

The NPL series [6] data for hulls with L/B of 7.5 indicate that there is a small increase in residuary resistance with LCB moving forward and that the significance decreases with increasing L/B (from L/B 4.5 to 7.5). Assuming that the trend can be extrapolated to higher length beam ratios one might expect a marginal increase in residuary resistance for 4b light over that for 4b in monohull configuration.

Effect of changing B/T from 2.0 to 2.35.

Analysing Molland's [4] results for systematic changes in beam draft ratio there appears to be very little change in value or trend for the form factor. Increasing B/T produces an increase in C_T and therefore C_w. However, the B/T change is relatively small compared to the range studied by Molland and so the increase in C_w and C_T will be small.

Effect of changing Prismatic from 0.693 to 0.657.

Tests on 5b, 5d, 5e indicate that reducing Prismatic should reduce residuary resistance at low speed and produce little difference at higher speeds.

Effect of changing Transom/Midship area from 0.524 to 0.374.

A reduction in transom area would prove beneficial to reducing resistance at low speed but as dynamic support increases one might expect the resistance curve to rise more steeply than that of a craft with a high transom to midship area ratio.

Effect of changing Length Displacement ratio.

Increasing the length displacement ratio reduces residuary resistance becoming more significant at higher Froude numbers. This ratio is regard as one of the major factors affecting the resistance of semi-displacement craft.

If 4b light was part of the systematic series then for a L/B = 9.4 its length displacement ratio would be 7.85. However, in the light displacement condition the hull is no longer part of the series and the actual length displacement ratio was 8.5. One would therefore expect a greater reduction in total resistance and form resistance.

The length to wetted surface area ratio and wetted surface area to displacement ratios are within a few percent of each other and should not affect the results to any extent.

Reviewing the above variables, LCB and B/T will all produce small increases in resistance. Length displacement ratio will have greater effects on reducing resistance. The overall effect would be to reduce the form resistance and total resistance with possibly a slightly greater reduction in hump resistance.

7 CONCLUSION AND RECOMMENDATIONS

7.1 Monohull

The effect of Prismatic coefficient on resistance is greater at lower speeds than at higher speeds with the lower Prismatic coefficient producing the lower resistance. The general trends for the variation in C_P appear to be as predicted by the Taylor series for the lower speeds.

This work indicates that for a monohull there is a higher value for optimum Prismatic for higher Froude numbers than that suggested bt Taylor. This is not surprising as Taylor's work did not include immersed transoms.

7.2 Catamarans

A lower Prismatic coefficient is significantly better for low Froude numbers.

At higher speeds there are marginal differences between high and low Prismatic coefficients, the lower C_P being beneficial at smaller hull separations.

There is greater (detrimental) hull interaction between forms with higher Prismatic coefficients than those with lower C_P. The interaction increases with decrease in hull separation and the interaction is stronger at low Froude numbers.

The work on model 4b at reduced draught suggests that useful additional data may be obtained by rerunning other models in the series at different displacements.

The fact that at low speeds model 4b light has noticeably lower Cw but not Cwp than model 5b suggests that there are more breaking waves generated by the lower L/B ratio hull.

REFERENCES

1) ITTC DICTIONARY OF SHIP HYDRODYNAMICS

MARITIME TECHNOLOGY MONOGRAPH NO 6 RINA 1978

2) INSEL M.
AN INVESTIGATION INTO THE RESISTANCE COMPONENTS OF HIGH SPEED CATAMARANS.

PhD THESIS, UNIVERSITY OF SOUTHAMPTON
1989

3) INSEL M. AND MOLLAND A.F.
AN INVESTIGATION INTO THE RESISTANCE COMPONENTS OF HIGH SPEED DISPLACEMENT CATAMARANS.

TRANSACTIONS OF THE ROYAL INSTITUTION OF NAVAL ARCHITECTS
1992

4) MOLLAND A.F. AND COUSER P.R.
RESISTANCE EXPERIMENTS ON A SYSTEMATIC SERIES OF HIGH SPEED DISPLACEMENT CATAMARAN FORMS: VARIATION OF LENGTH TO DISPLACEMENT RATIO AND BREADTH-DRAUGHT RATIO

SHIP SCIENCE REPORT NO.71
UNIVERSITY OF SOUTHAMPTON 1994

5) MOLLAND A.F. AND LEE A.R.
THE THEORETICAL INVESTIGATION OF A SERIES OF HIGH SPEED DISPLACEMENT CATAMARAN FORMS: VARIATION OF PRISMATIC COEFFICIENT

SHIP SCIENCE REPORT NO.87
UNIVERSITY OF SOUTHAMPTON 1995

6) BAILEY D.
THE NPL HIGH SPEED ROUND BILGE DISPLACEMENT HULL SERIES

MARINE TECHNOLOGY MONOGRAPH, No: 4 RINA 1976

7) TAYLOR D.
THE SPEED AND POWER OF SHIPS

THE UNITED STATES GOVERNMENT PRINTING OFFICE
1943

8) LACKENBY H.
ON THE SYSTEMATIC GEOMETRICAL VARIATION OF SHIP FORMS

TRANSACTIONS OF THE ROYAL INSTITUTION OF NAVAL ARCHITECTS
1950

9) CAMBELL I, CLAUGHTON A.
THE INTERPRETATION OF RESULTS FROM TANK TESTS ON 12m YACHTS

THE EIGHT CHESAPEAK SAILING YACHT SYMPOSIUM, SNAME 1987

10) CORDIER S, DUMEZ F.
SCALE EFFECTS ON THE RESISTANCE COMPONENTS OF A HIGH SPEED SEMI-DISPLACEMENT CRAFT

FAST 93
PROCEEDINGS OF THE SECOND INTERNATIONAL CONFERENCE ON FAST SEA TRANSPORT
THE SOCIETY OF NAVAL ARCHITECTS OF JAPAN, 1993

11) NORDSTROM H.
SOME TESTS WITH MODELS OF SMALL VESSELS

THE SWEDISH STATE SHIPBUILDING EXPERIMENTAL TANK
NO. 19 1951

12) WIGLEY W.
CALCULATED AND MEASURED WAVE RESISTANCE OF A SERIES OF FORMS DEFINED ALGEBRAICALLY.
INA TRANSACTIONS 1942

13) DOCTORS L, RENILSON M.
THE INFLUENCE OF DEMI-HULL SEPARATION AND RIVER BANKS ON THE RESISTANCE OF A CATAMARAN

FAST 93
PROCEEDINGS OF THE SECOND INTERNATIONAL CONFERENCE ON FAST SEA TRANSPORT
THE SOCIETY OF NAVAL ARCHITECTS OF JAPAN, 1993

Table 1 **THE SHIP SCIENCE SYSTEMATIC SERIES**

	B/T			
	1.5	2	2.5	
$L/\nabla^{1/3}$		MODEL		C_P
6.3	-	3b	-	0.693
7.4	4a	4b	4c	0.693
8.5	5a	5b	5c	0.693
9.5	6a	6b	6c	0.693
8.5	-	5d	-	0.653
8.5	-	5e	-	0.733

Table 2 **HYDROSTATIC DATA**

MODEL	5d	5b	5e	4b Reduced Displmnt.	4b Original Displmnt.
C_P	0.653	0.693	0.733	0.657	0.693
C_B	0.396	0.397	0.398	0.334	0.397
C_M	0.606	0.572	0.543	0.509	0.572
C_W	0.756	0.762	0.770	0.737	0.762
L/B	11	11	11	9.4	9.0
B/T	2	2	2	2.3	2
L	1.6	1.6	1.6	1.58	1.6
LCB	56.4	56.4	56.4	54.5	56.4
$L/\nabla^{1/3}$	8.479	8.479	8.479	8.504	7.41
WSA	0.2707	0.276	0.2714	0.2745	0.338
TRANSOM A/ MIDSHIP A	0.472	0.524	0.597	0.374	0.524
$L/WSA^{1/2}$	3.07	3.05	3.08	3.016	2.752
$WSA/\nabla^{2/3}$	7.60	7.75	7.62	7.95	7.23
β	1.66	2.0	2.19	1.6	1.5

Table 3 **FORM FACTORS**

Model	Cp	S/L 0.5	S/L 0.4	S/L 0.3	S/L 0.2	MONO
5d	0.653	1.46	1.43	1.41	1.39	1.26
5b	0.693	1.41		1.46	1.41	1.26
5e	0.733	1.46	1.46	1.46	1.40	1.21

Table 4 **FORM RESISTANCE INTERFERENCE FACTOR, β**

Model	S/L 0.5	S/L 0.4	S/L 0.3	S/L 0.2
5d	1.77	1.65	1.58	1.50
5b	1.58	-	1.77	1.58
5e	2.19	2.19	2.19	1.90

Table 5 **NORDSTROM HULL DATA**

MODEL	49	301
∇	24.04	12
$L/\nabla^{1/3}$	7	7.04
$B/\nabla^{1/3}$	1.15	1.16
$T/\nabla^{1/3}$	0.265	0.270
MAX AREA/$\nabla^{2/3}$	0.222	0.209
L/B	6.07	6.07
B/T	4.35	4.3
C_B	0.467	0.453
C_p	0.644	0.681
LCB	52.69	52.63

FIGURE 1

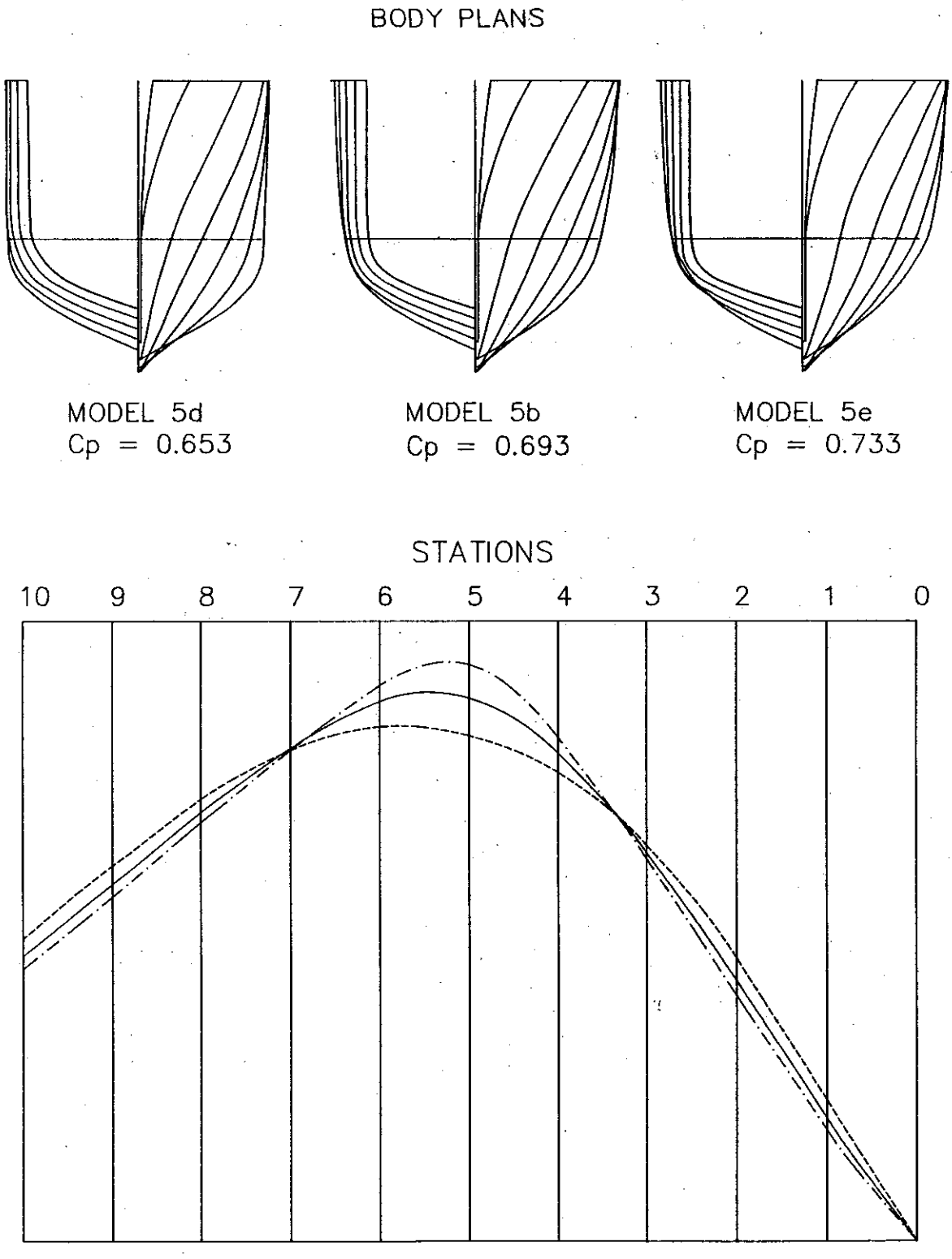
BODY PLANS
MODEL 5d
Cp = 0.653
MODEL 5b
Cp = 0.693
MODEL 5e
Cp = 0.733
STATIONS
10 9 8 7 6 5 4 3 2 1 0
SECTIONAL AREA CURVES
Cp = 0.653
Cp = 0.693
Cp = 0.733

FIGURE 2 RESISTANCE COMPONENTS 4B MONOHULL (RETESTS)

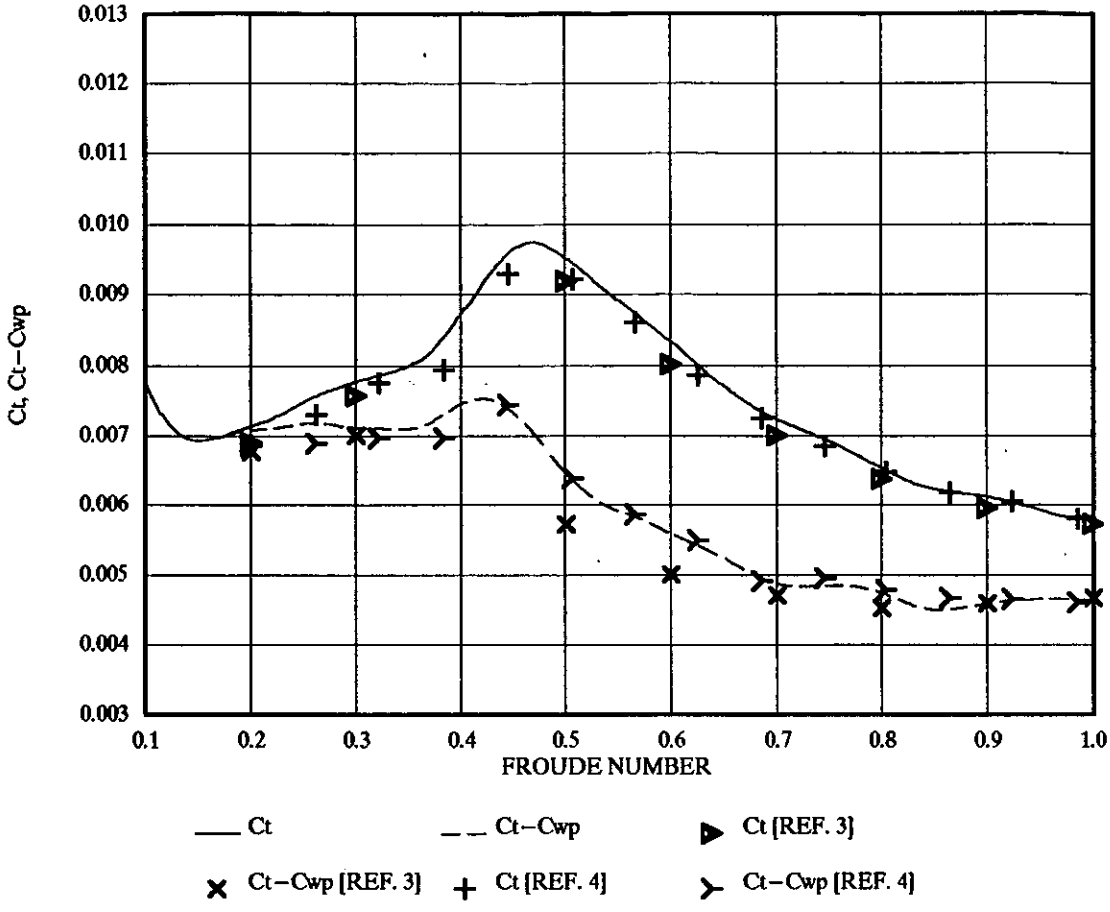

FIGURE 3 RESISTANCE COMPONENTS 4b S/L 0.3 (RETESTS)

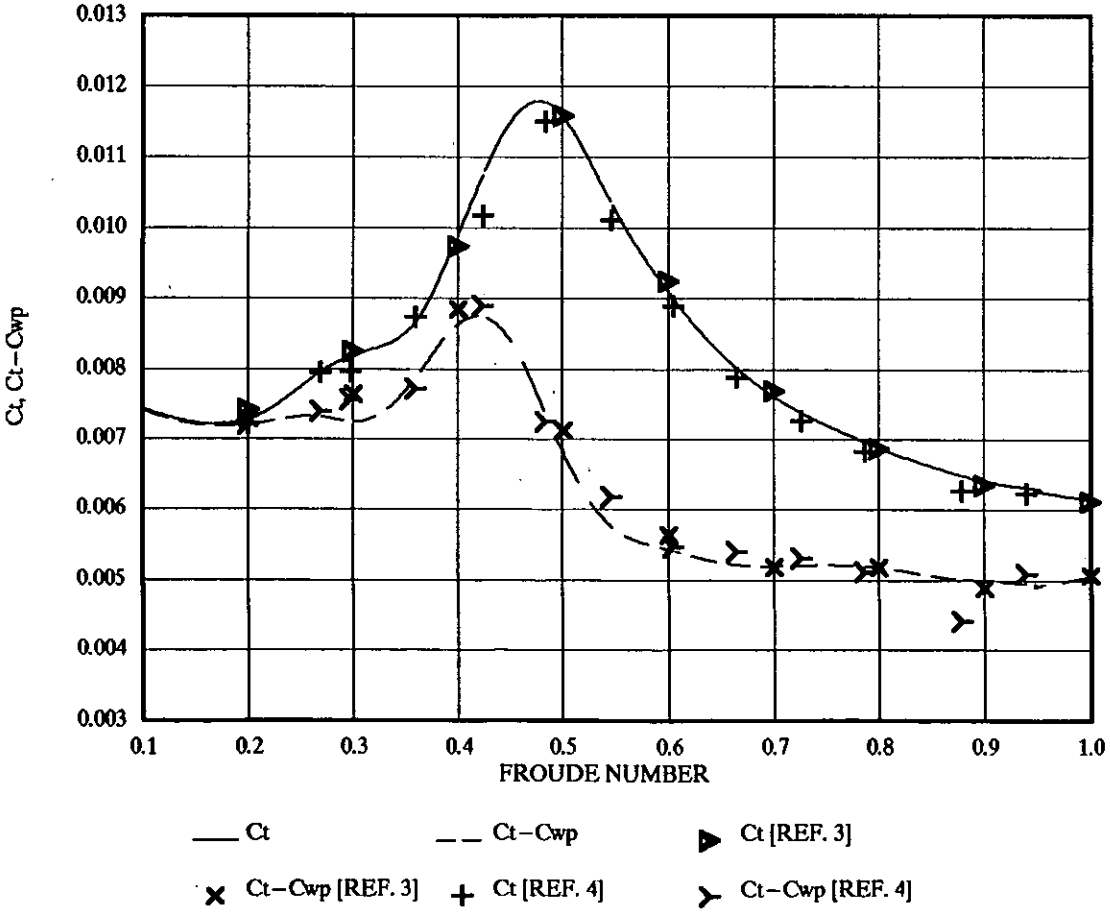

FIGURE 4 RESISTANCE COMPONENTS 5b MONOHULL (RETESTS)

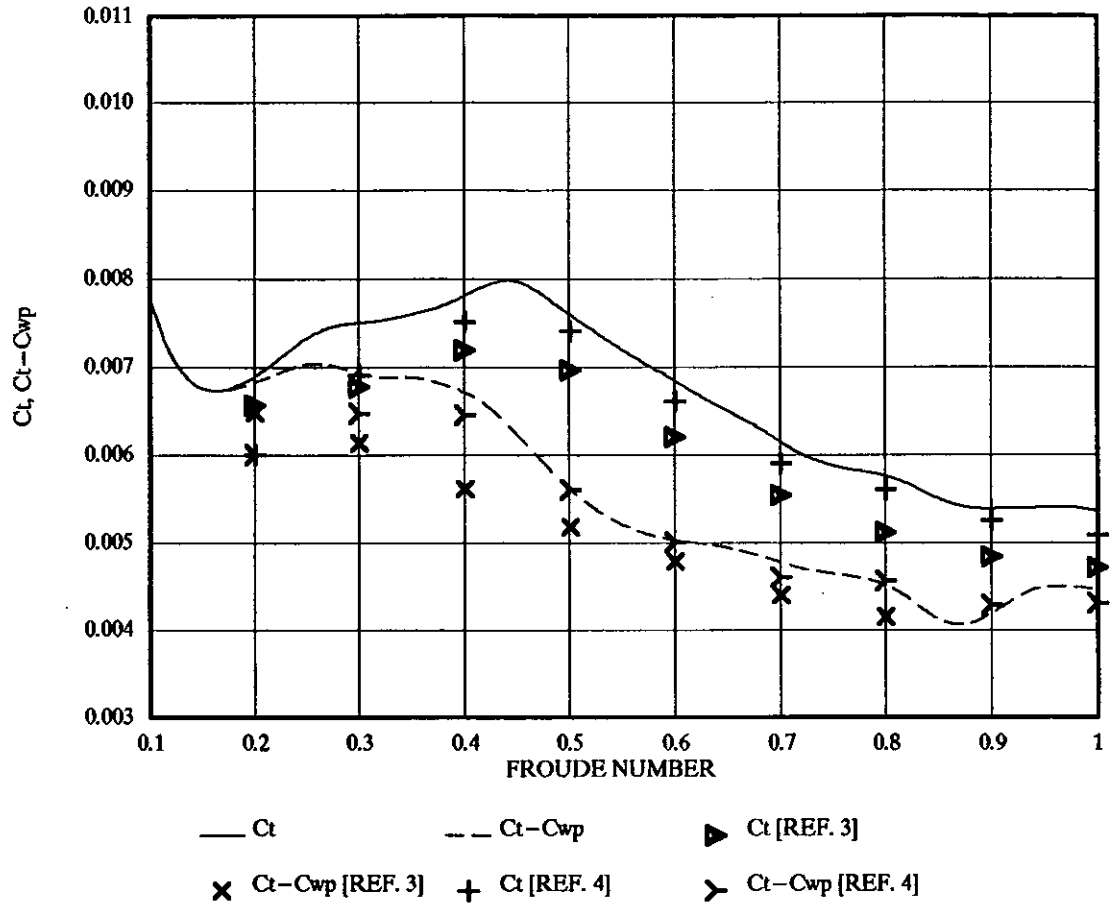

FIGURE 5 RESISTANCE COMPONENTS 5d MONOHULL

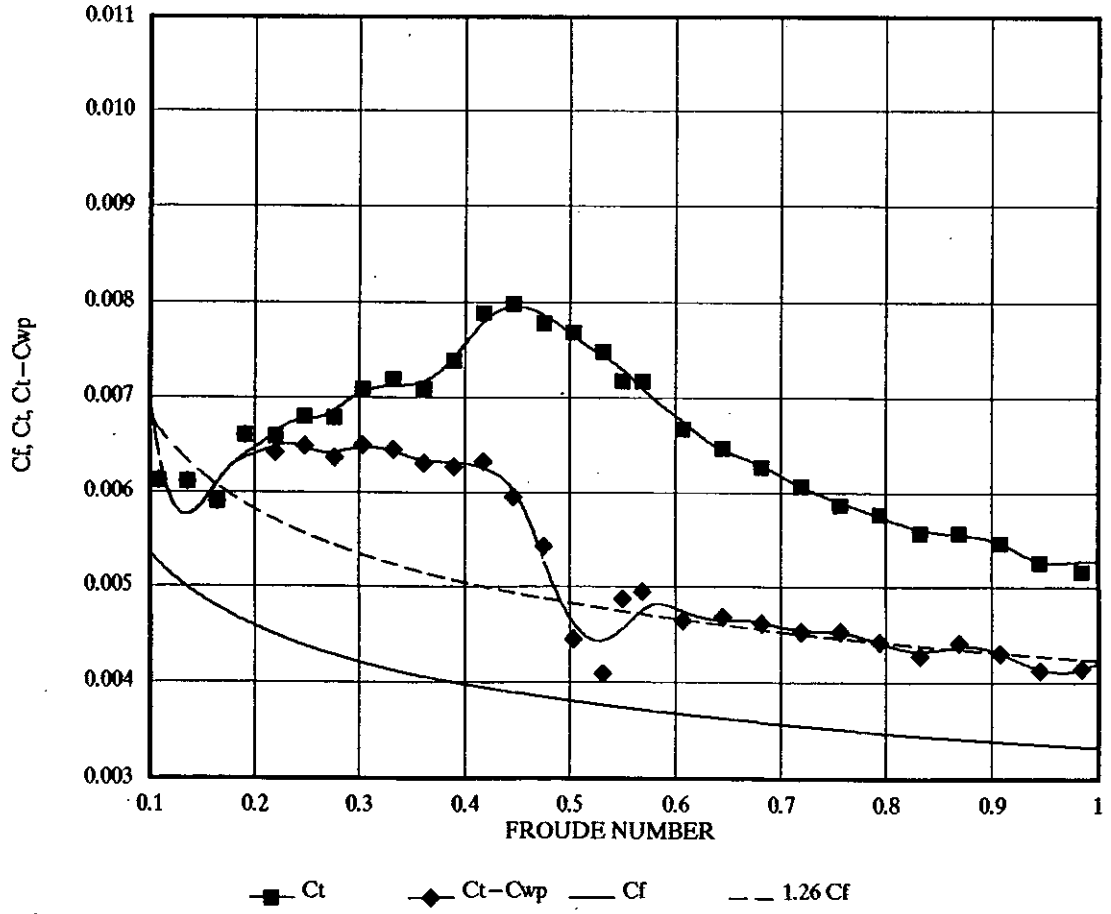

FIGURE 6 RESISTANCE COMPONENTS 5d S/L 0.2

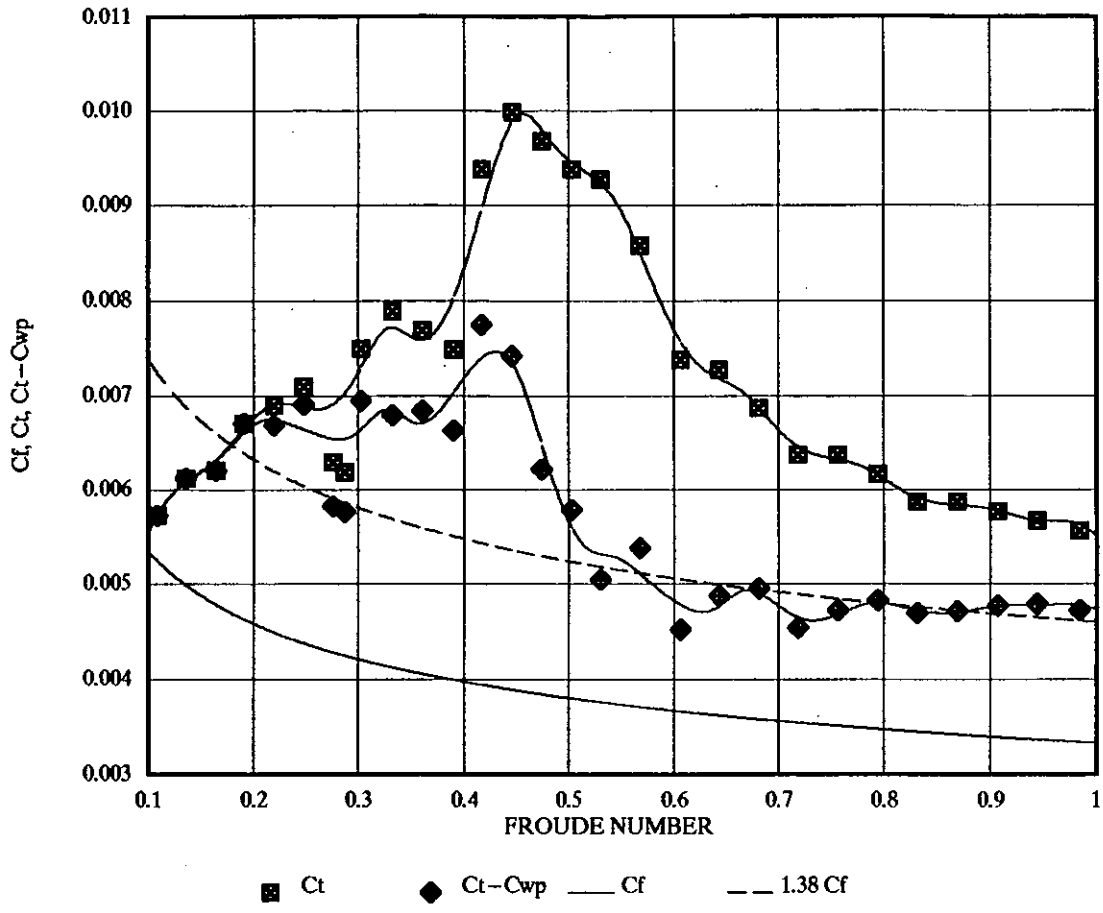

FIGURE 7 RESISTANCE COMPONENTS 5d S/L 0.3

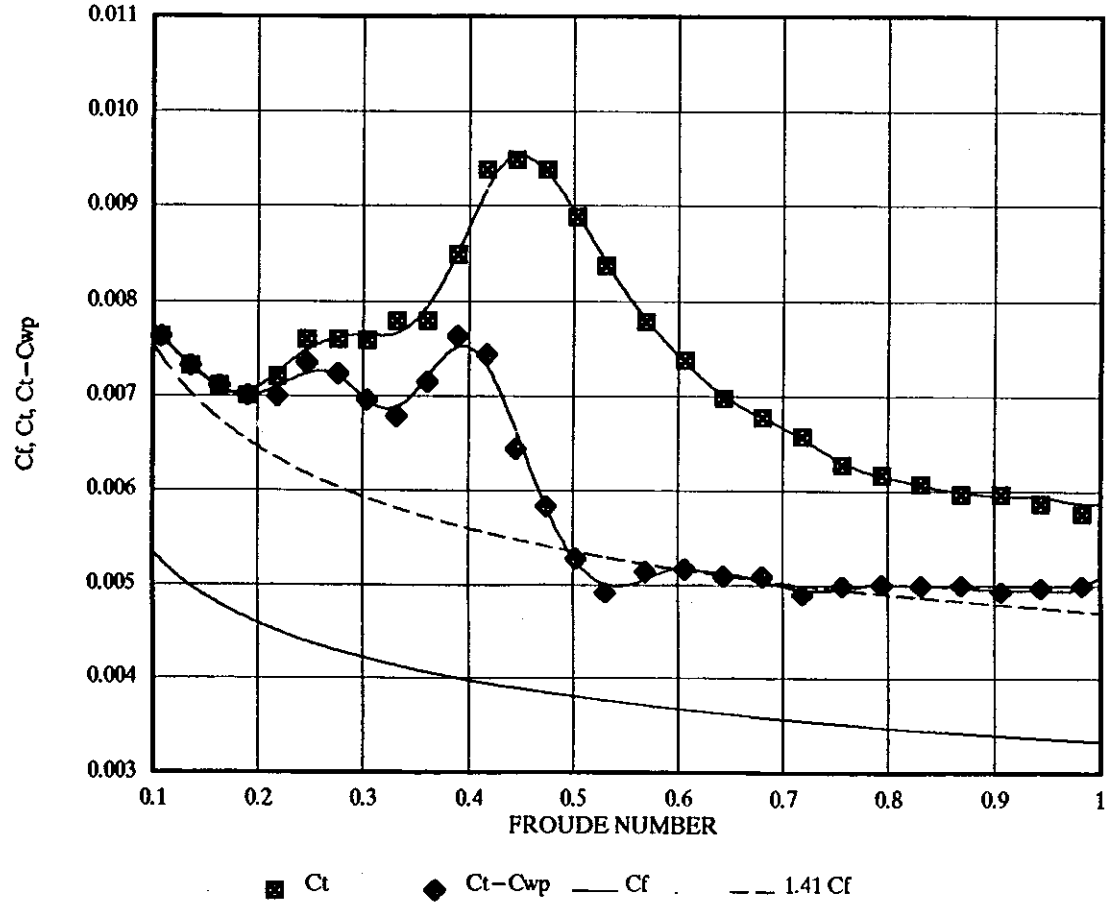

FIGURE 8 RESISTANCE COMPONENTS 5d S/L 0.4

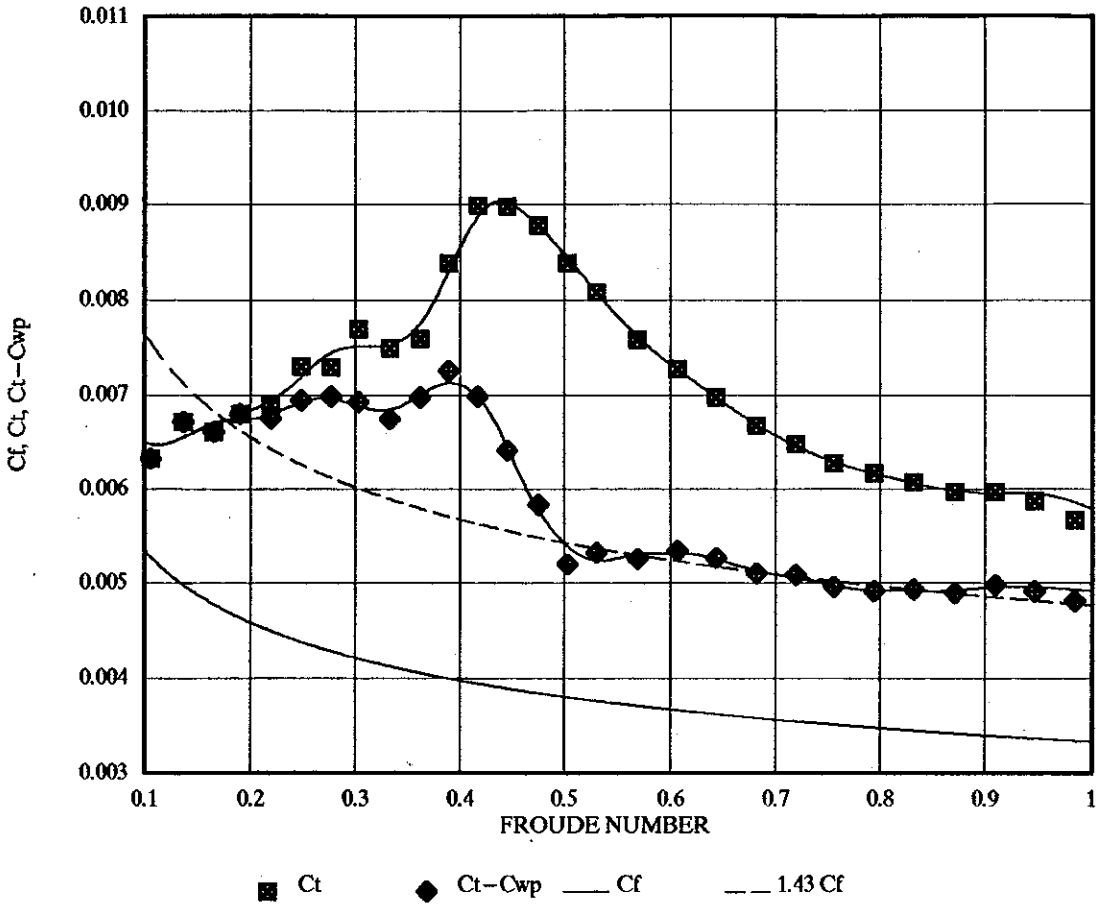

FIGURE 9 RESISTANCE COMPONENTS 5d S/L 0.5

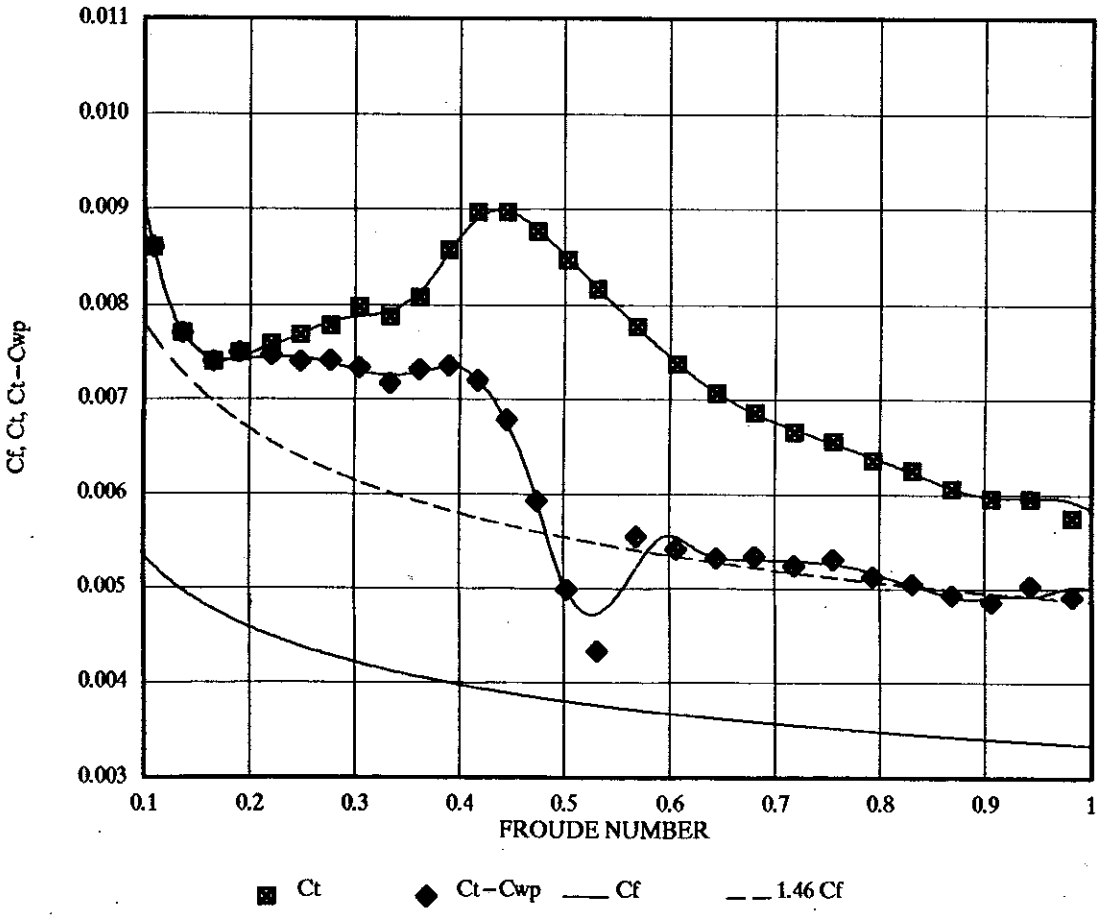

FIGURE 10 RESISTANCE COMPONENTS 5b MONOHULL

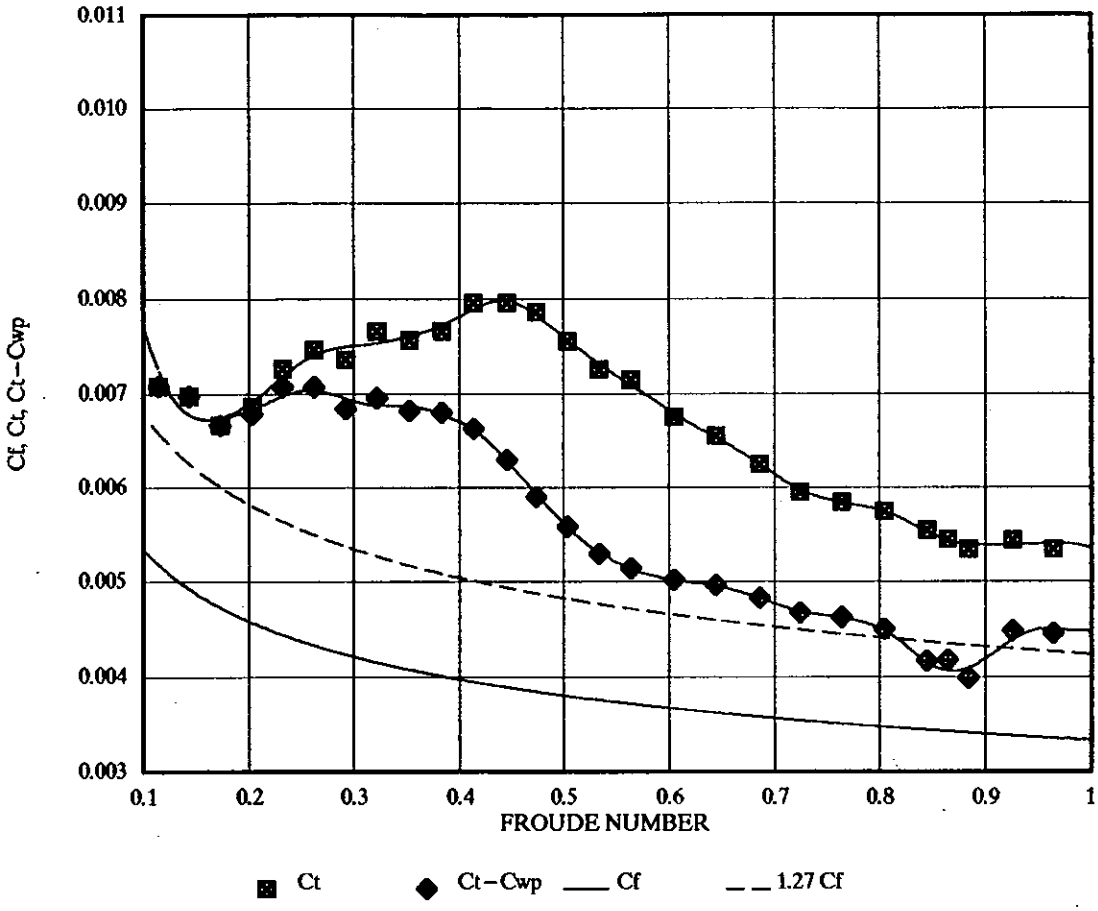

FIGURE 11 RESISTANCE COMPONENTS 5b S/L 0.2

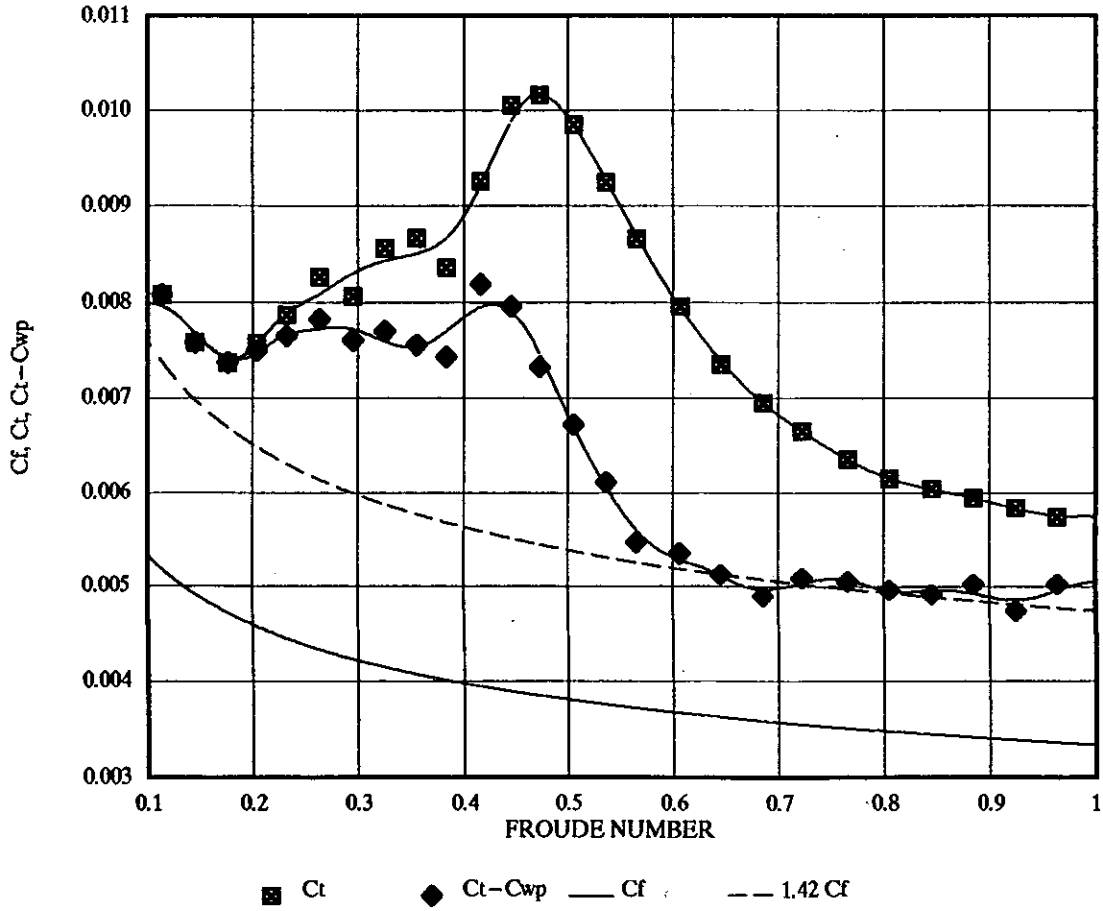

FIGURE 12 RESISTANCE COMPONENTS 5b S/L 0.3

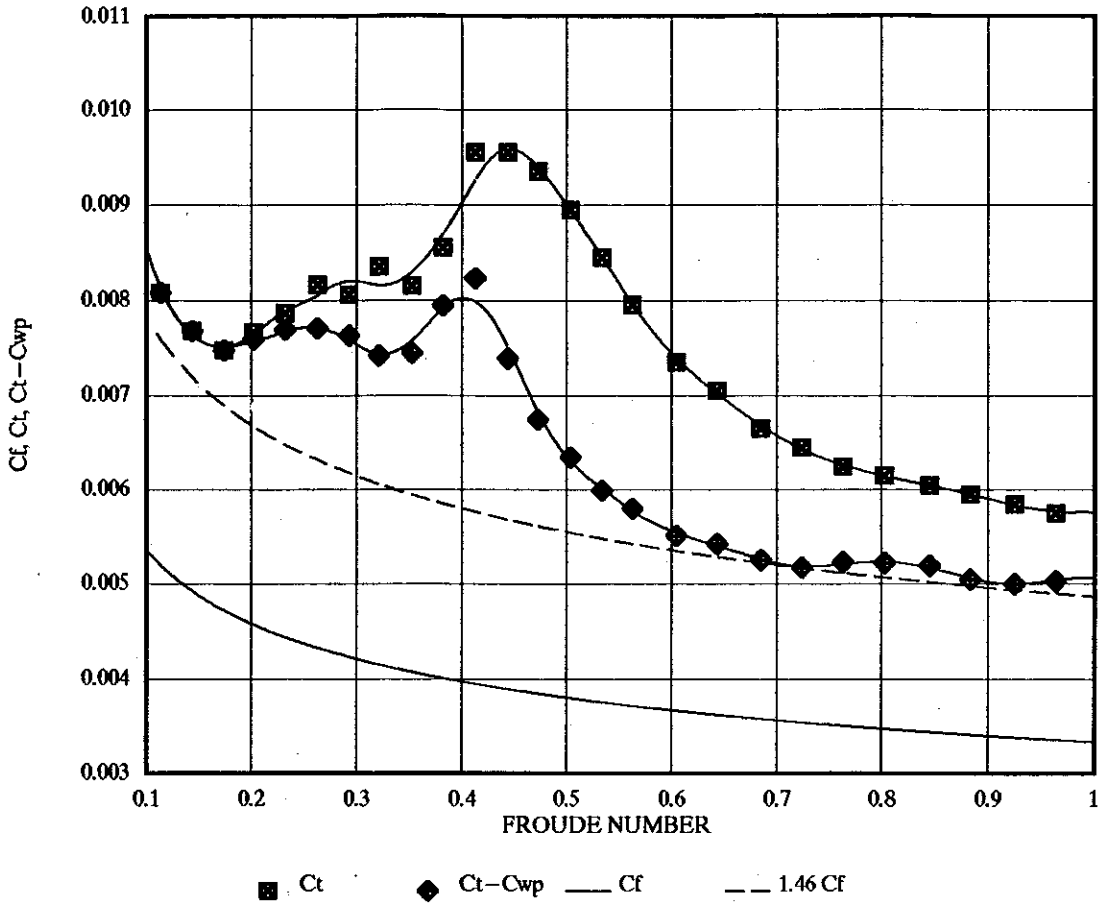

FIGURE 13 RESISTANCE COMPONENTS 5b S/L 0.5

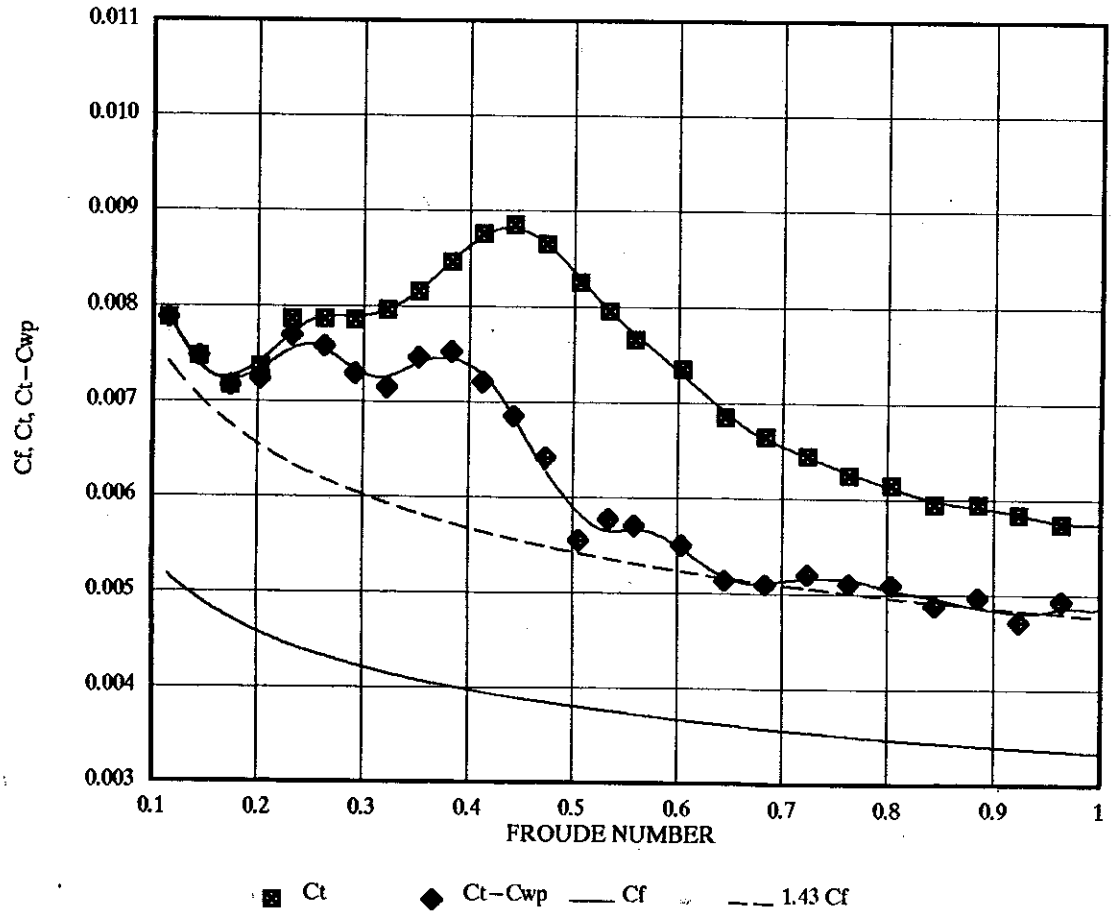

FIGURE 14 RESISTANCE COMPONENTS 5e MONOHULL

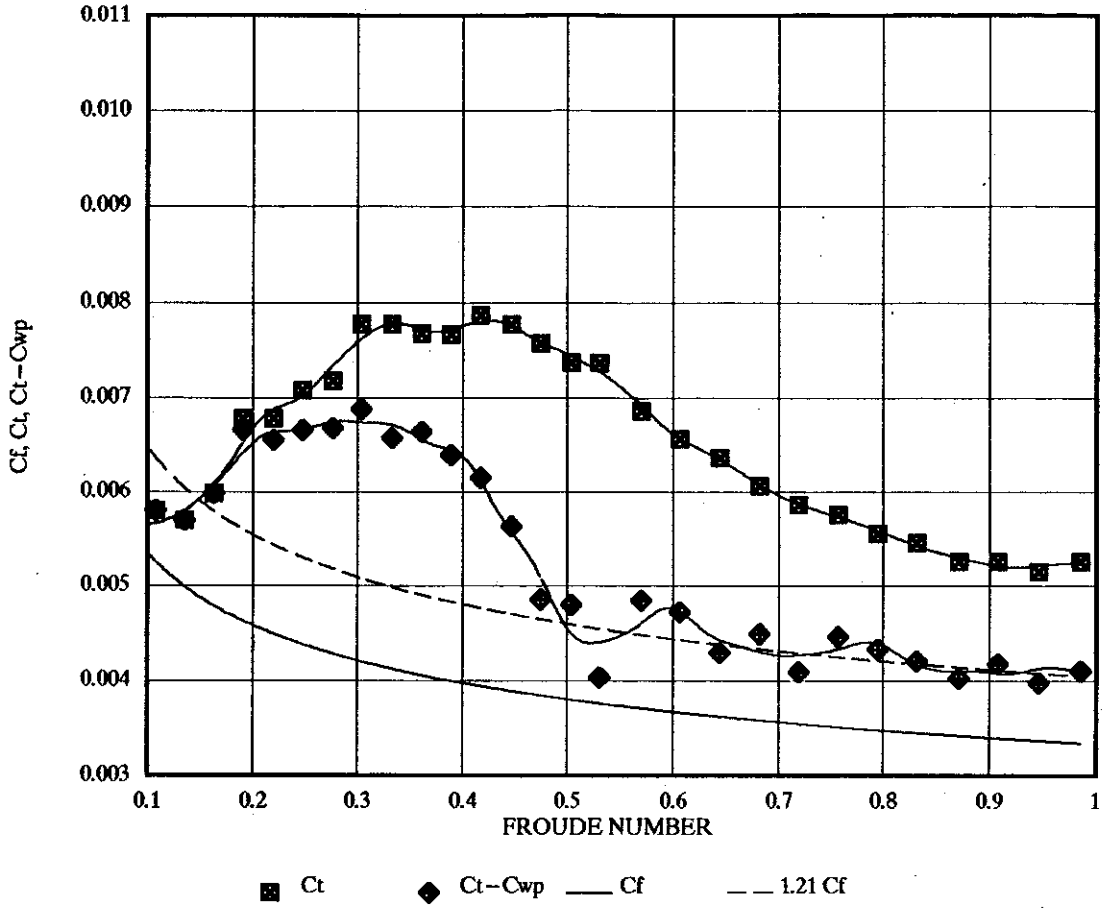

FIGURE 15 RESISTANCE COMPONENTS 5e S/L 0.2

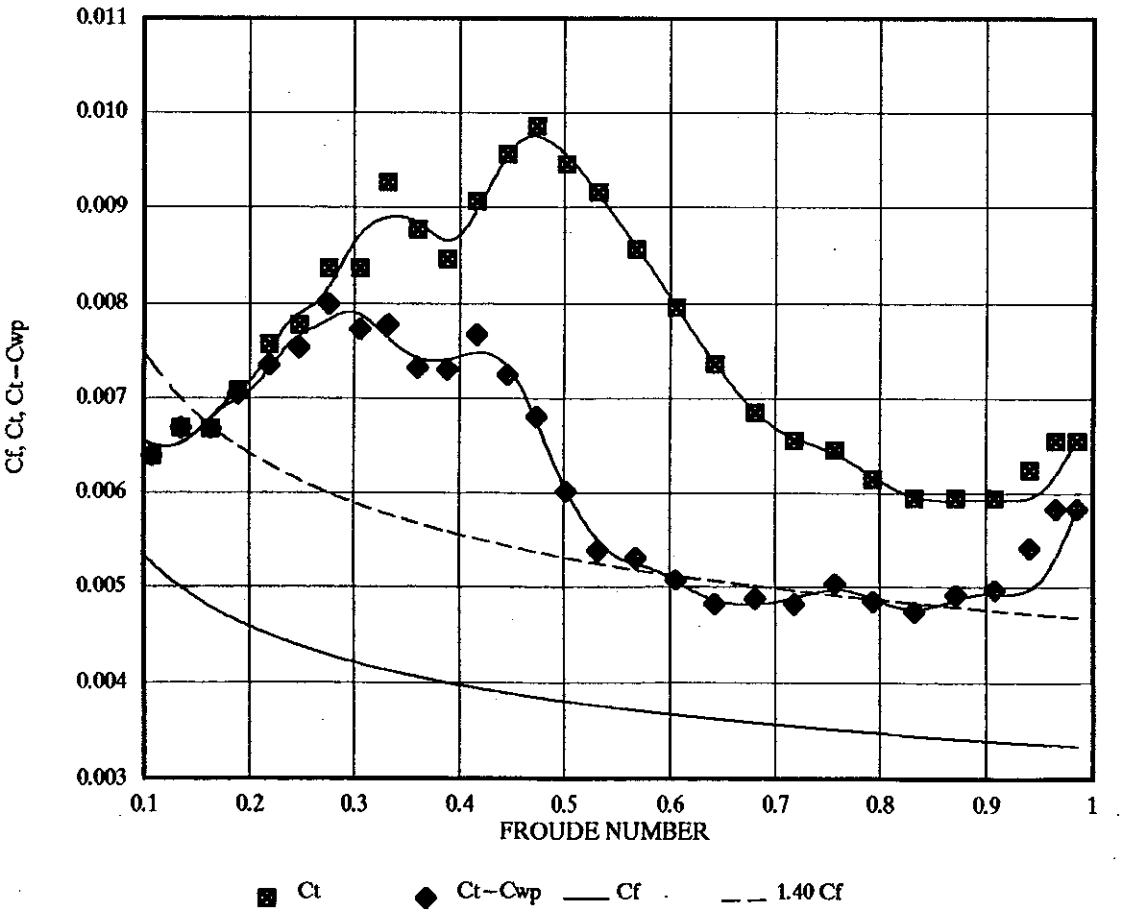

FIGURE 16 RESISTANCE COMPONENTS 5e S/L 0.3

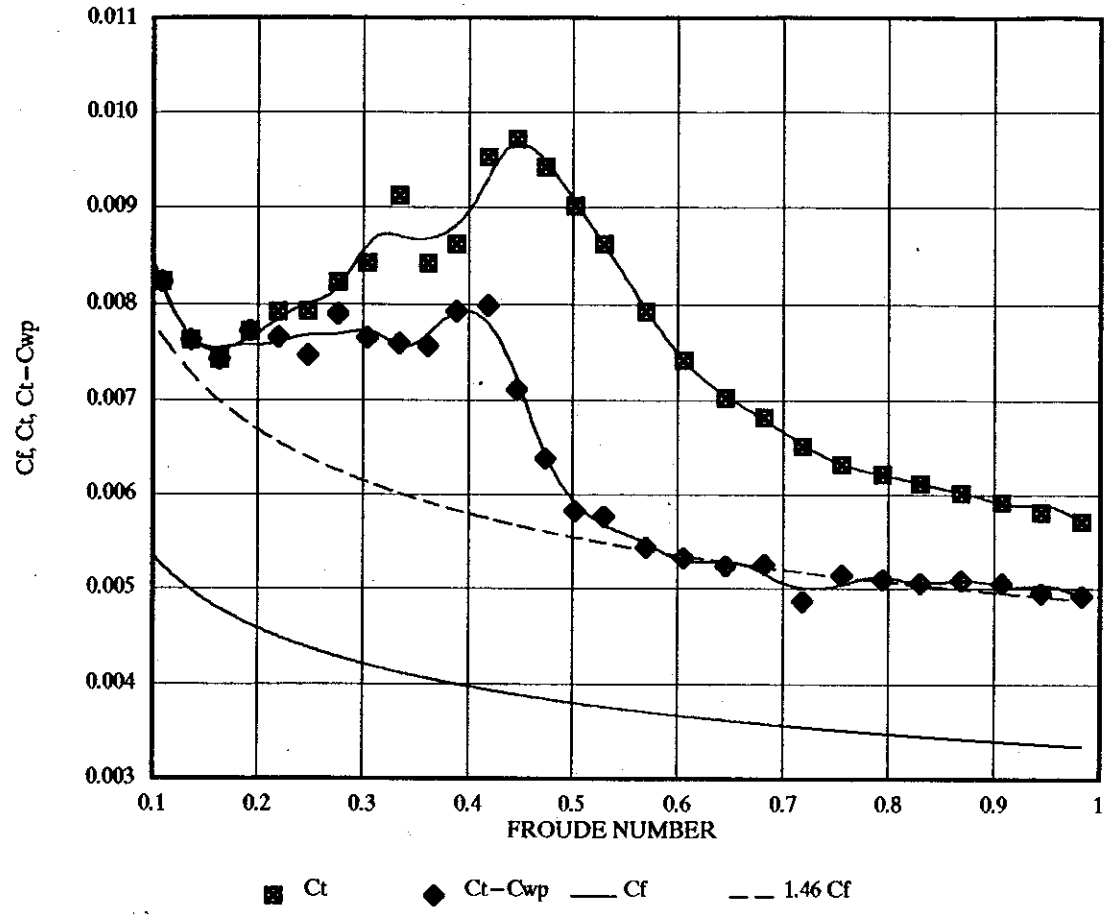

FIGURE 17 RESISTANCE COMPONENTS 5e S/L 0.4

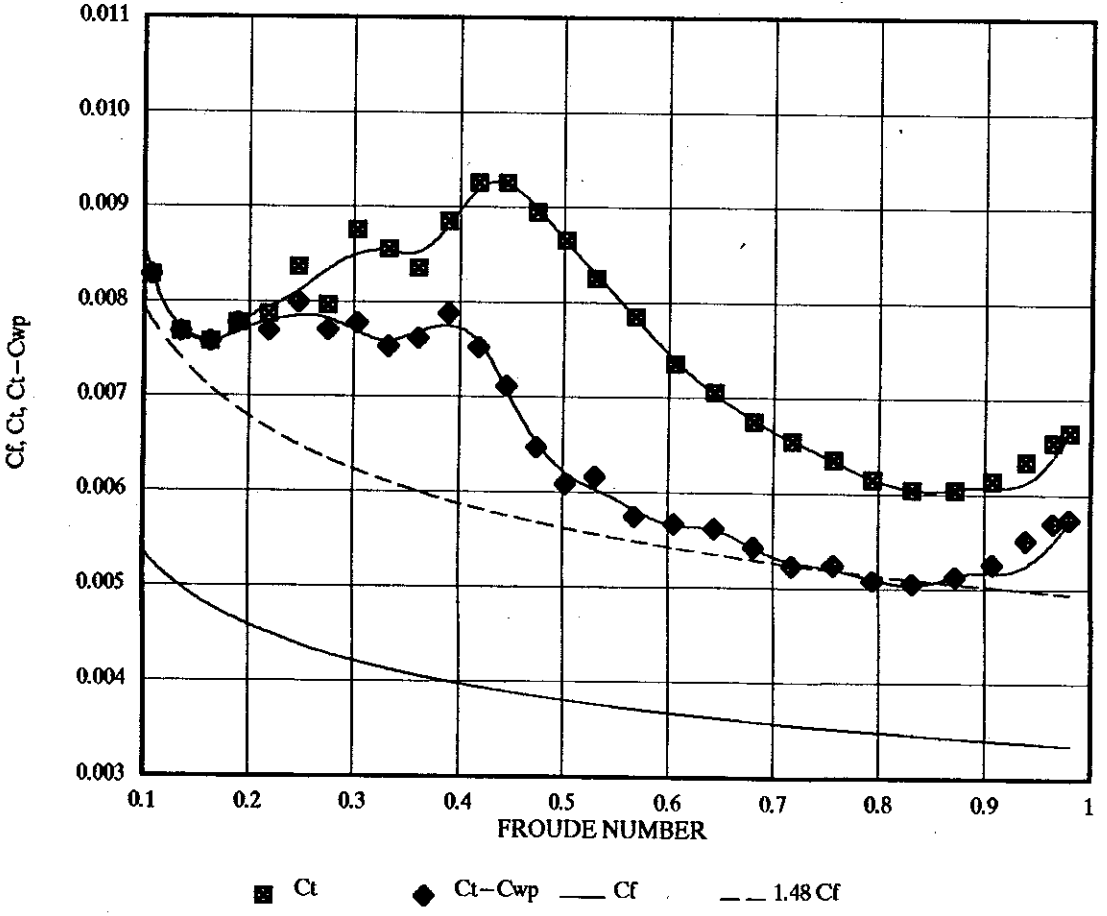

FIGURE 18 RESISTANCE COMPONENTS 5e S/L 0.5

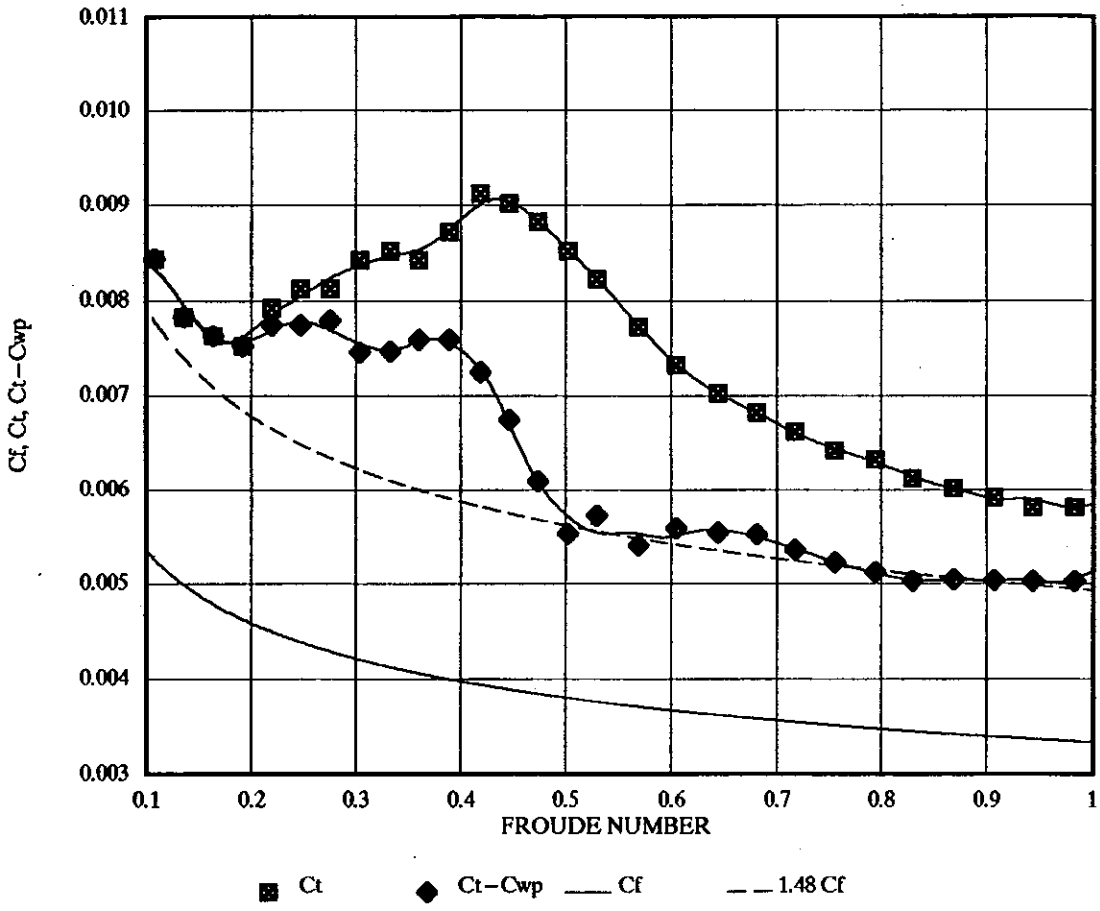

FIGURE 19 RESISTANCE COMPONENTS 4b MONOHULL
LIGHT DISPLACEMENT

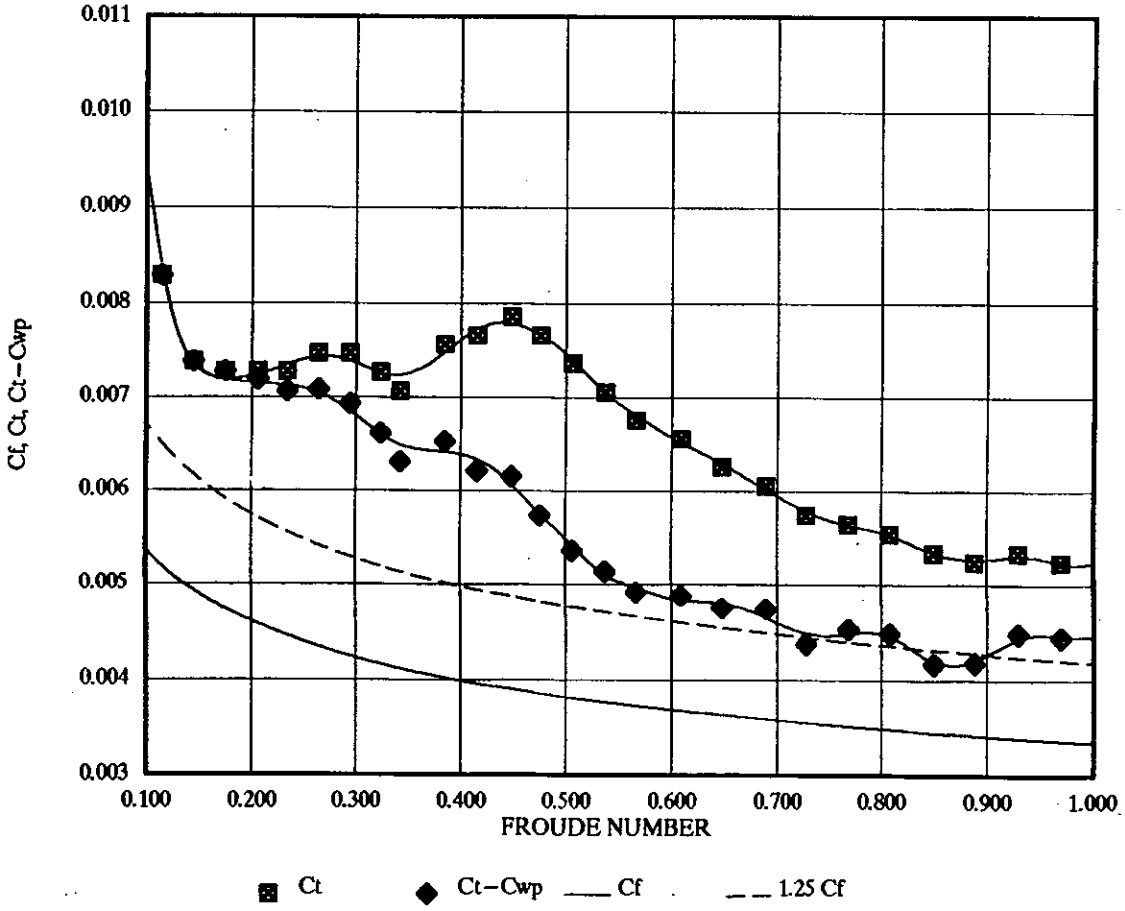

FIGURE 20

RESISTANCE COMPONENTS 4b S/L 0.3
LIGHT DISPLACEMENT

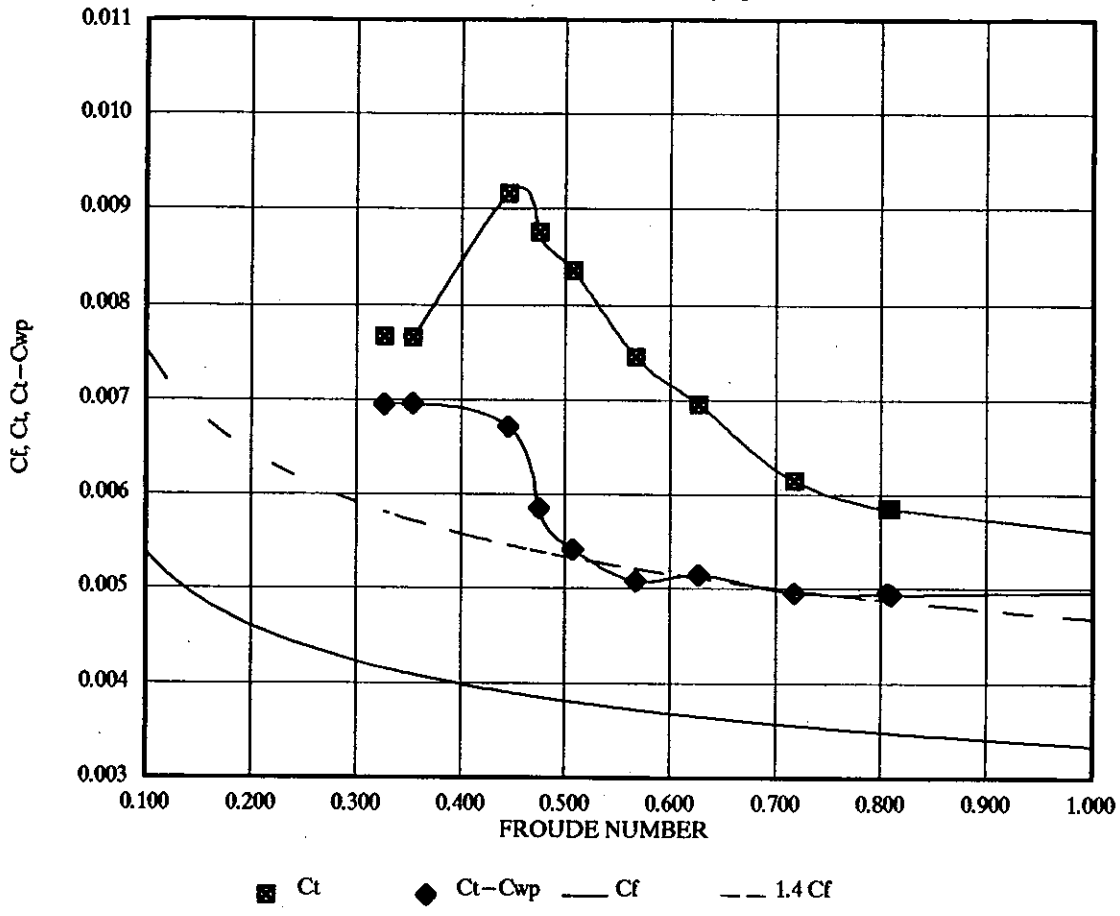

FIGURE 21

RESISTANCE COMPONENTS 4b S/L 0.5
LIGHT DISPLACEMENT

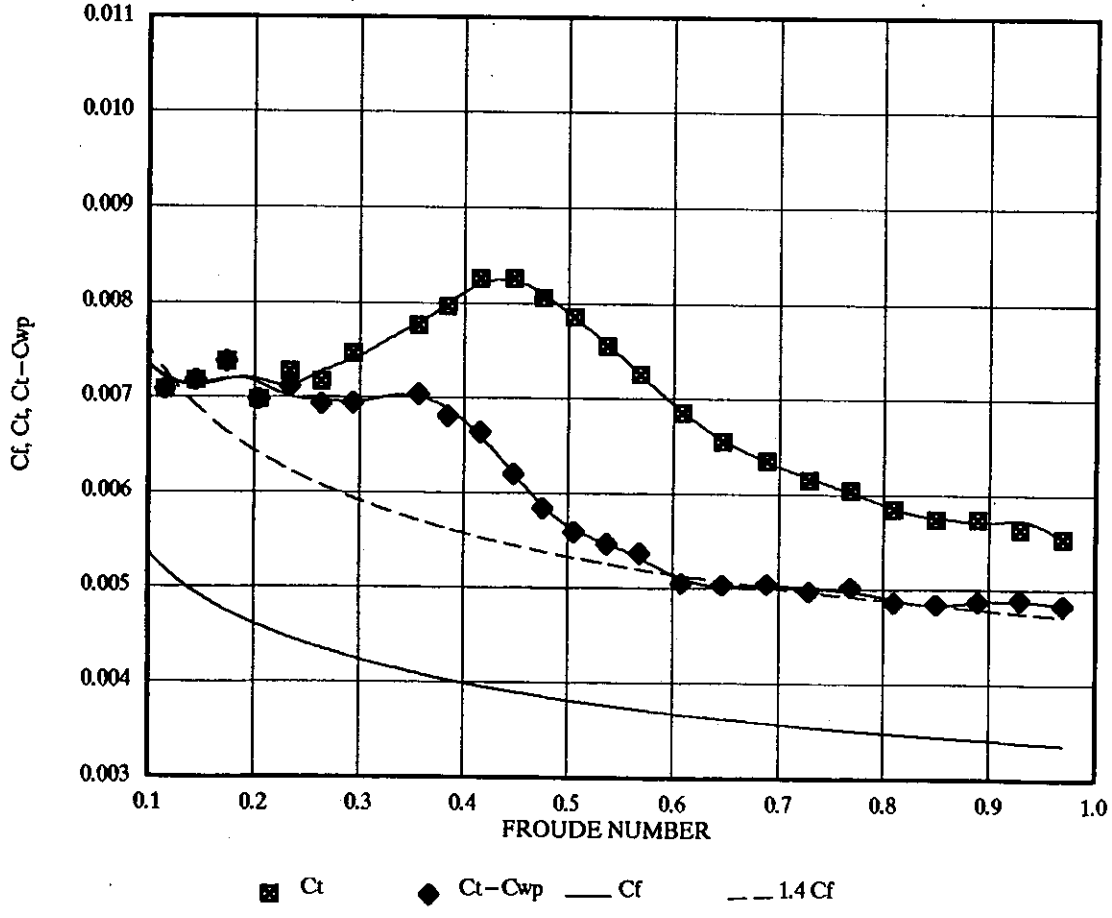

FIGURE 22

5d RUNNING TRIM

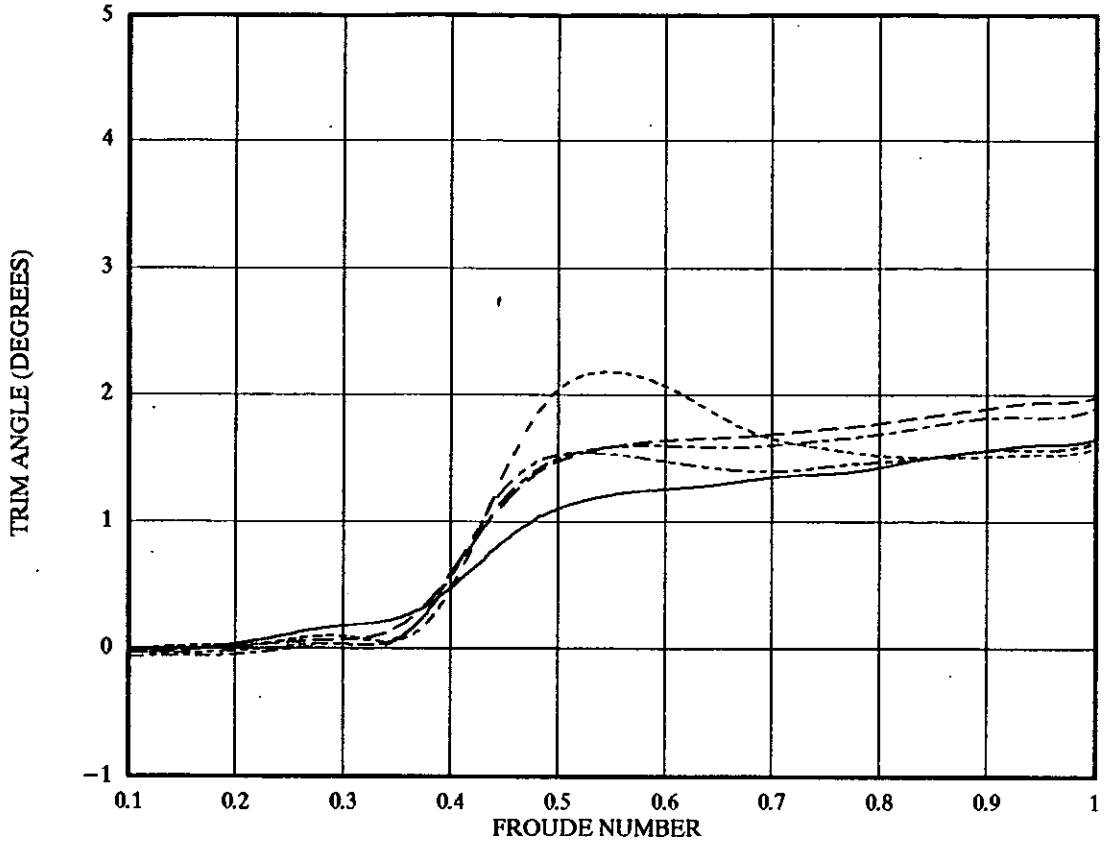

FIGURE 23

5b RUNNING TRIM

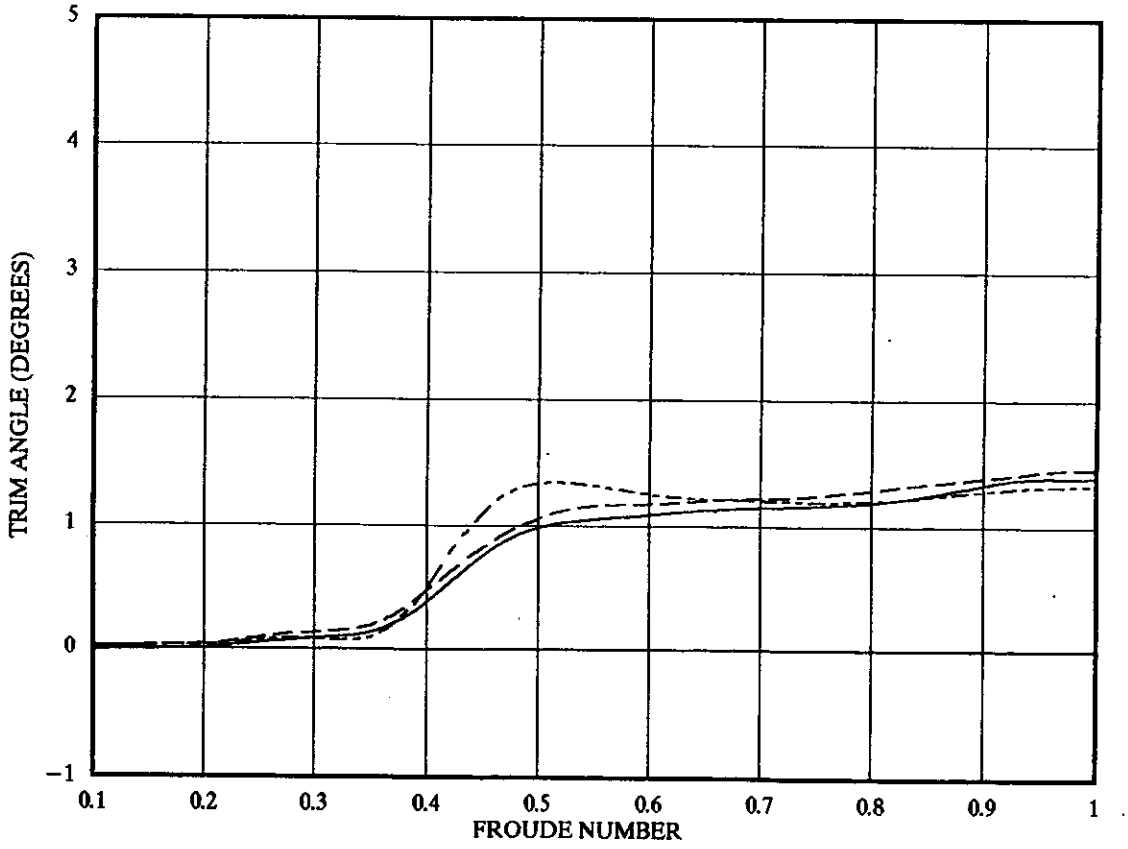

FIGURE 24 5e RUNNING TRIM

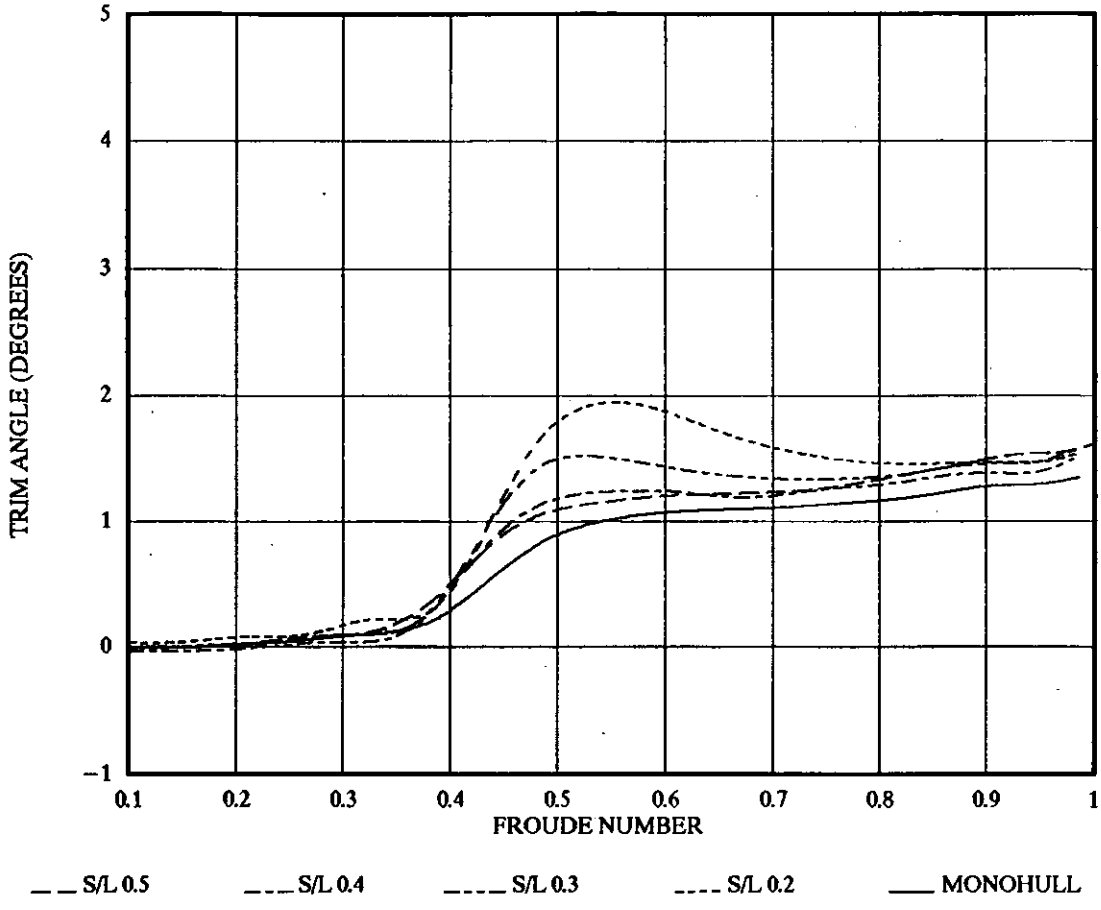

FIGURE 25 RUNNING TRIM MONOHULL
5b, 5d, 5e

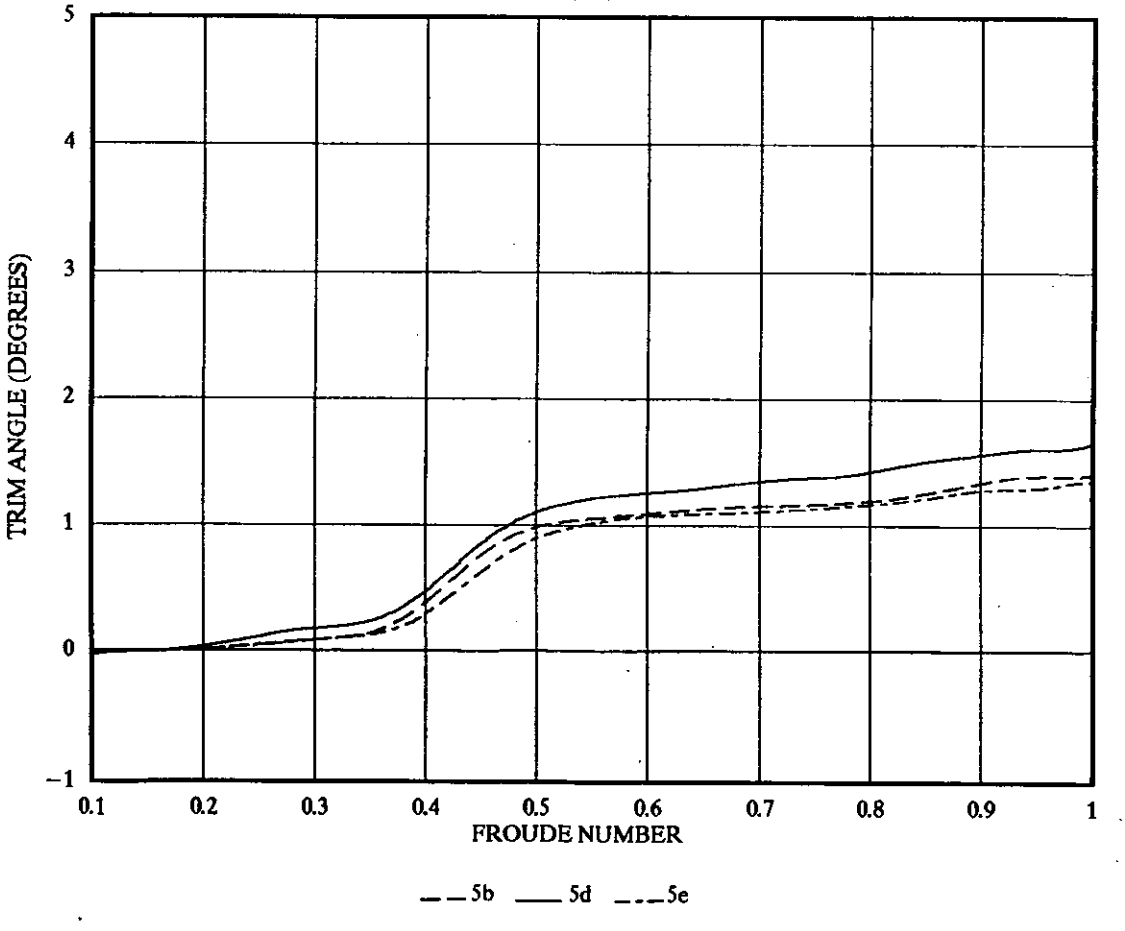

FIGURE 26

RUNNING TRIM FOR S/L 0.2
5d, 5e

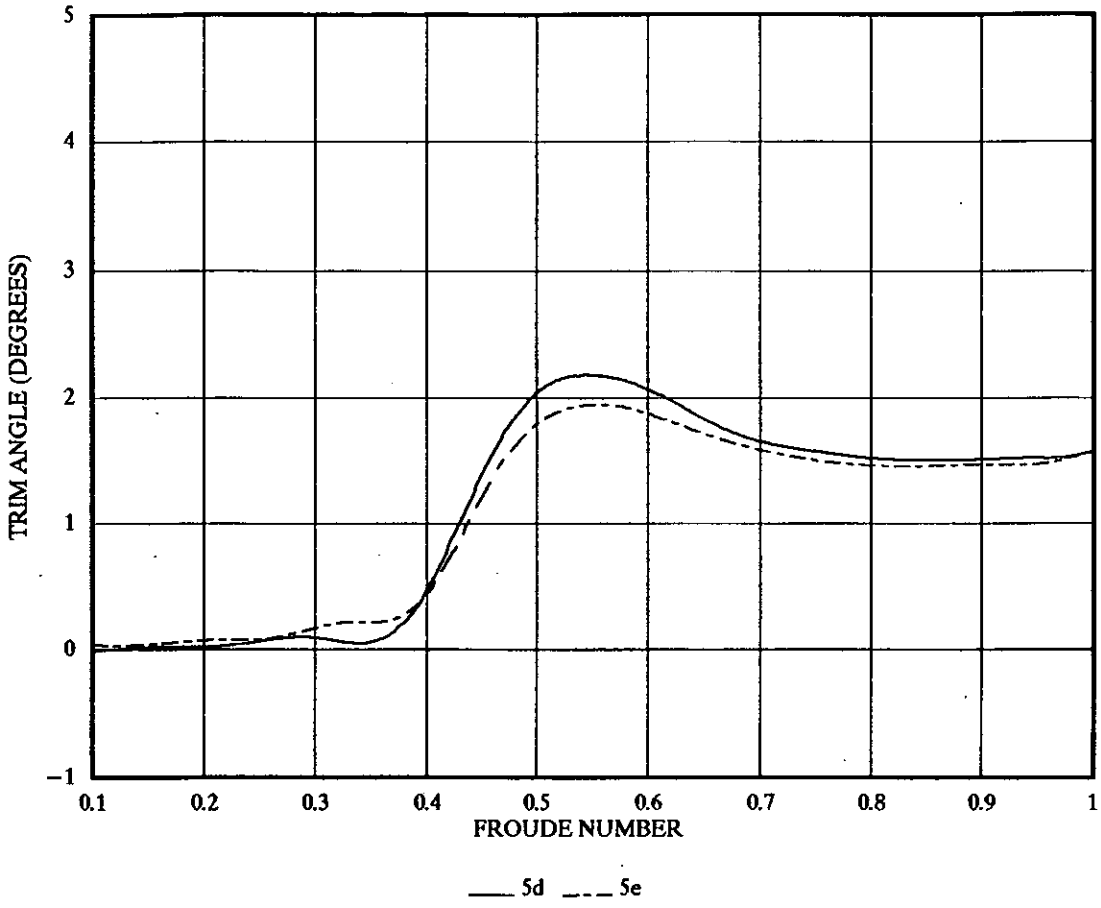

FIGURE 27

RUNNING TRIM FOR S/L 0.3
5b, 5d, 5e

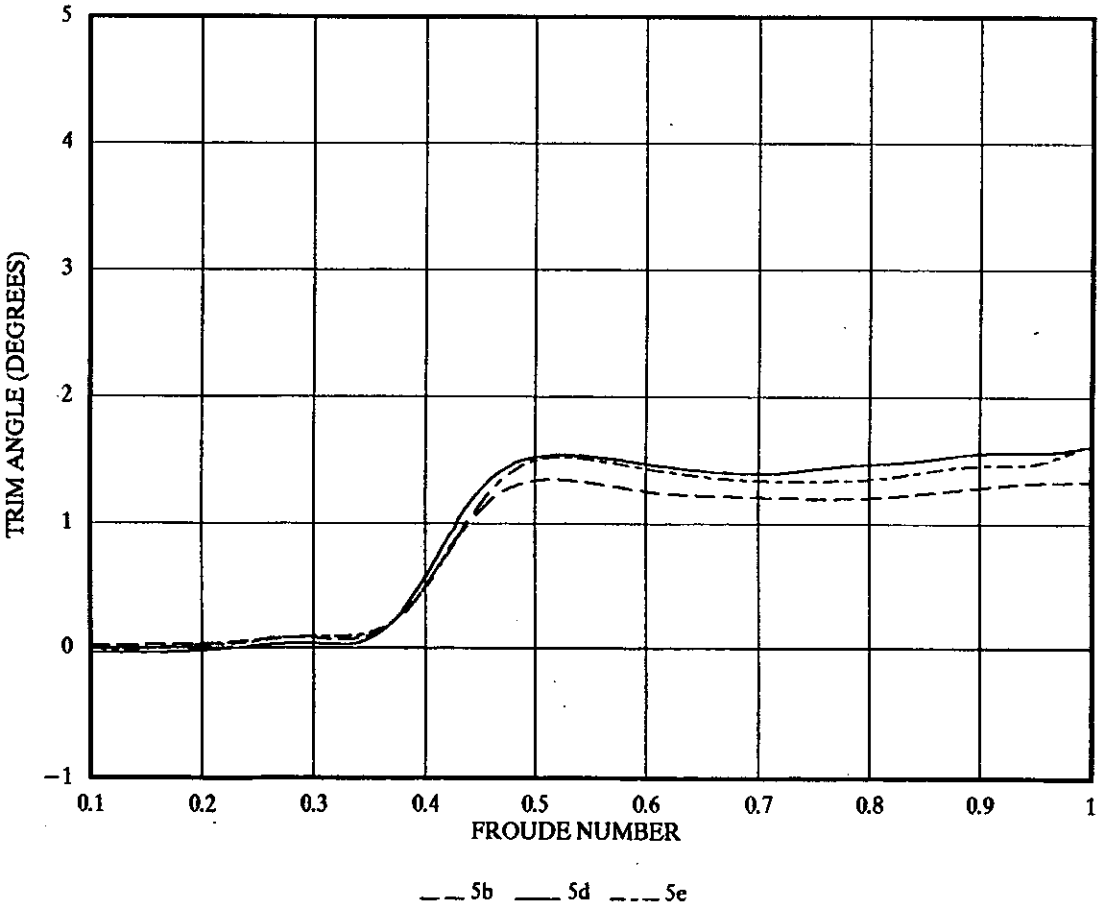

FIGURE 28

RUNNING TRIM FOR S/L 0.4
5d, 5e

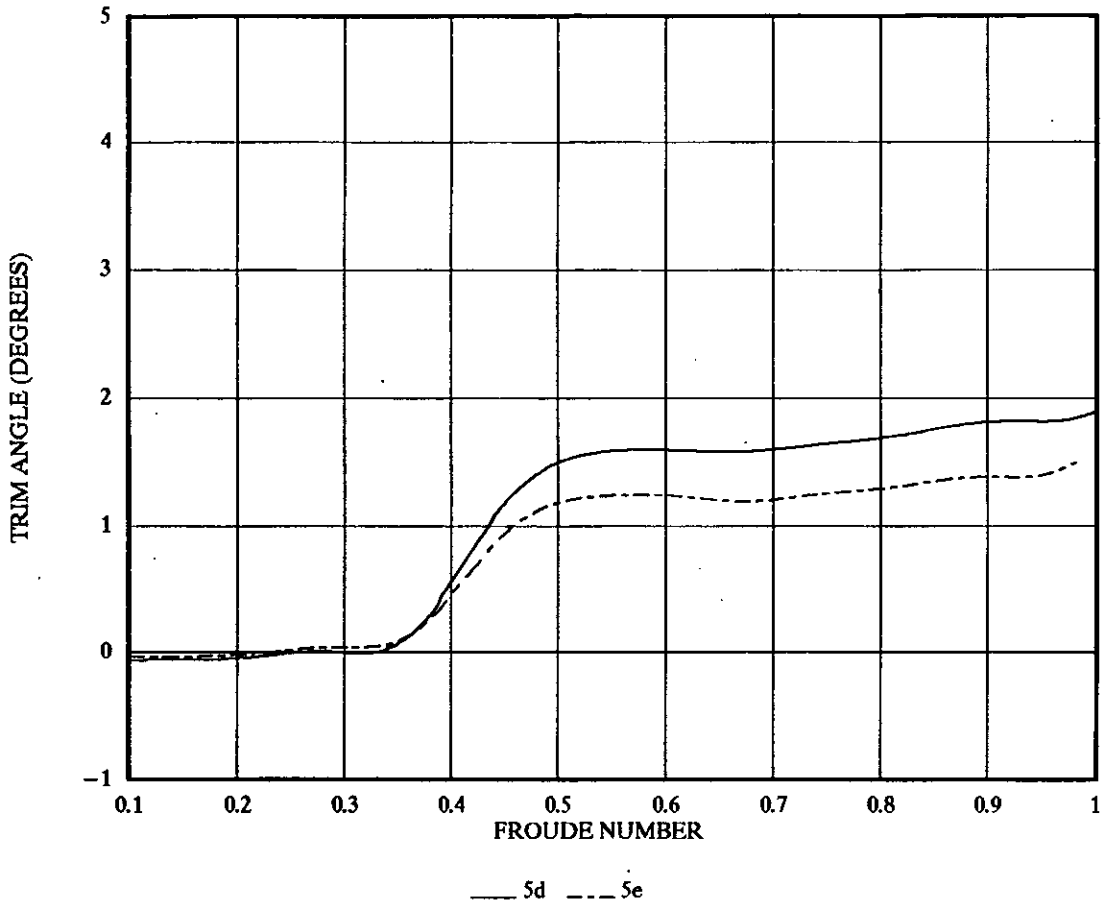

FIGURE 29

RUNNING TRIM S/L 0.5
5b, 5d, 5e

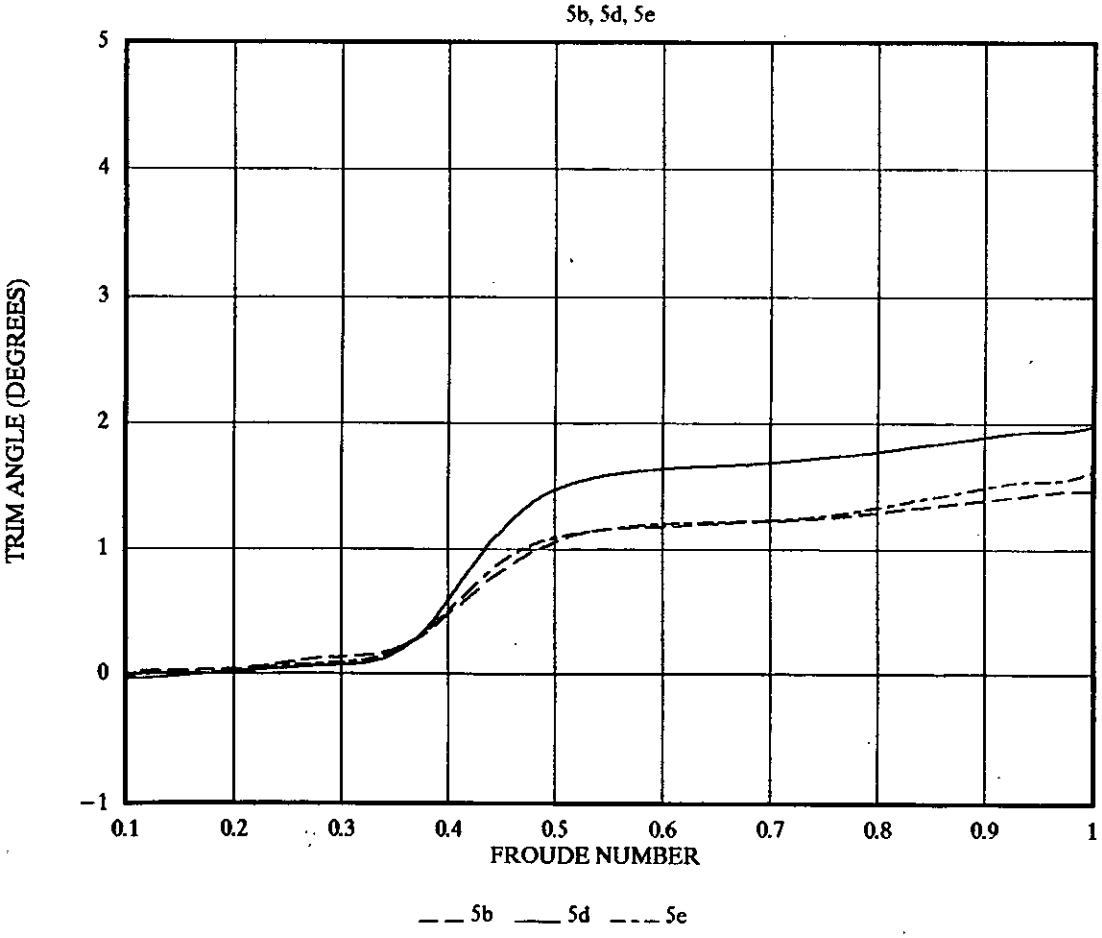

FIGURE 30

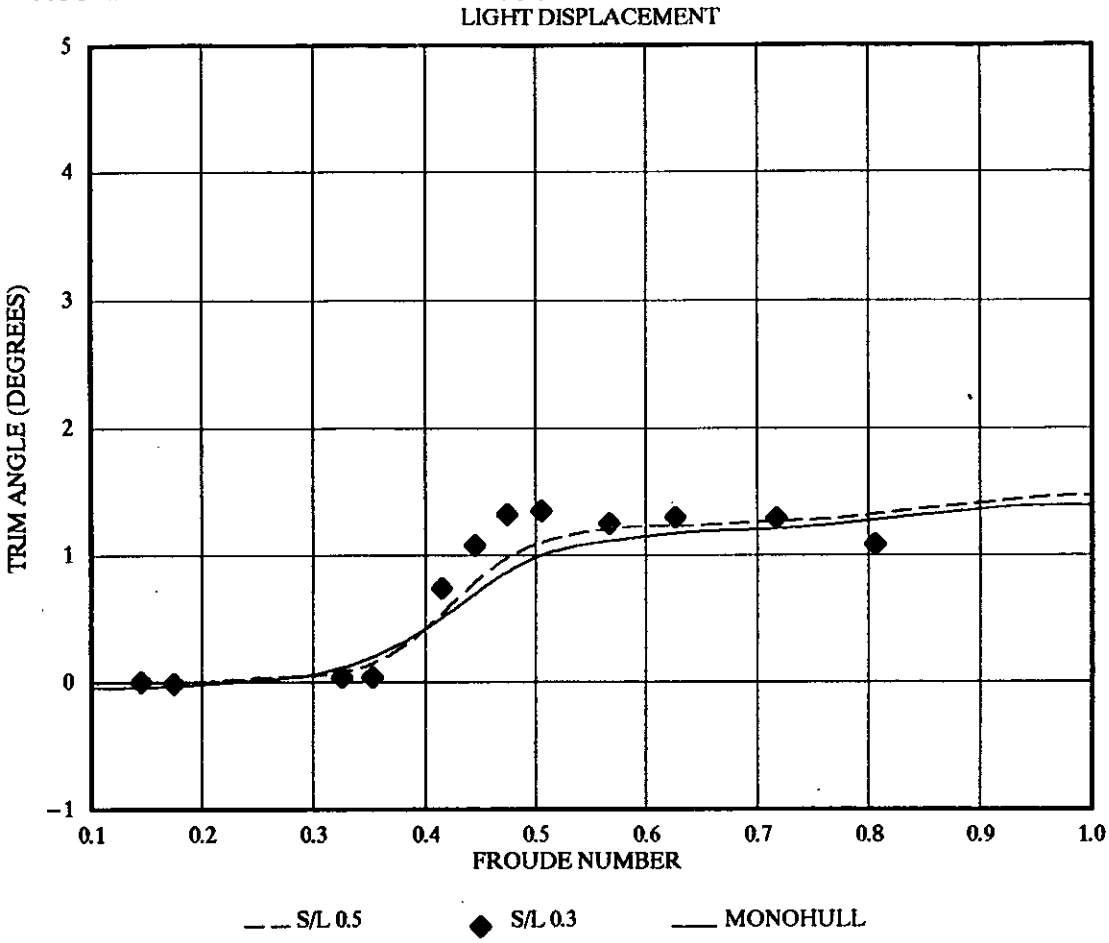
4b RUNNING TRIM
LIGHT DISPLACEMENT
TRIM ANGLE (DEGREES)
5
4
3
2
1
0
−1
0.1
0.2
0.3
0.4
0.5
0.6
0.7
0.8
0.9
1.0
FROUDE NUMBER
S/L 0.5
S/L 0.3
MONOHULL

FIGURE 31

5d SINKAGE

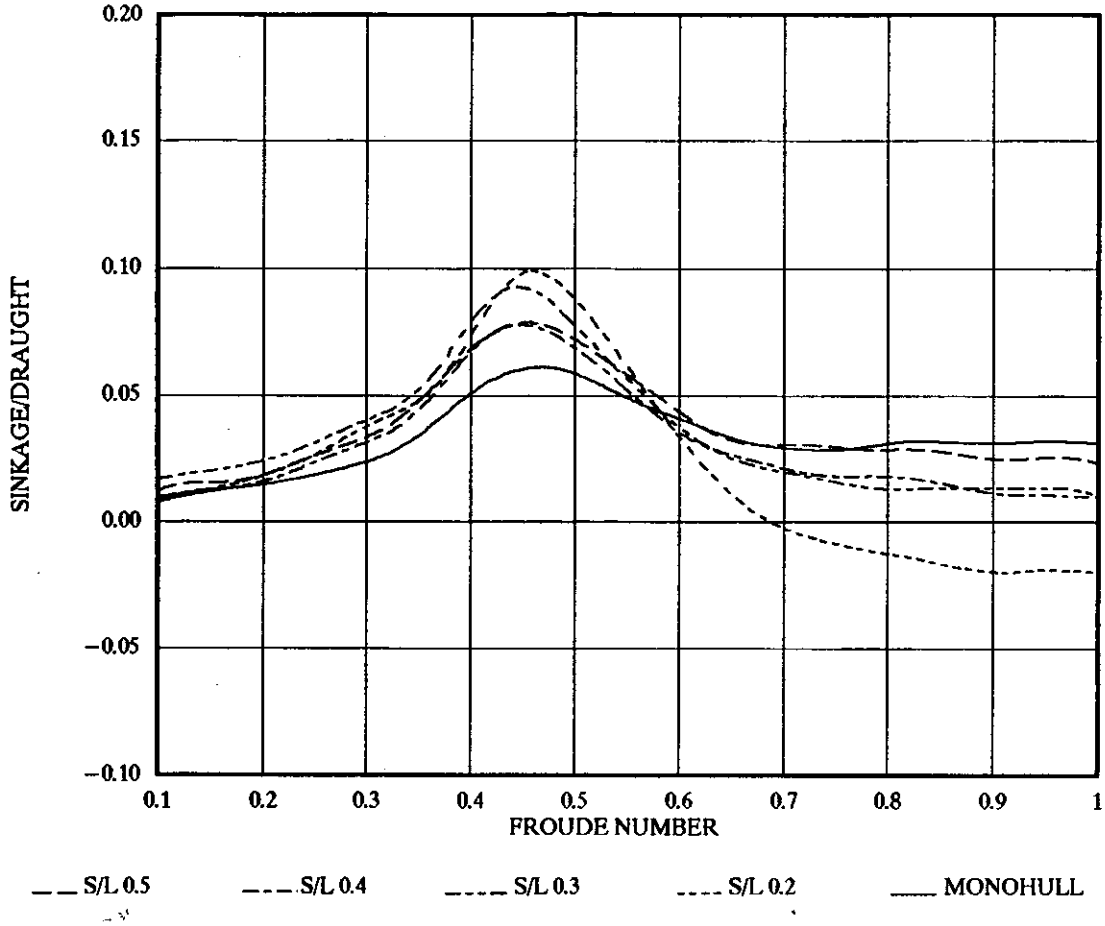

FIGURE 32

5b SINKAGE

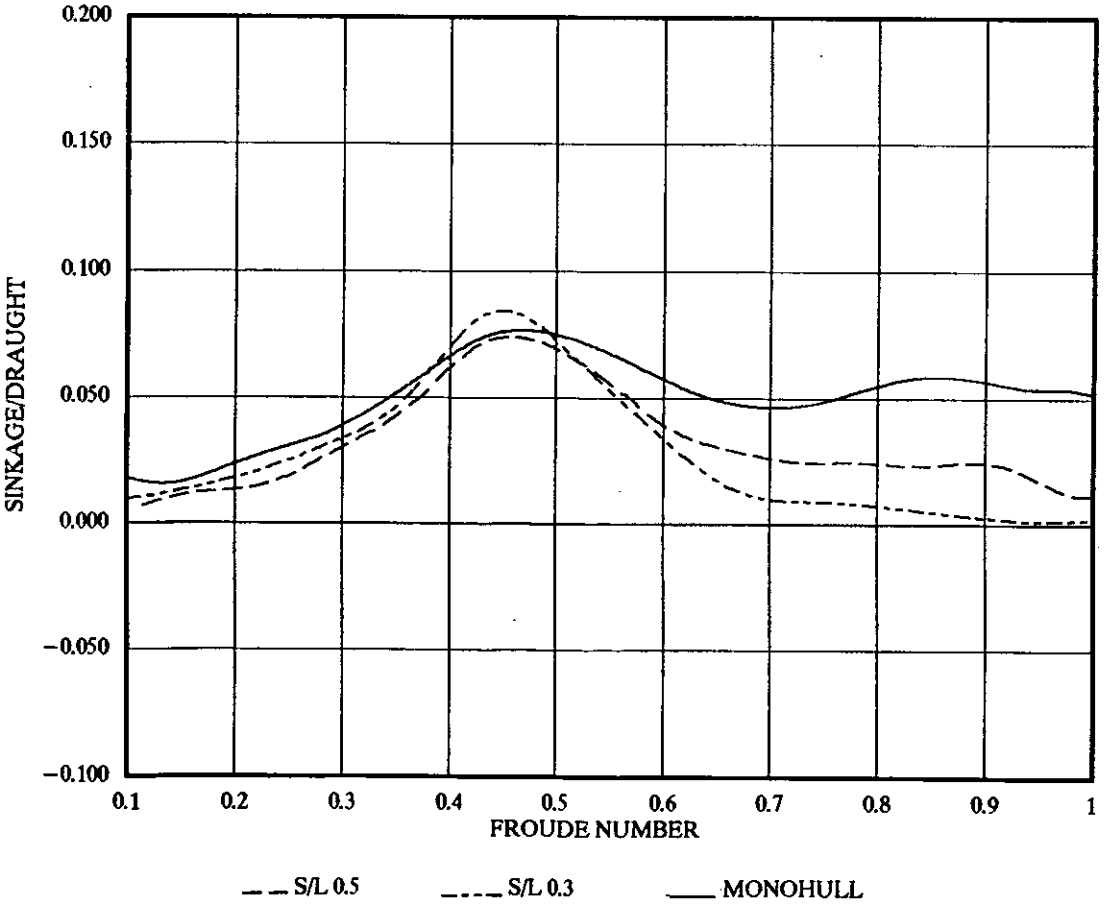

FIGURE 33 5e SINKAGE

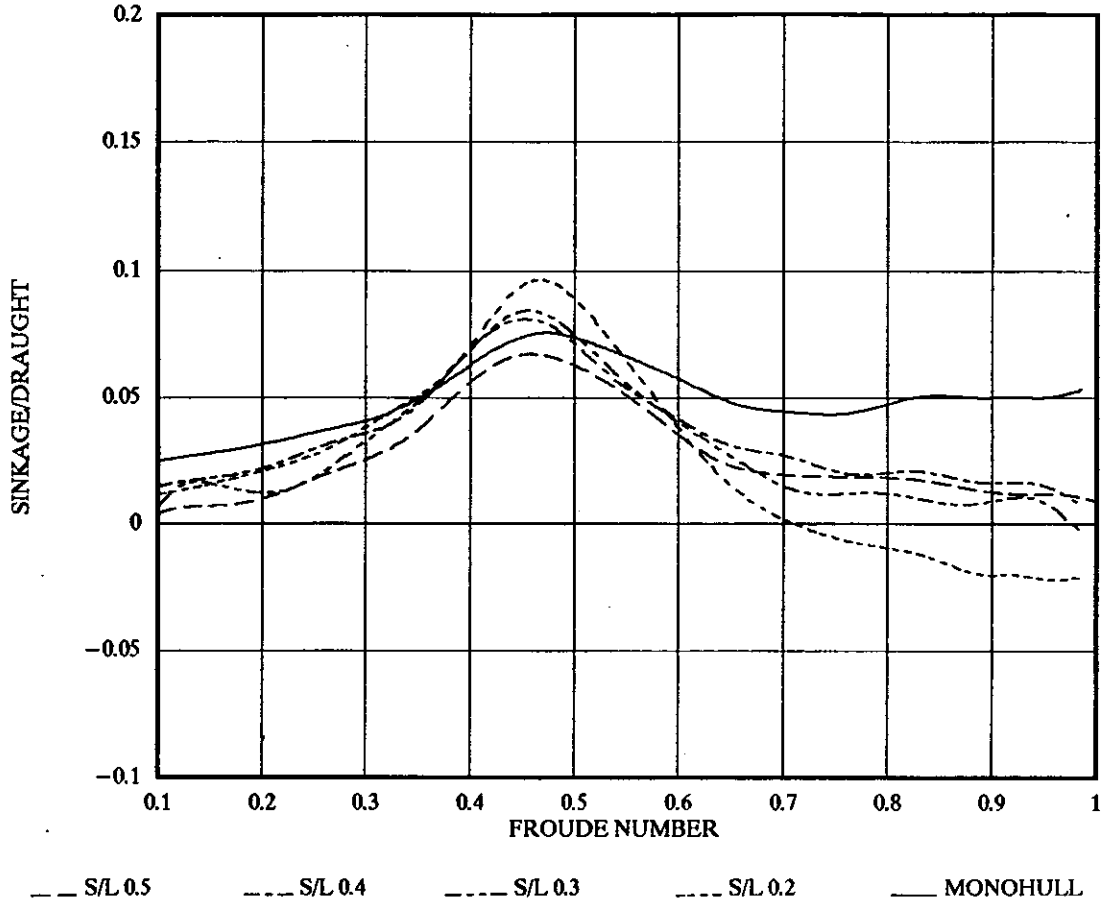

FIGURE 34 SINKAGE FOR MONOHULL
5b, 5d, 5e

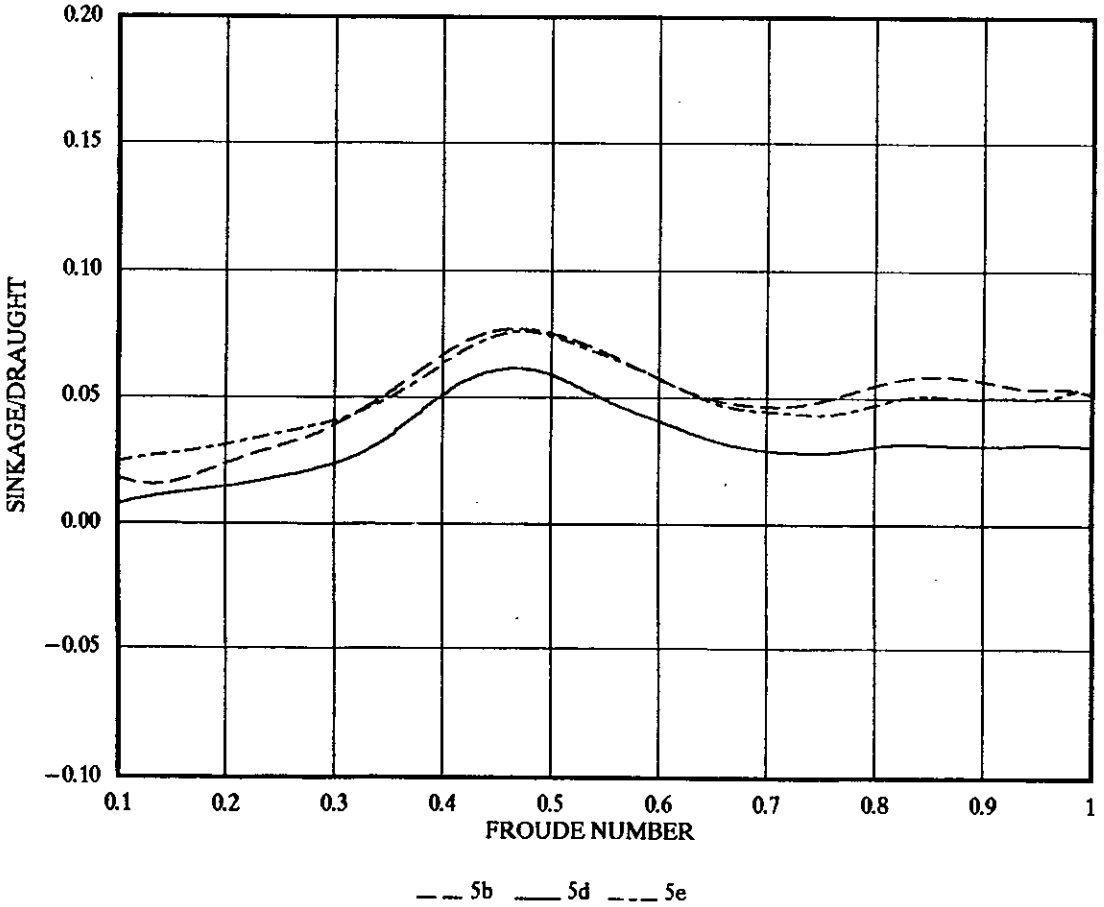

FIGURE 35

SINKAGE FOR S/L 0.2
5d, 5e

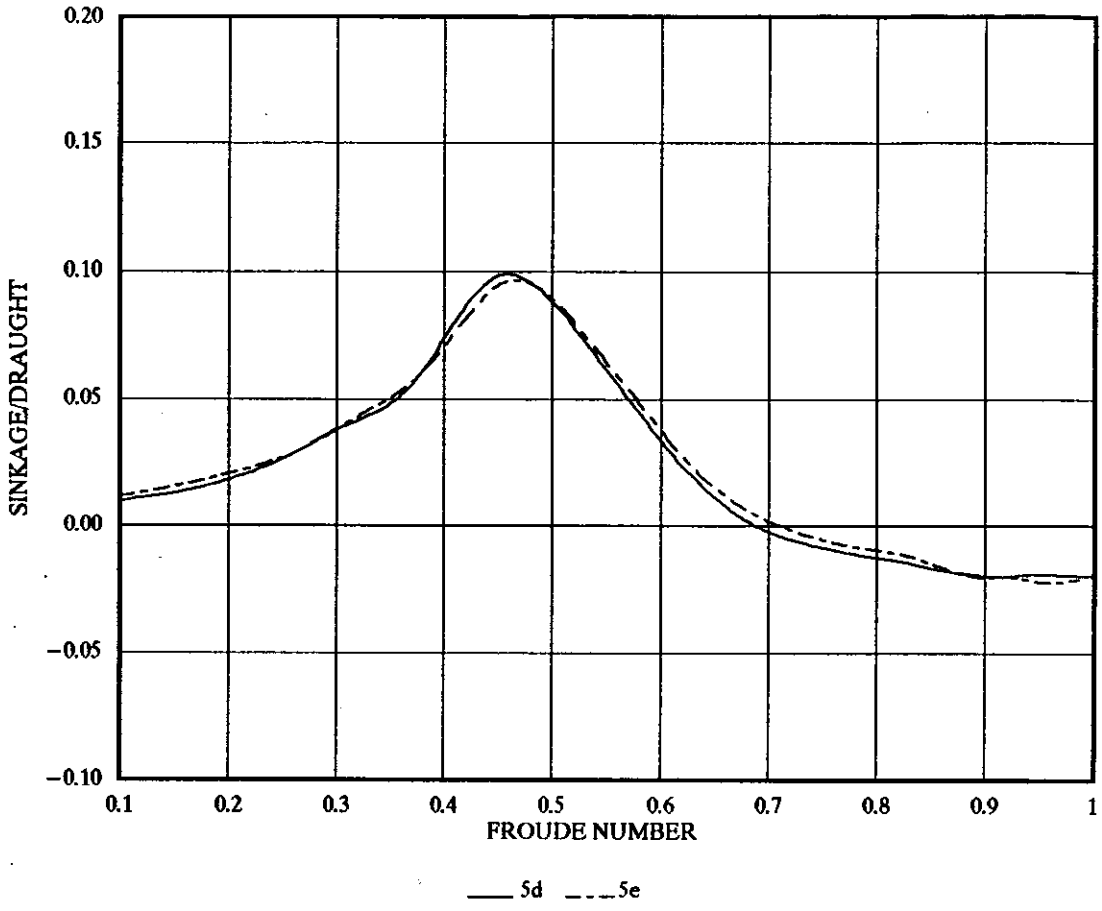

FIGURE 36

SINKAGE FOR S/L 0.3
5b, 5d, 5e

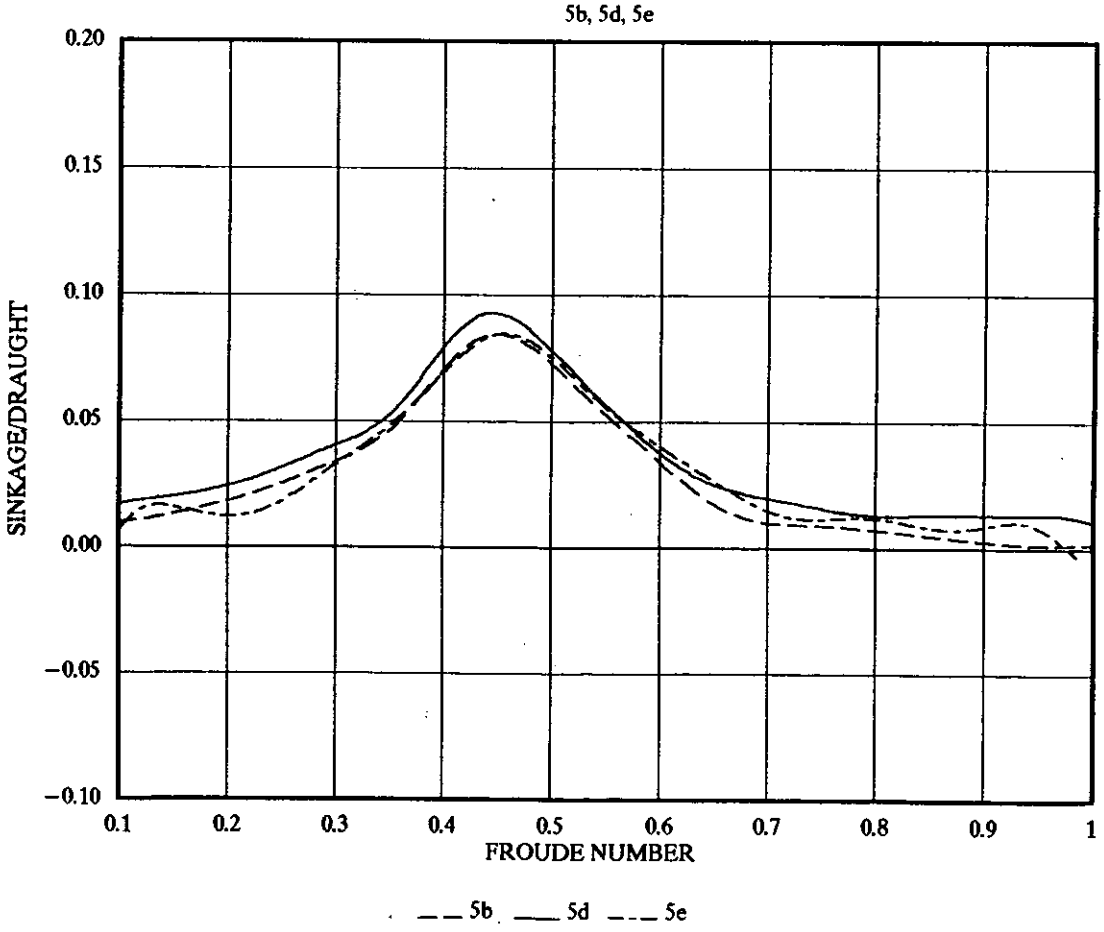

FIGURE 37

SINKAGE FOR S/L 0.4
5d, 5e

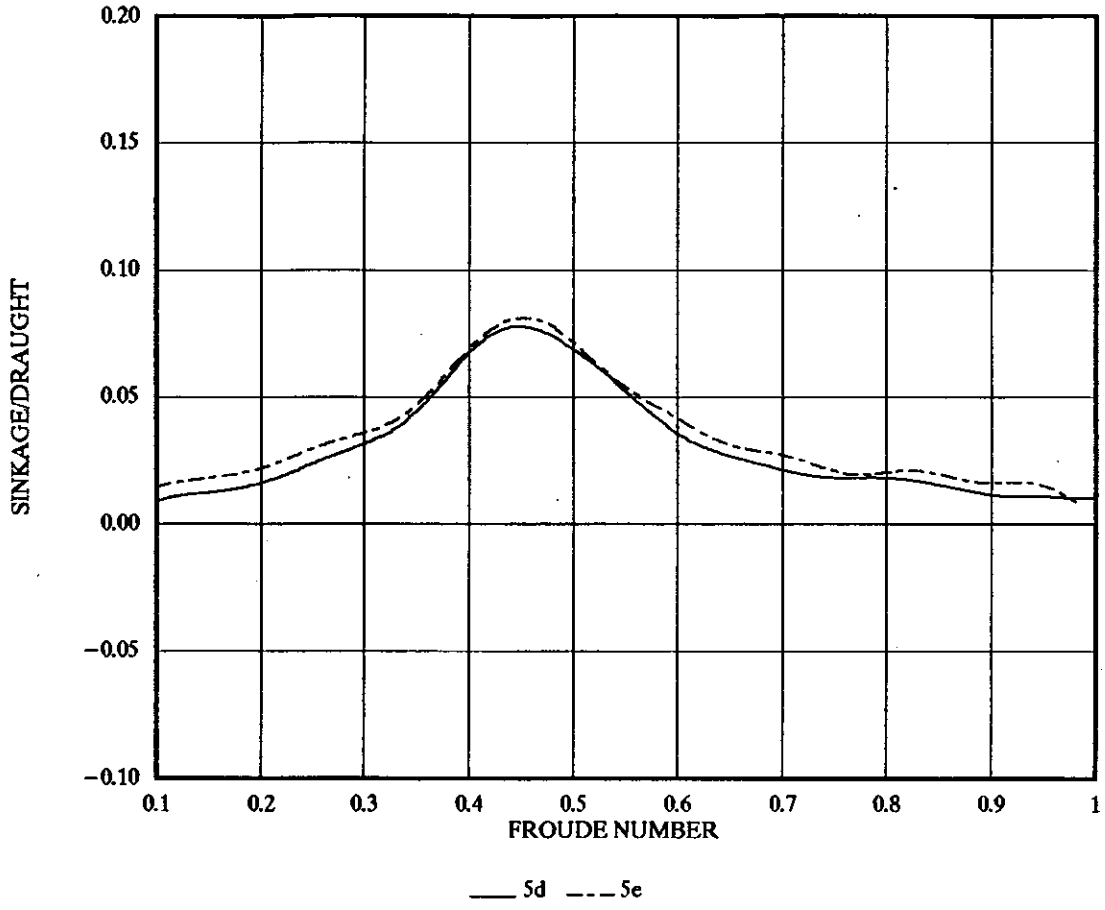

FIGURE 38

SINKAGE S/L 0.5
5b, 5d, 5e

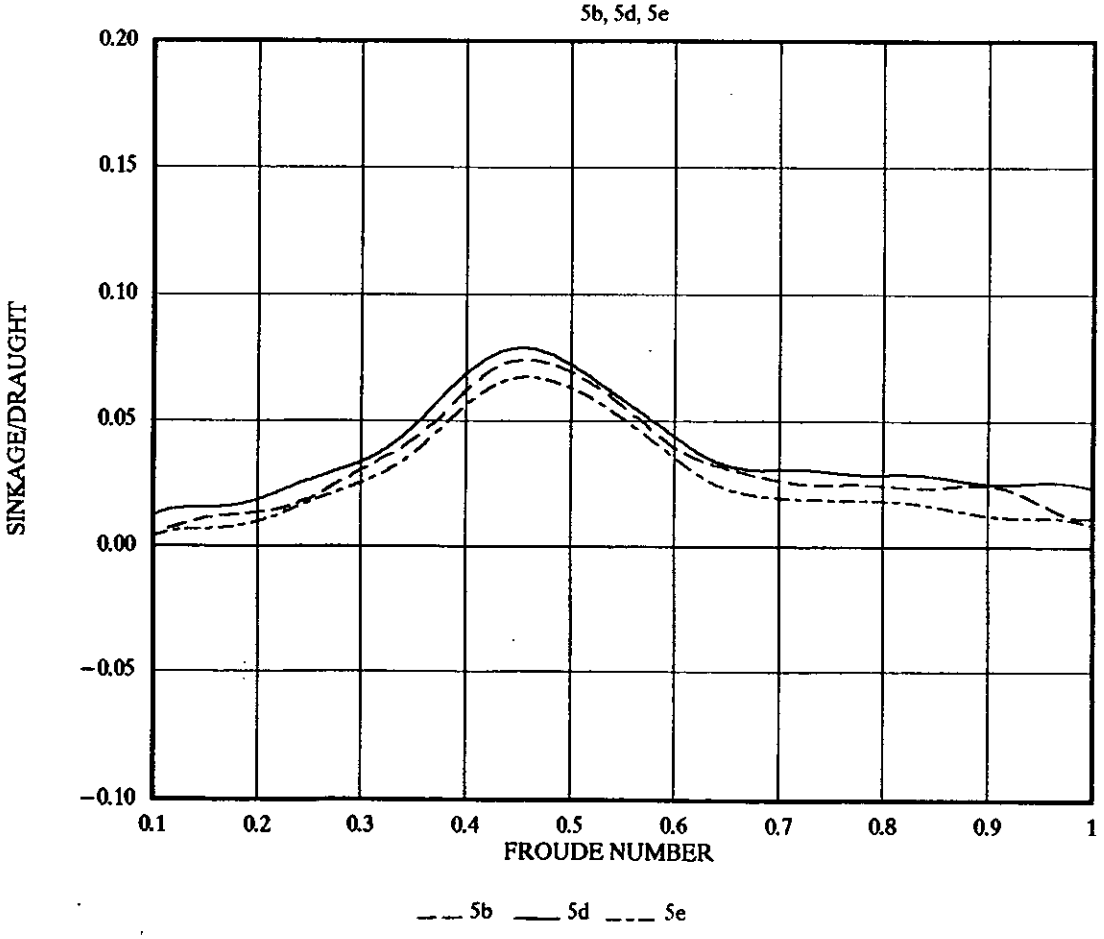

FIGURE 39

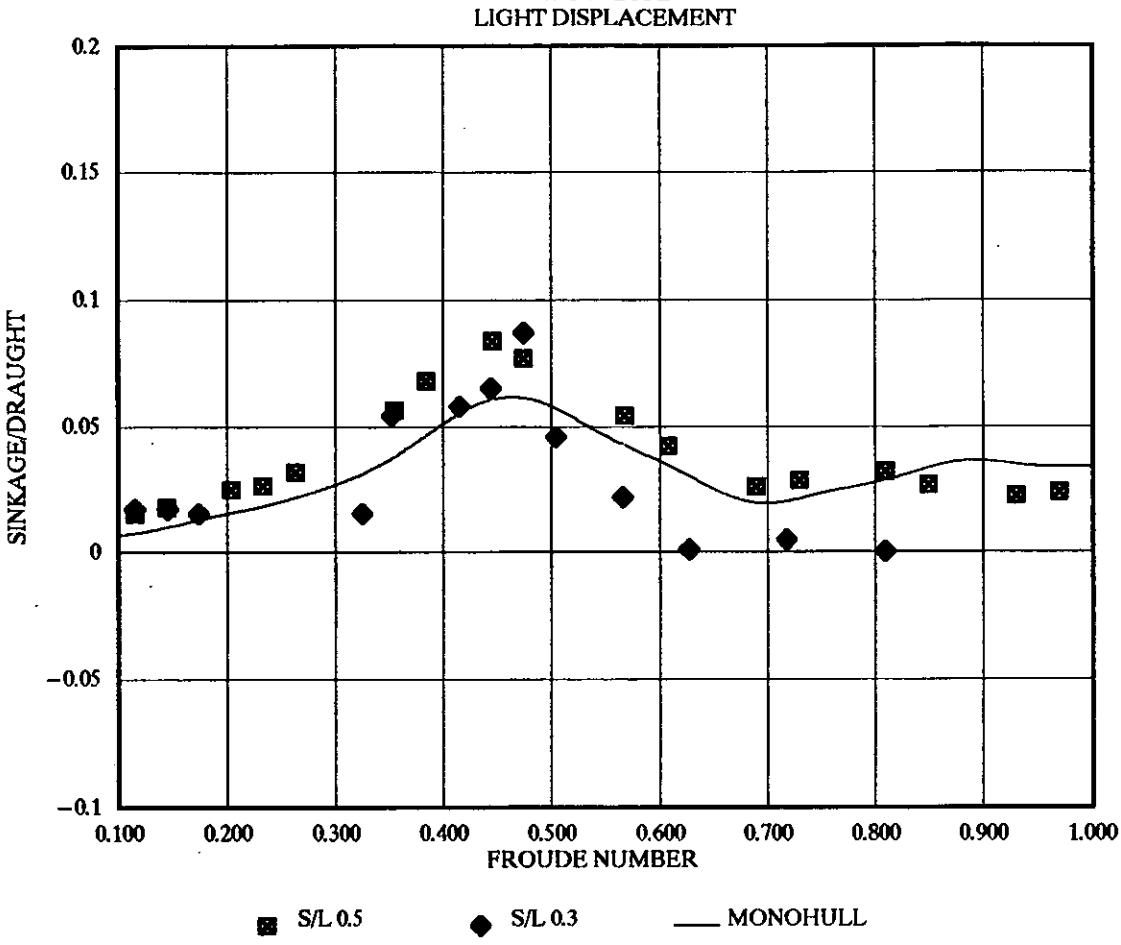
4b SINKAGE
LIGHT DISPLACEMENT
SINKAGE/DRAUGHT
0.2
0.15
0.1
0.05
0
−0.05
−0.1
0.100
0.200
0.300
0.400
0.500
0.600
0.700
0.800
0.900
1.000
FROUDE NUMBER
S/L 0.5
S/L 0.3
MONOHULL

FIGURE 40

RESIDUARY RESISTANCE Cr
5d

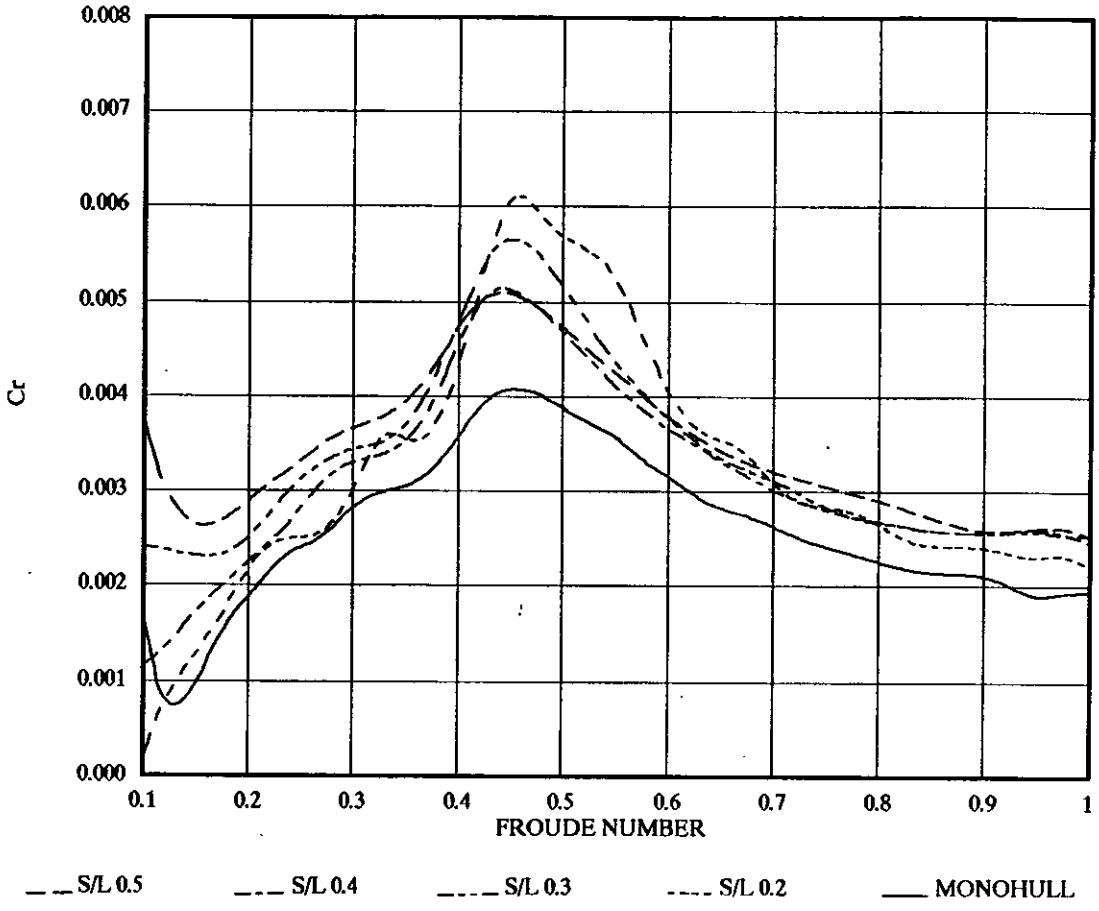

FIGURE 41

RESIDUARY RESISTANCE Cr FOR 5b

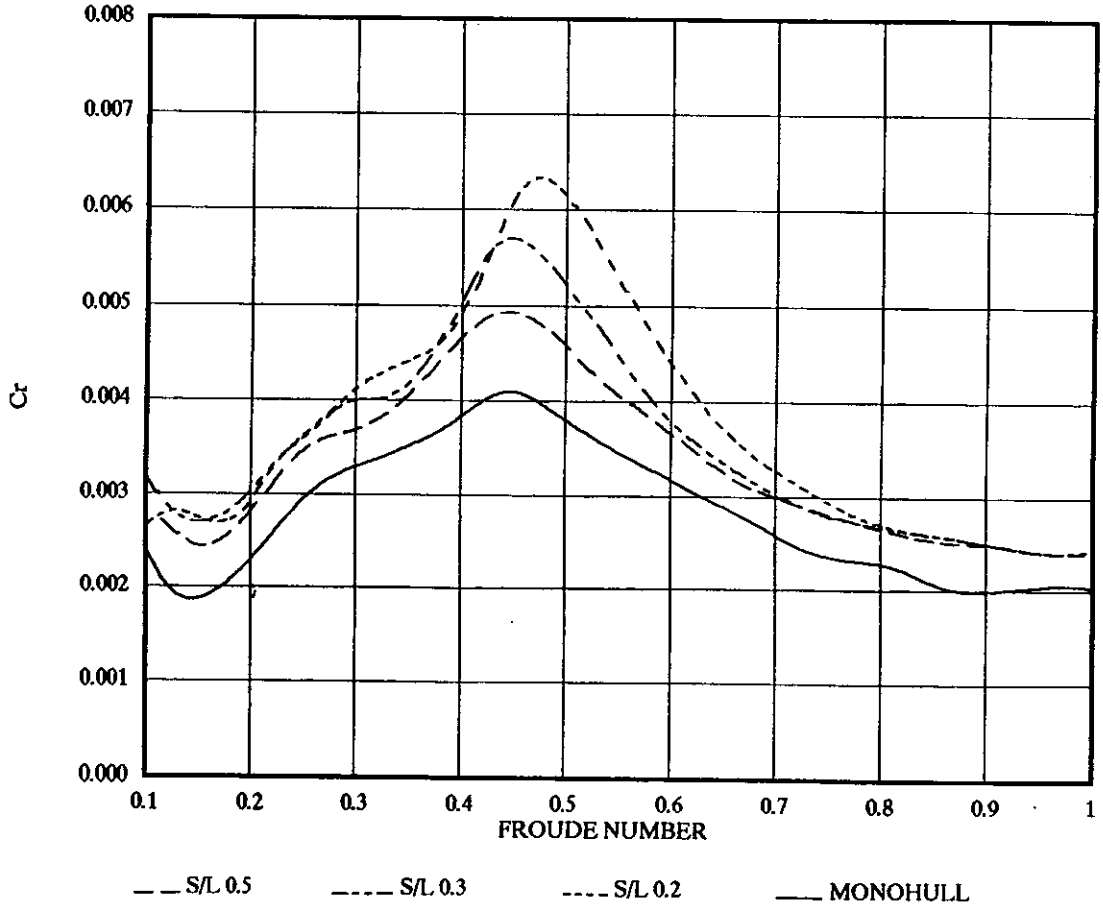

FIGURE 42

RESIDUARY RESISTANCE Cr
5e

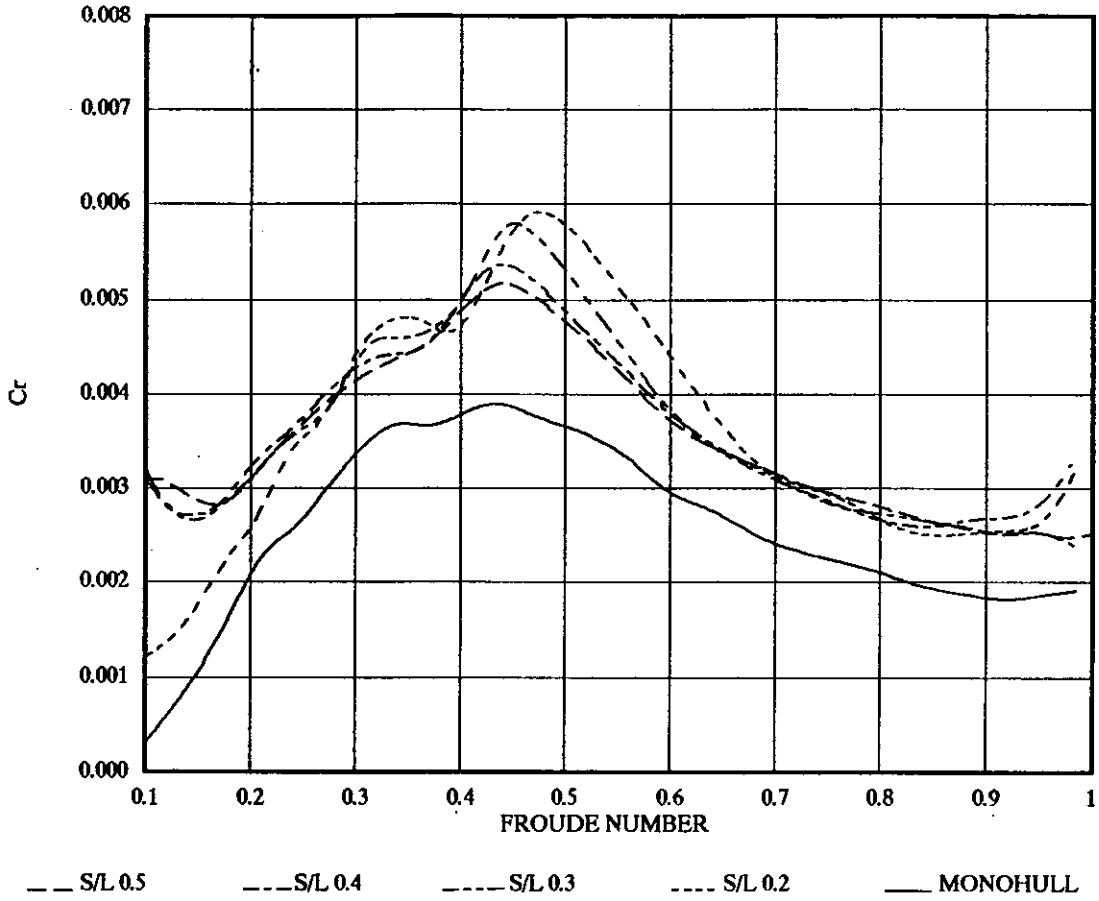

FIGURE 43

RESIDUARY RESISTANCE Cr
4b LIGHT DISPLACEMENT

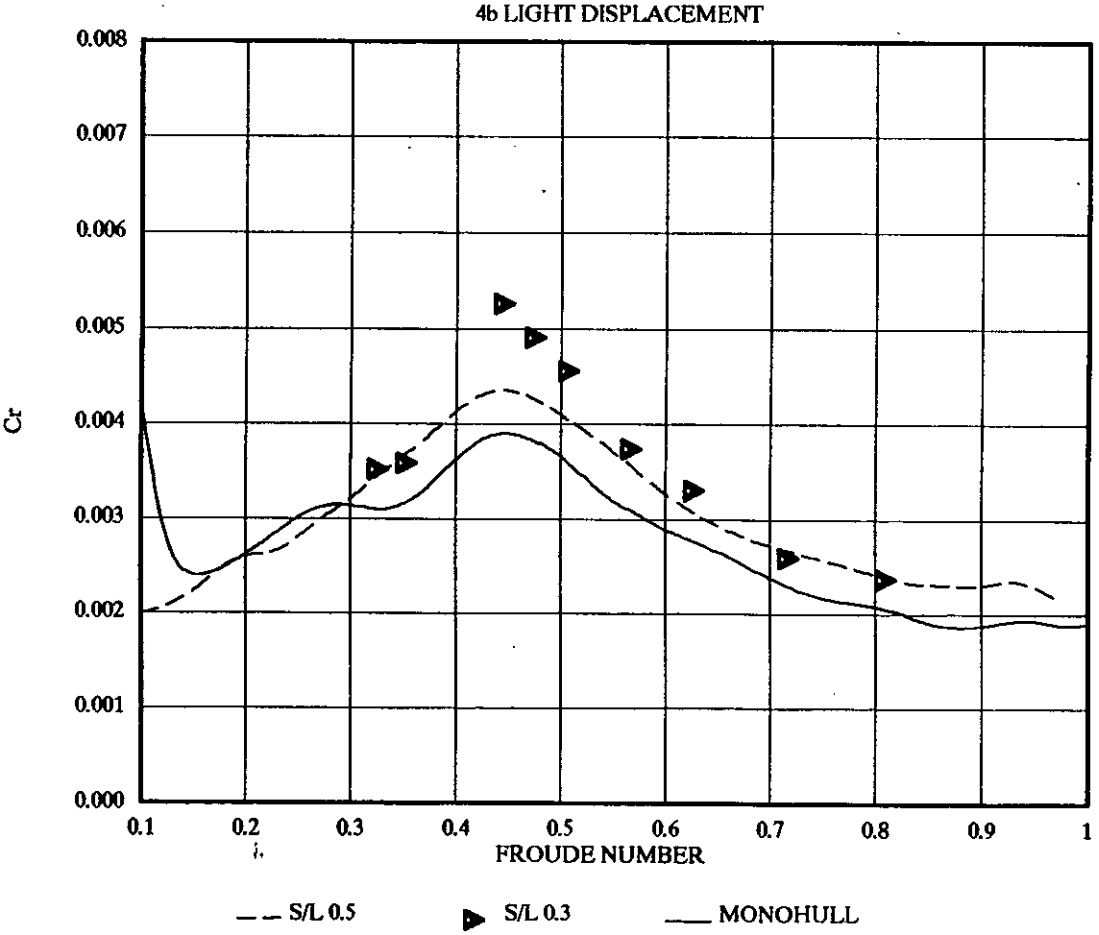

FIGURE 44

RESIDUARY RESISTANCE Cr FOR MONOHULL
5b, 5d, 5e

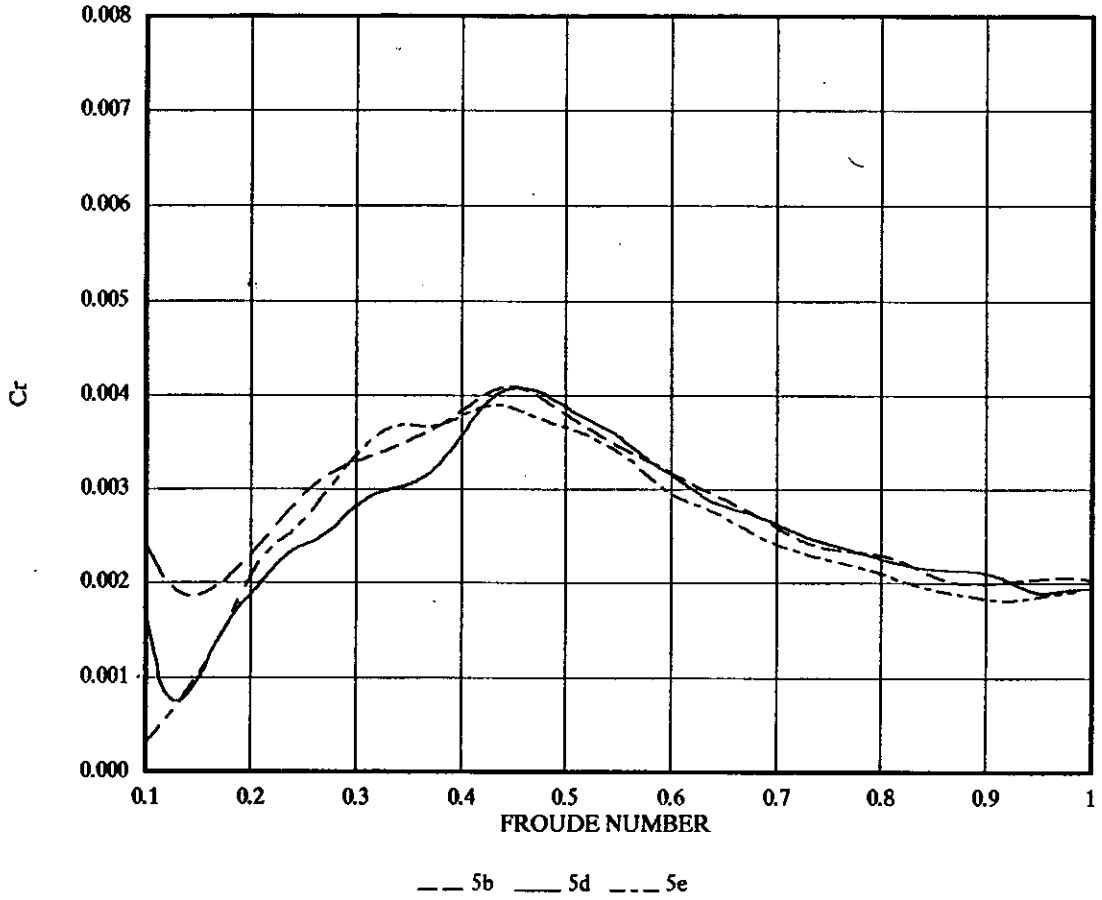

FIGURE 45

RESIDUARY RESISTANCE Cr FOR S/L 0.2
5b, 5d, 5e

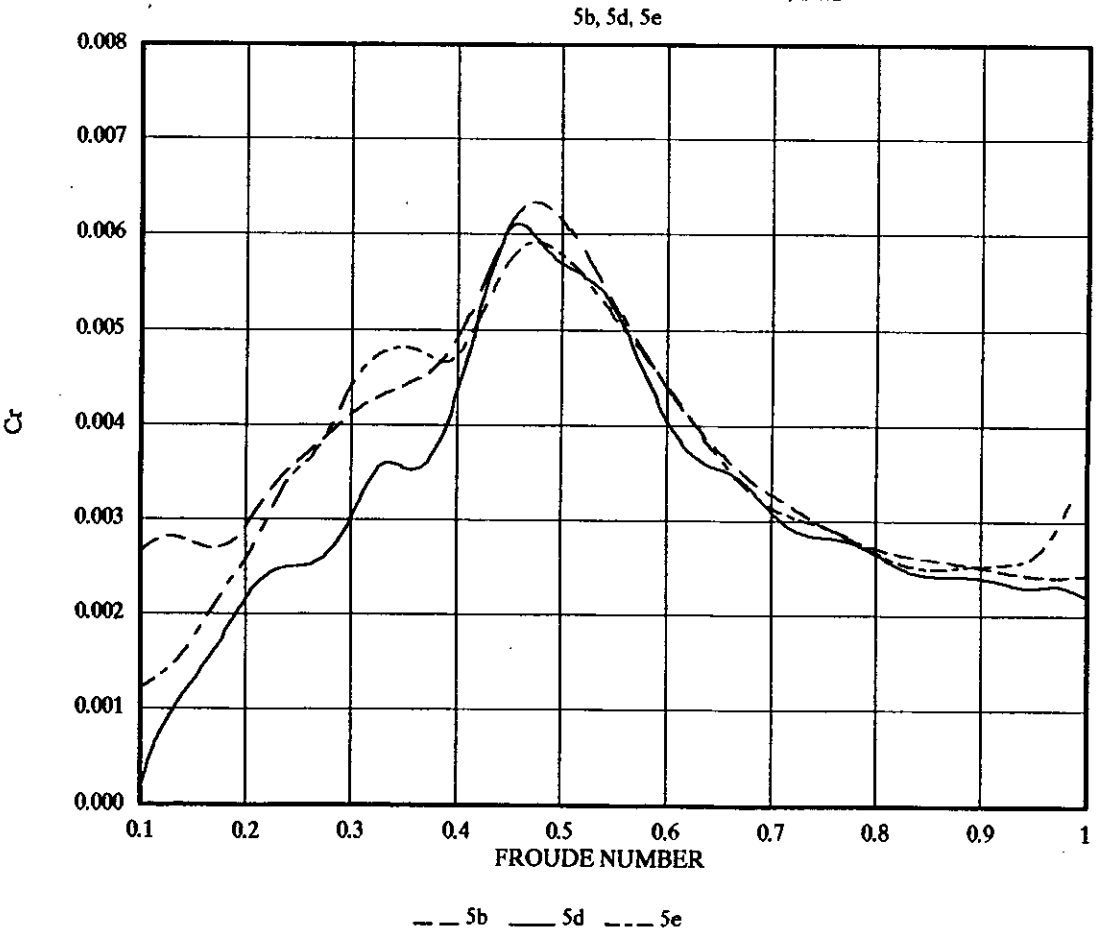

FIGURE 46

RESIDUARY RESISTANCE Cr FOR S/L 0.3
5b, 5d, 5e

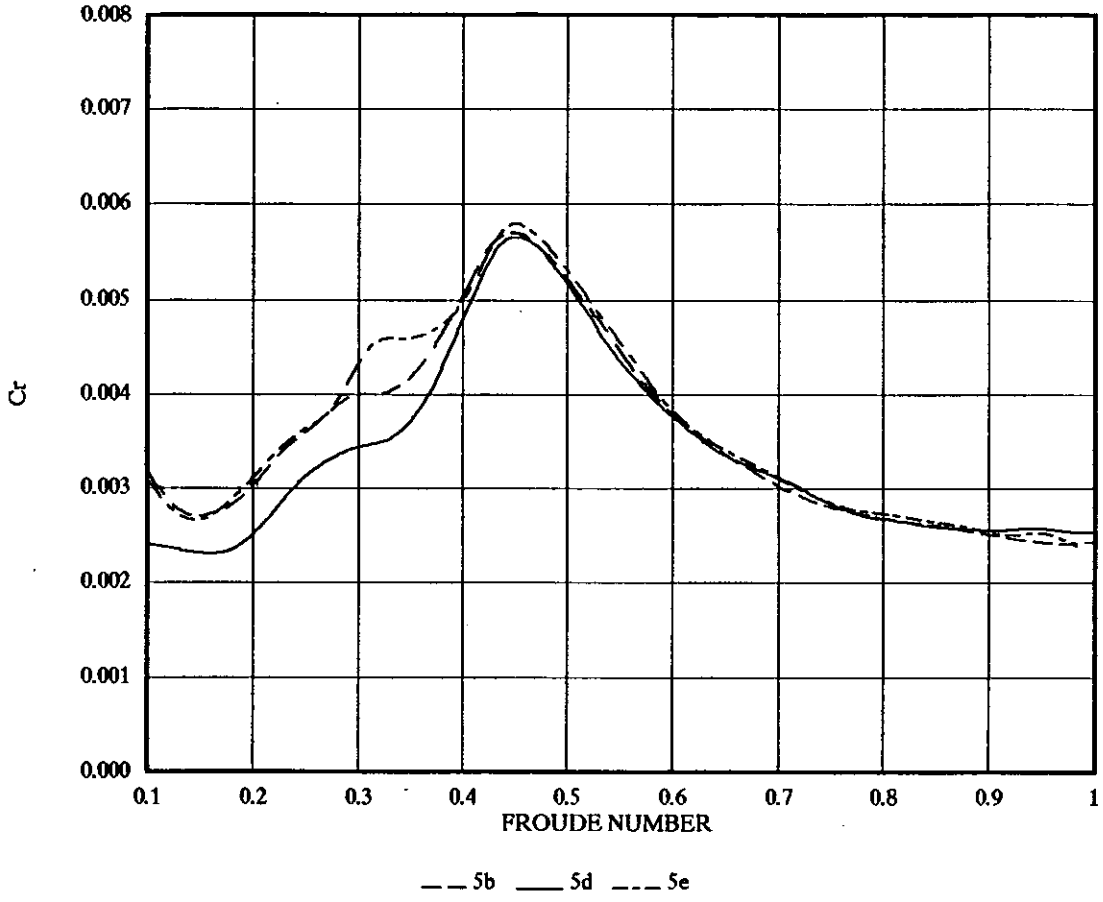

FIGURE 47

RESIDUARY RESISTANCE Cr FOR S/L 0.4
5d, 5e

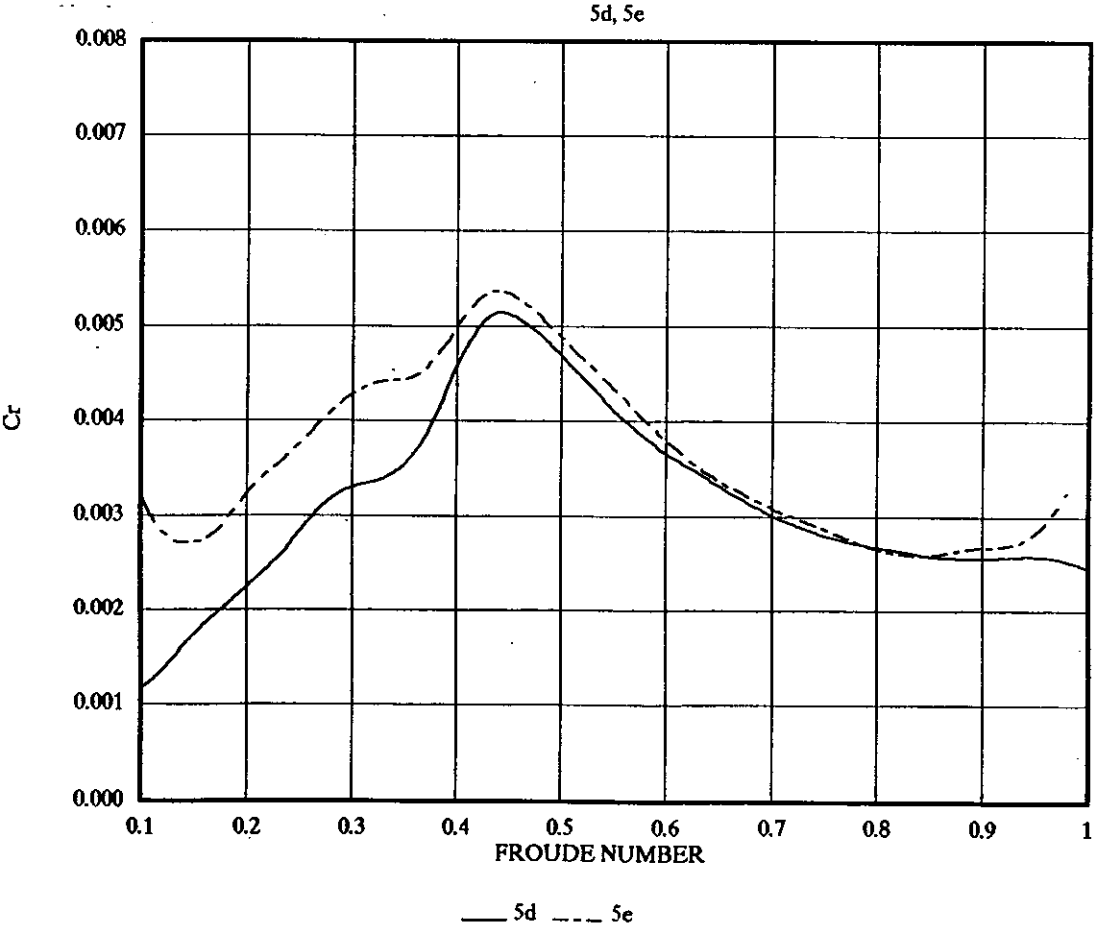

FIGURE 48 RESIDUARY RESISTANCE Cr FOR S/L 0.5

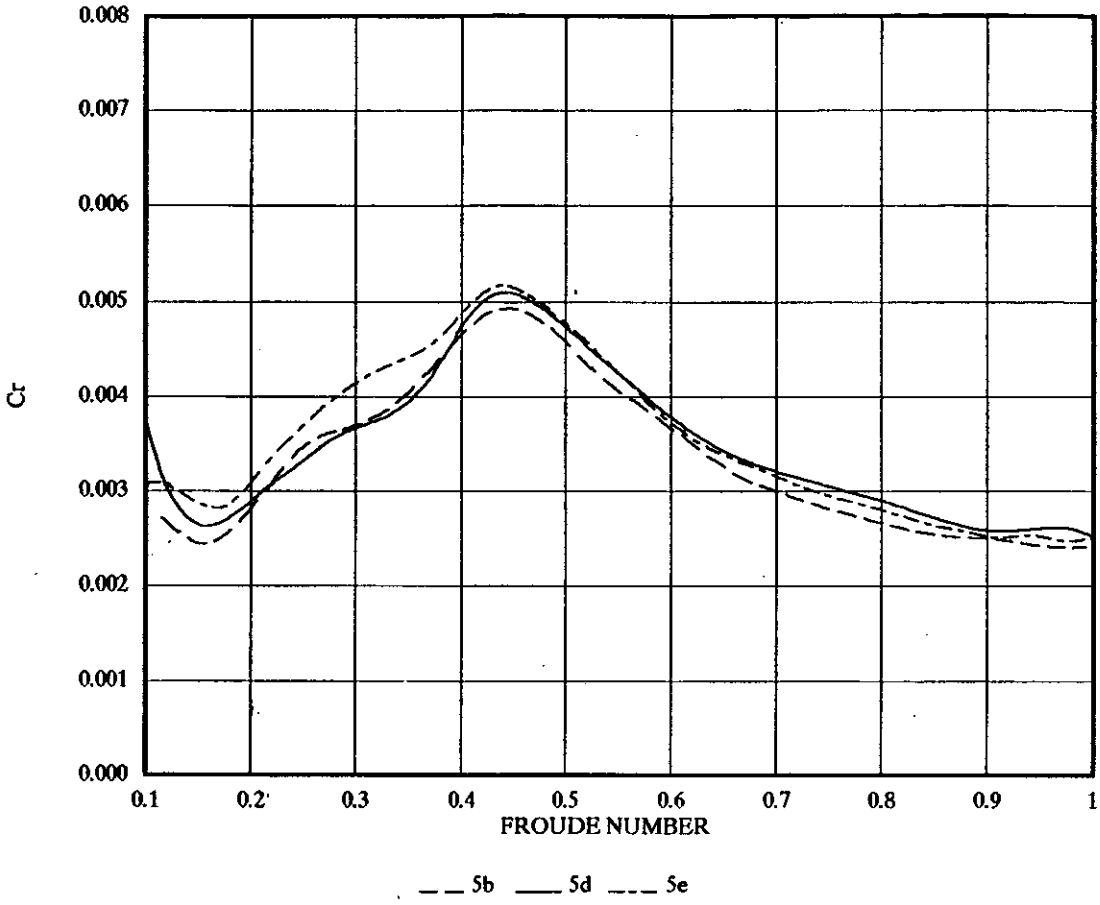

FIGURE 49 RESIDUARY RESISTANCE Cr FOR MONOHULL
4b, 4b LIGHT, 5b, 5d

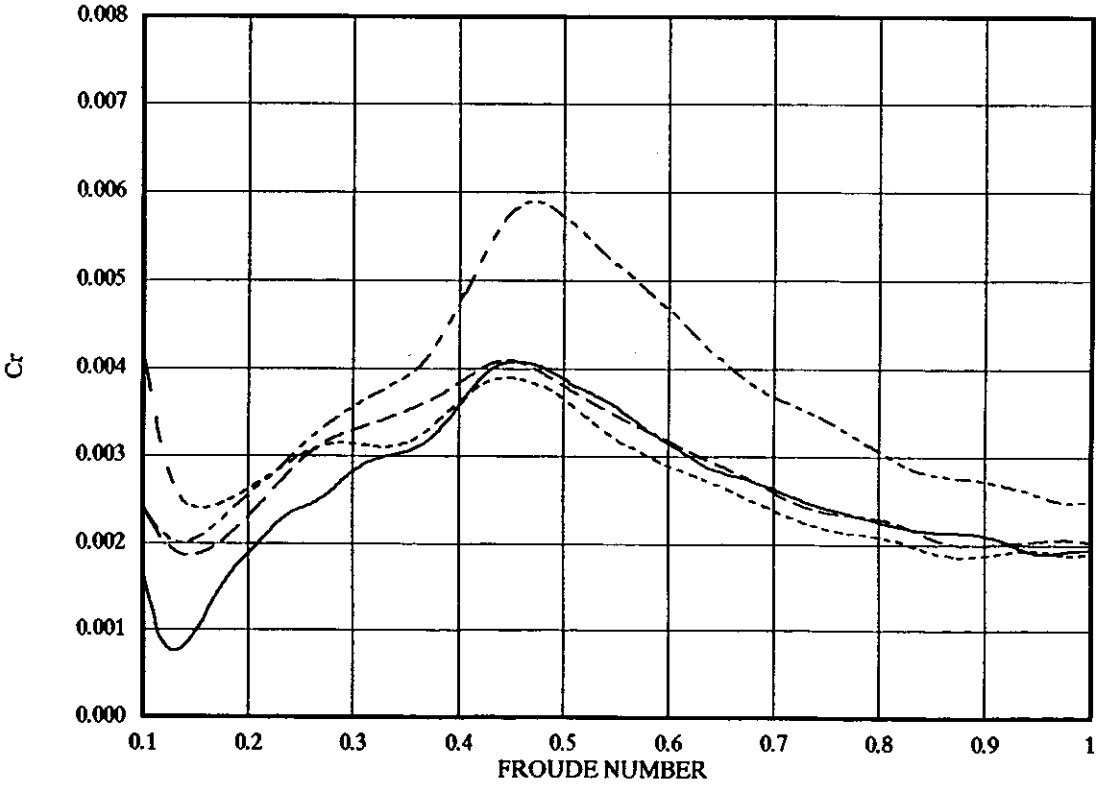

FIGURE 50

RESIDUARY RESISTANCE Cr FOR S/L 0.3
4b, 4b LIGHT, 5b, 5d

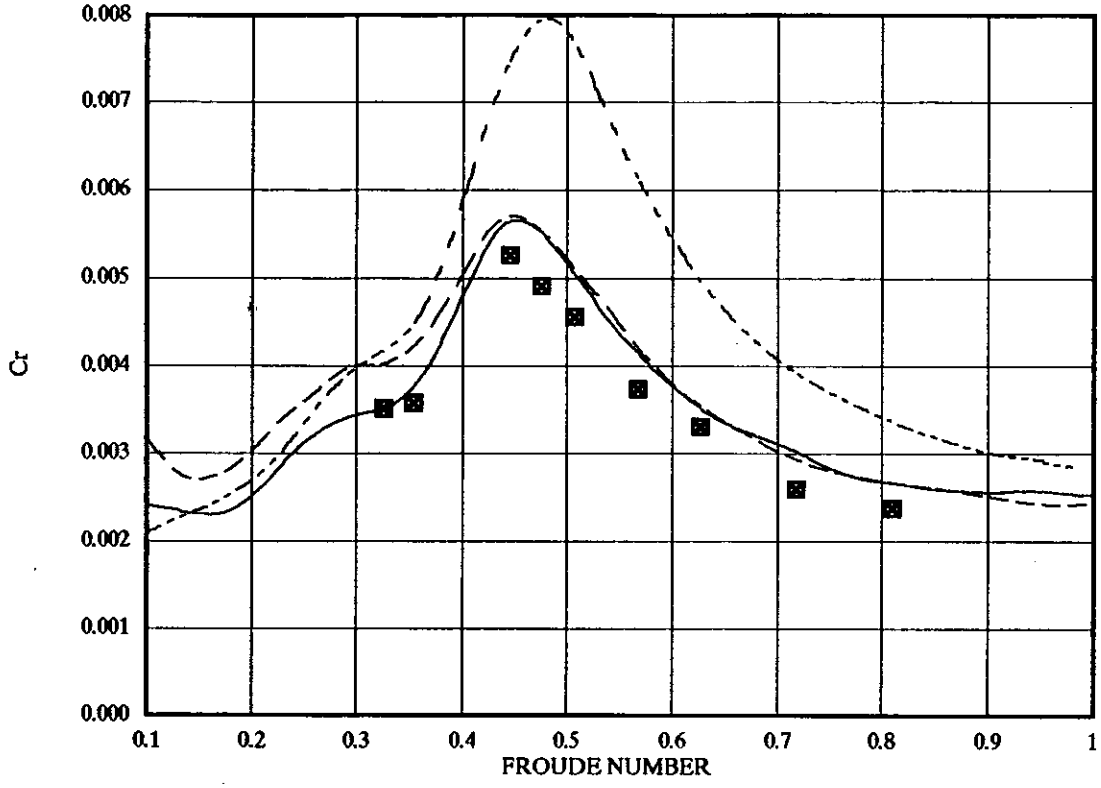

4b LIGHT DISPLMNT. ---- 4b NORMAL DISPLMNT.

— — 5b ——— 5d

FIGURE 51

RESIDUARY RESISTANCE Cr FOR S/L 0.5
4b, 4b LIGHT, 5b, 5d

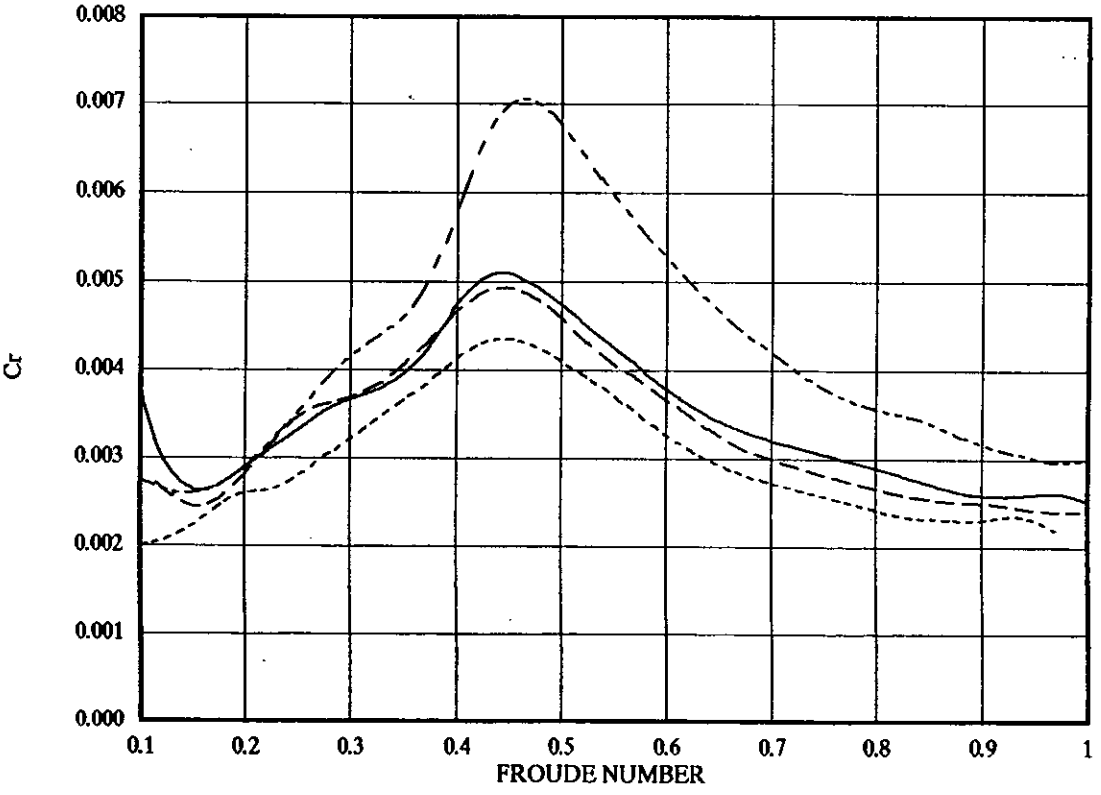

---- 4b LIGHT DISPLMNT. ---- 4b NORMAL DISPLMNT

— — 5b ——— 5d

FIGURE 52 RESIDUARY RESISTANCE INTERFERENCE FACTOR
5d

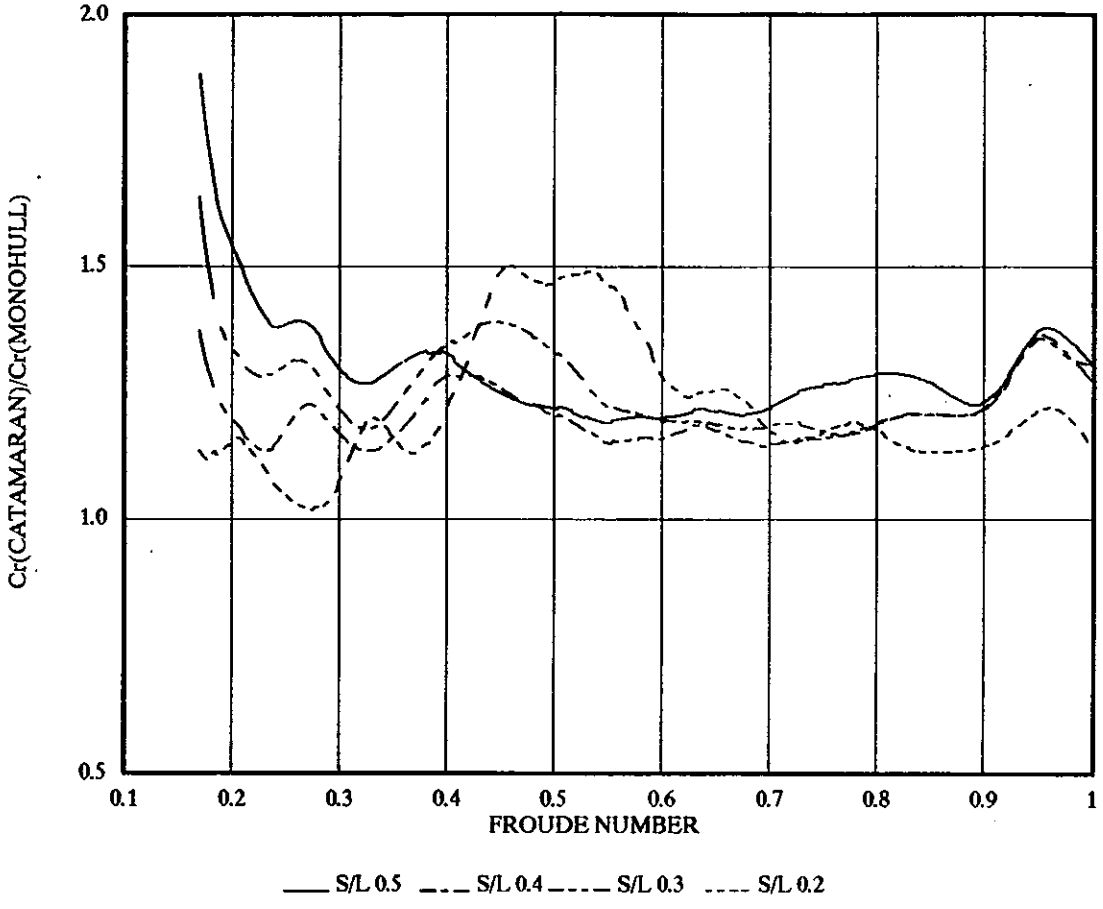

FIGURE 53 RESIDUARY RESISTANCE INTERFERANCE FACTOR
5b

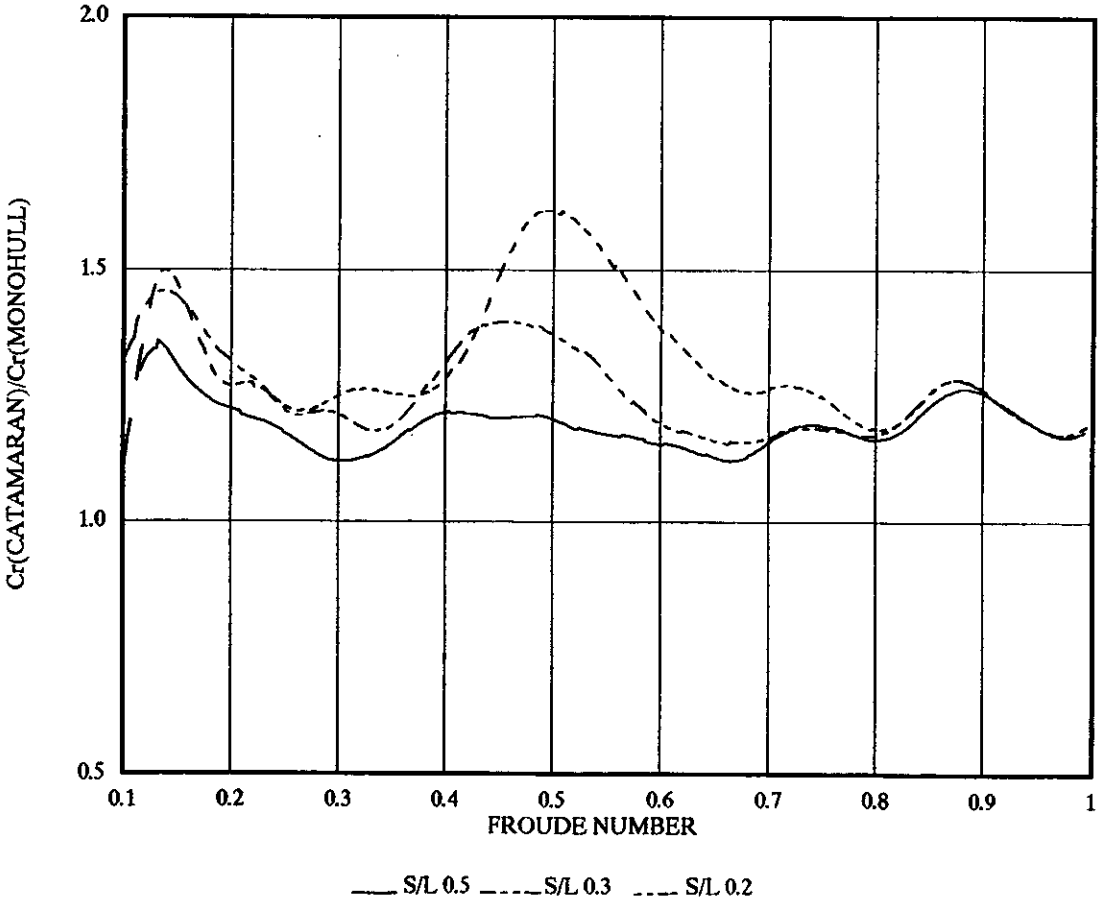

FIGURE 53

FIGURE 54 RESIDUARY RESISTANCE INTERFERANCE FACTOR
5e

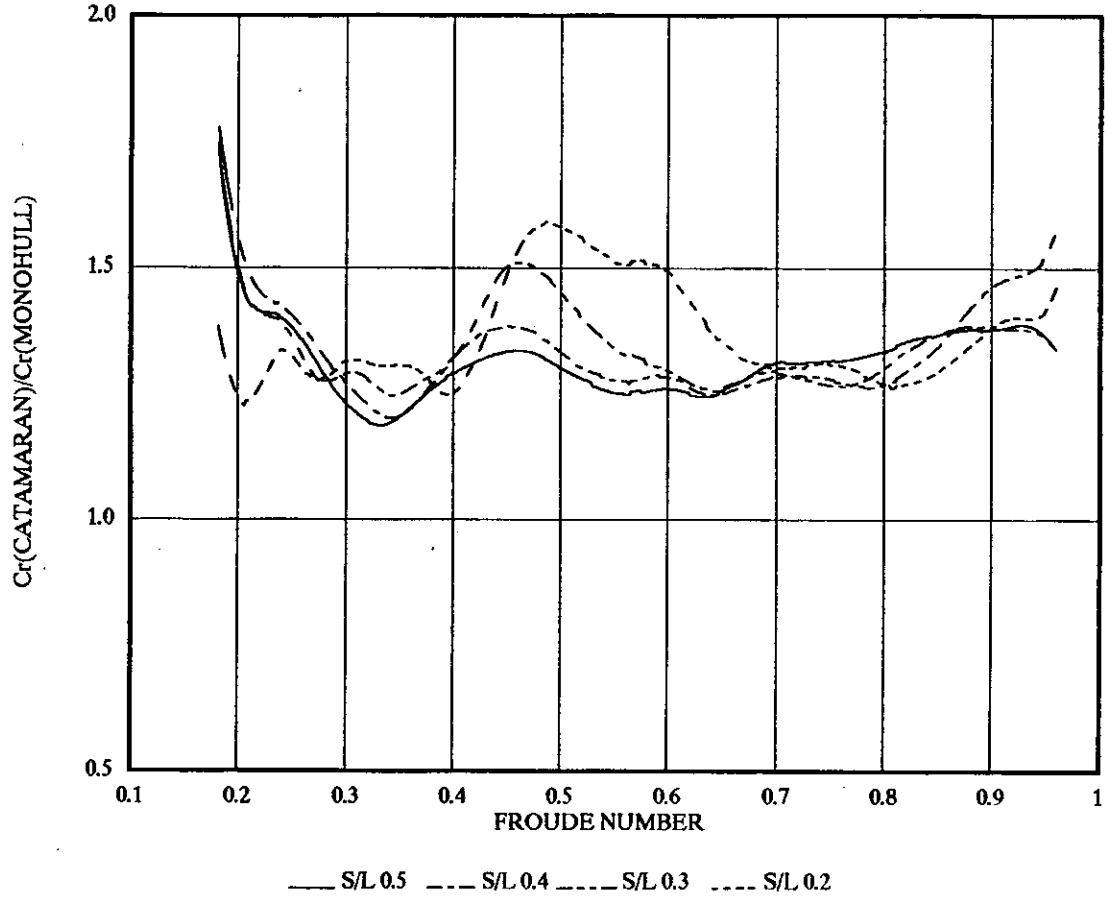

FIGURE 55 RESIDUARY RESISTANCE INTERFERANCE FACTOR
4b LIGHT DISPLACEMENT

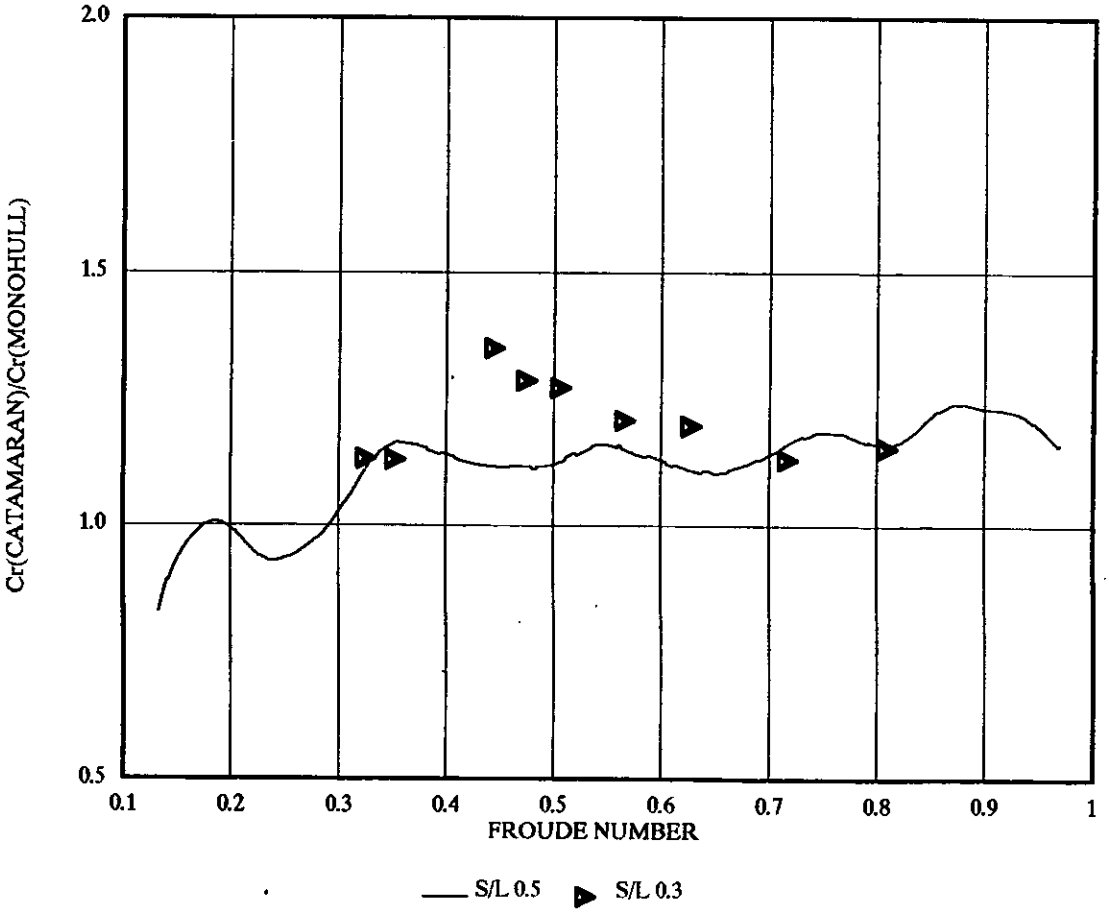

FIGURE 56 RESIDUARY RESISTANCE INTERFERENCE FACTOR
5d AND 5e S/L 0.2

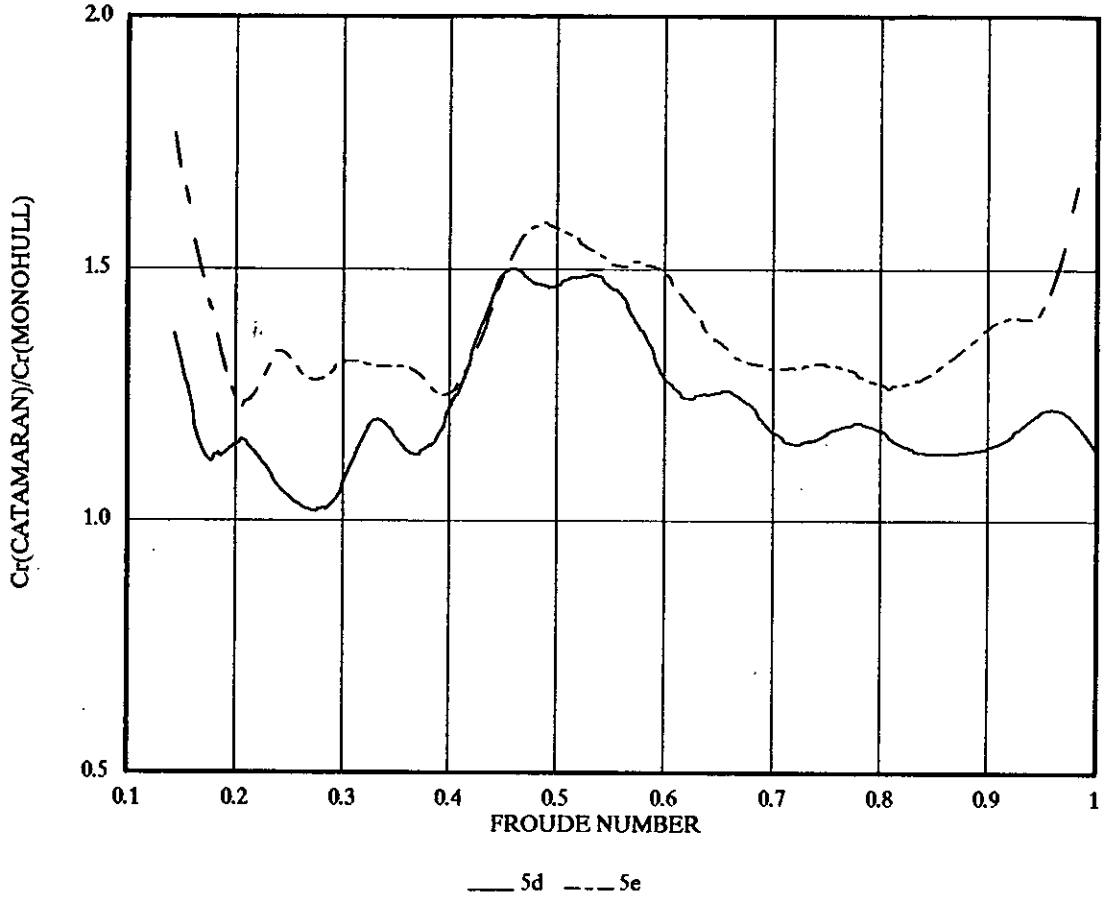

FIGURE 57 RESIDUARY RESISTANCE INTERFERENCE FACTOR
5b, 5d, 5e S/L 0.3

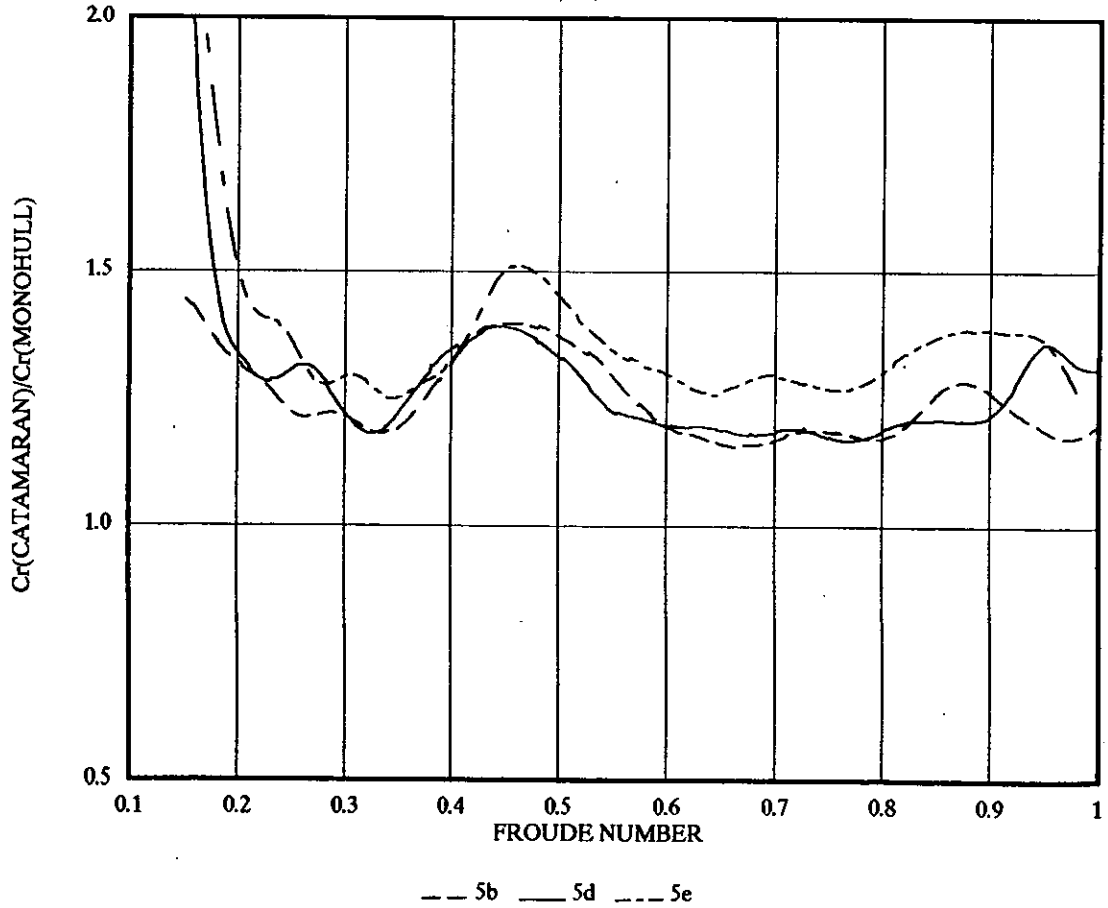

FIGURE 58 RESIDUARY RESISTANCE INTERFERENCE FACTOR
5d AND 5e S/L 0.4

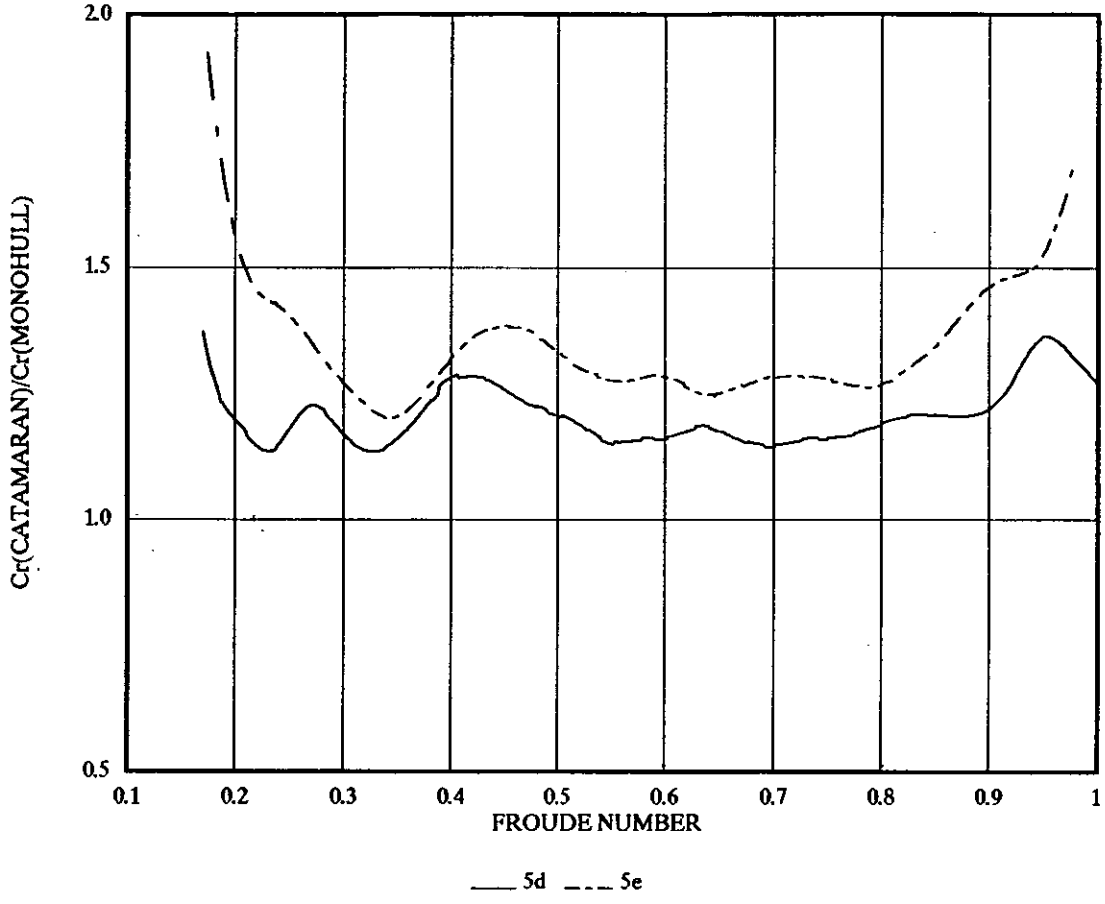

FIGURE 59 RESIDUARY RESISTANCE INTERFERENCE FACTOR
5b, 5d, 5e S/L 0.5

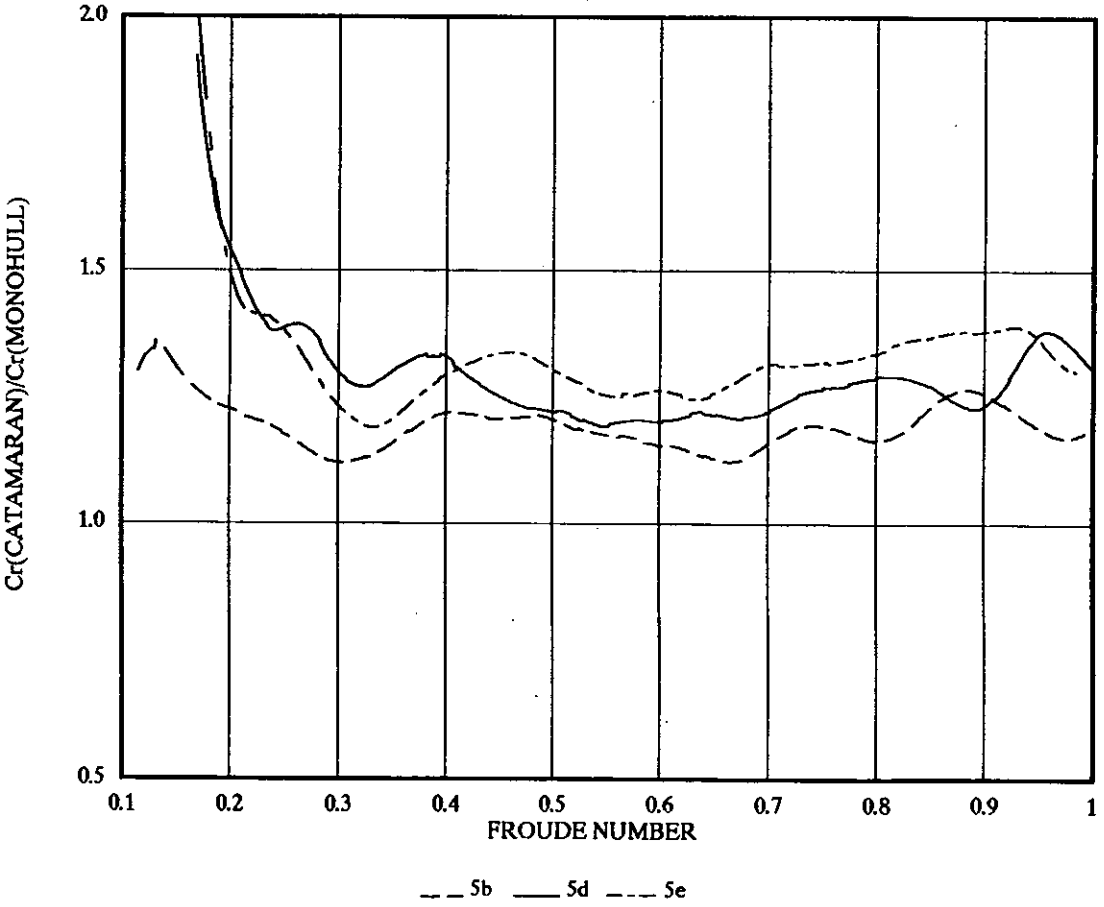

FIGURE 60 RESIDUARY RESISTANCE INTERFERENCE FACTOR
4b, 4b LIGHT, 5b, 5d S/L 0.3

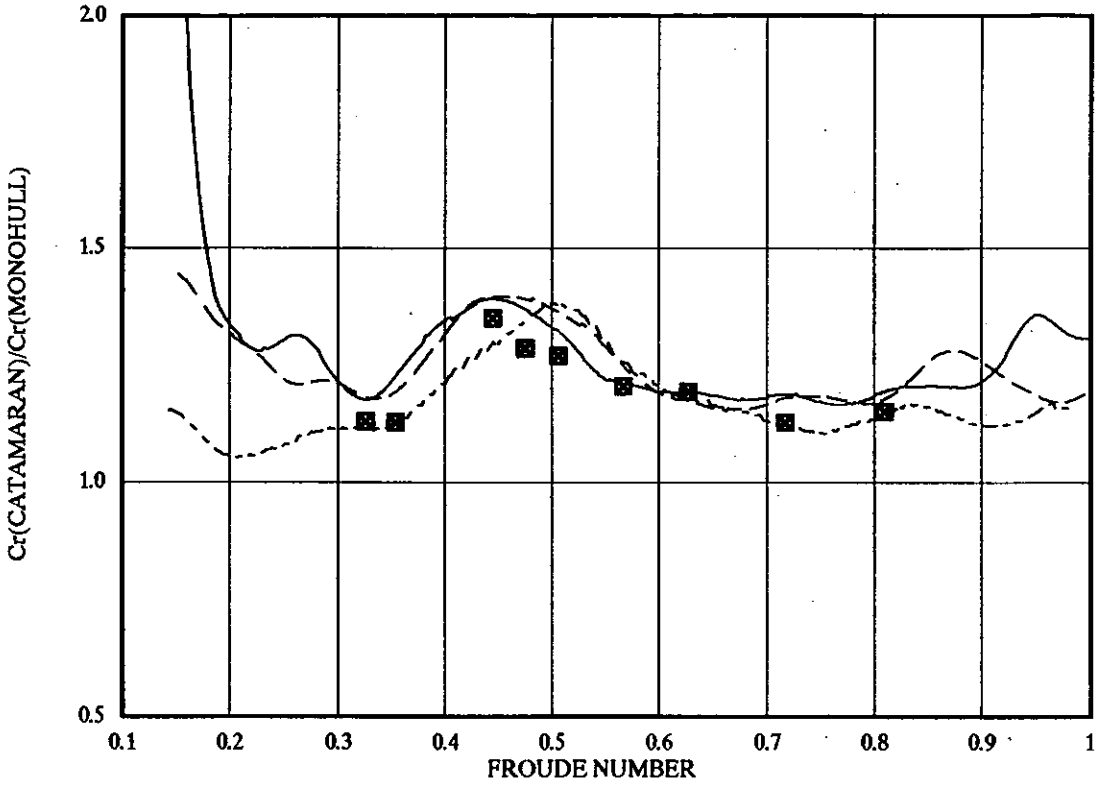

4b LIGHT DISPLMNT. 4b NORMAL DISPLMNT.

5b 5d

FIGURE 61 RESIDUARY RESISTANCE INTERFERENCE FACTOR
4b LIGHT, 5b, 5d S/L 0.5

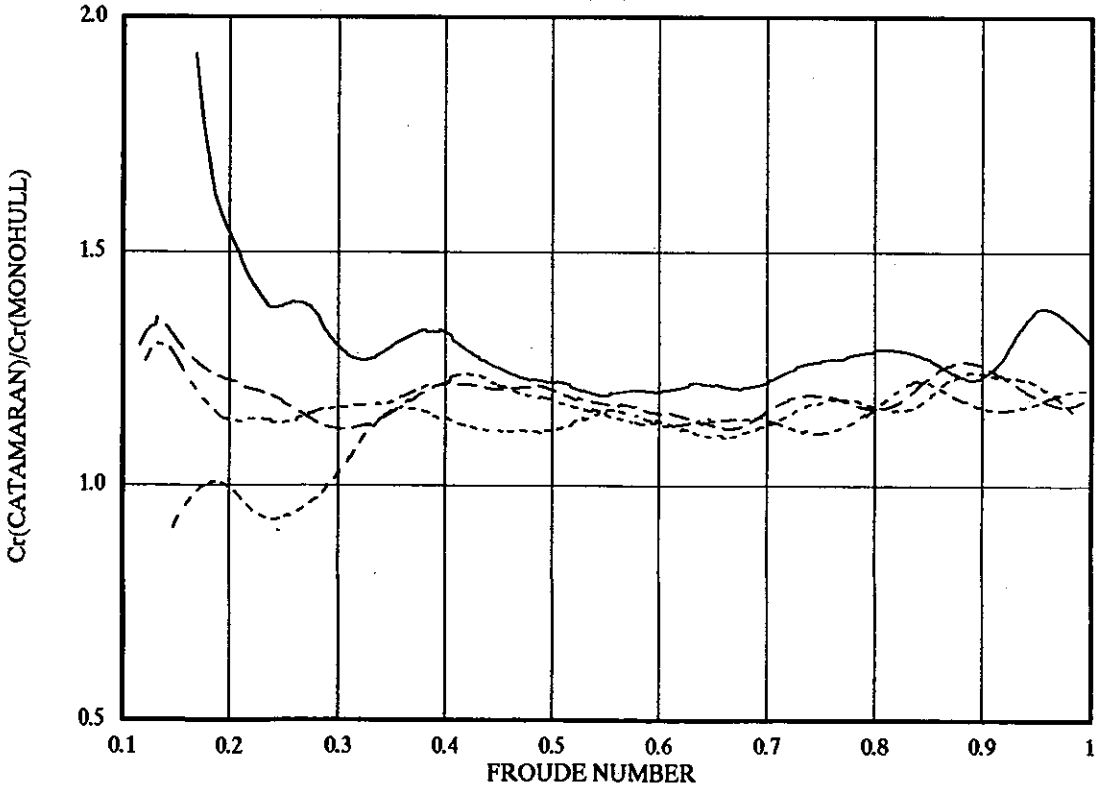

4b LIGHT DISPLMNT. 4b NORMAL DISPLMNT.

5b 5d

FIGURE 62

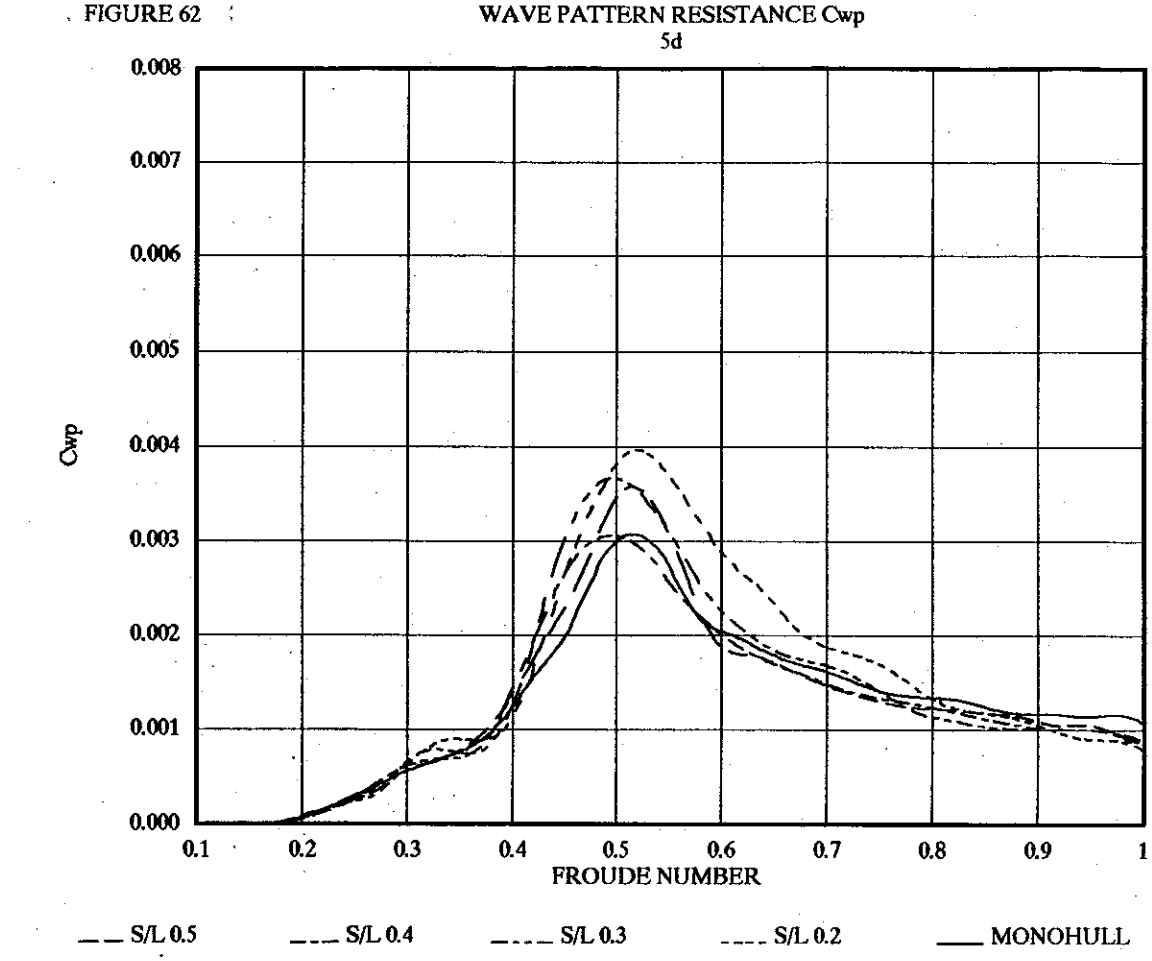

FIGURE 63

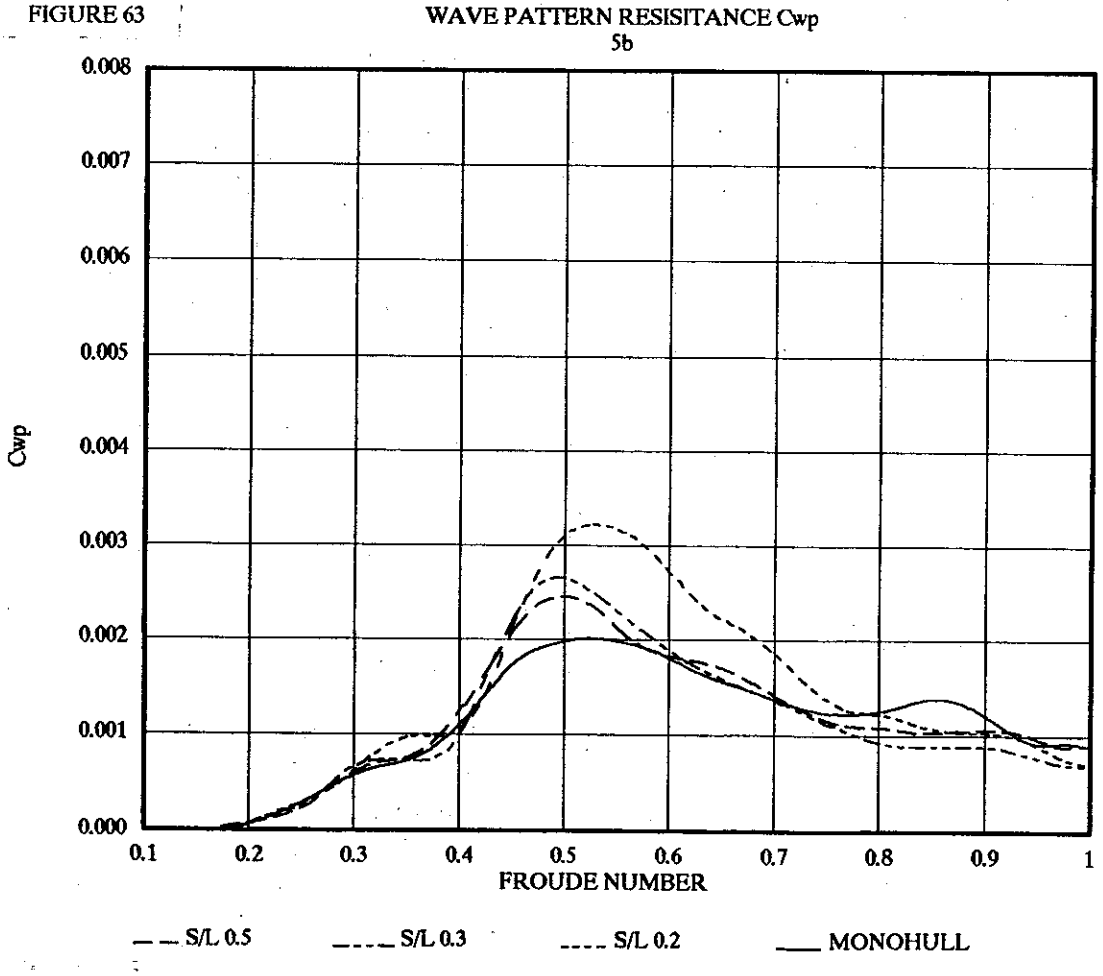

FIGURE 64

WAVE PATTERN RESISTANCE Cwp
5e

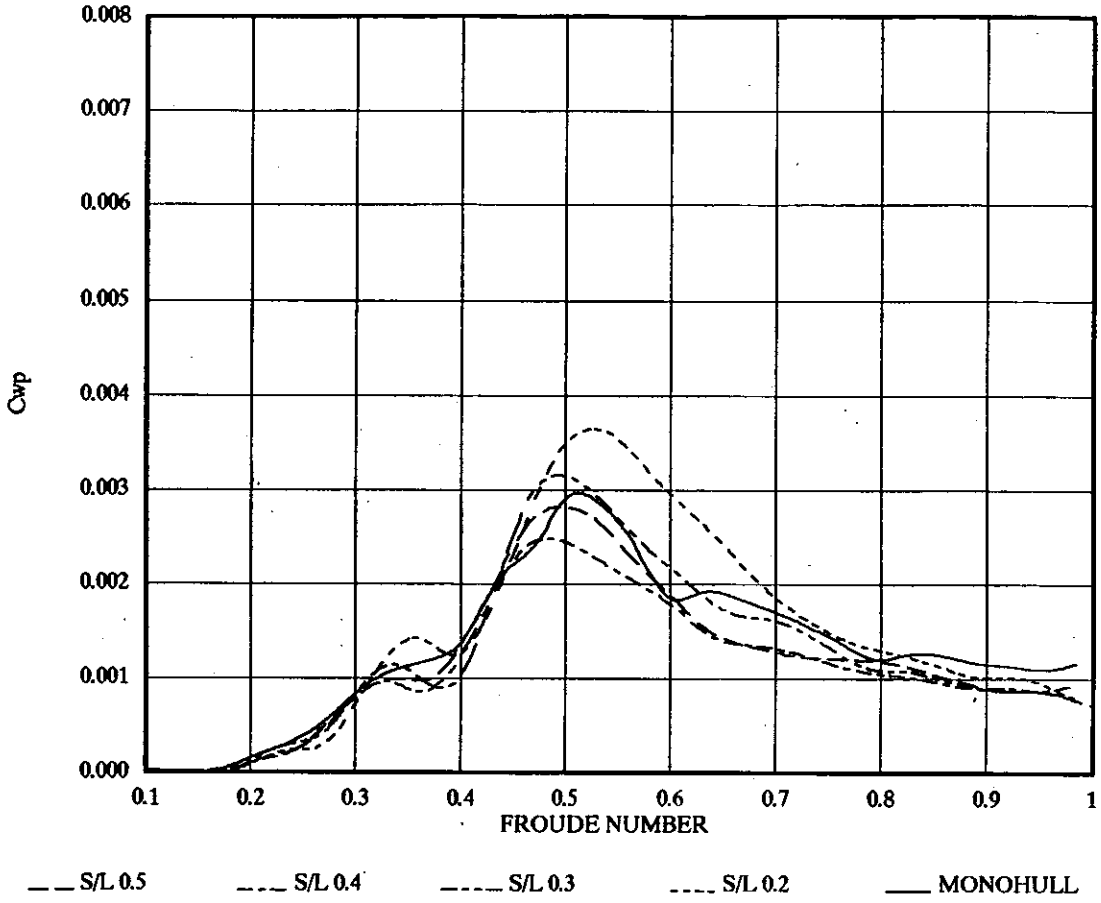

FIGURE 65

WAVE PATTERN RESISTANCE Cwp
4b LIGHT DISPLACEMENT

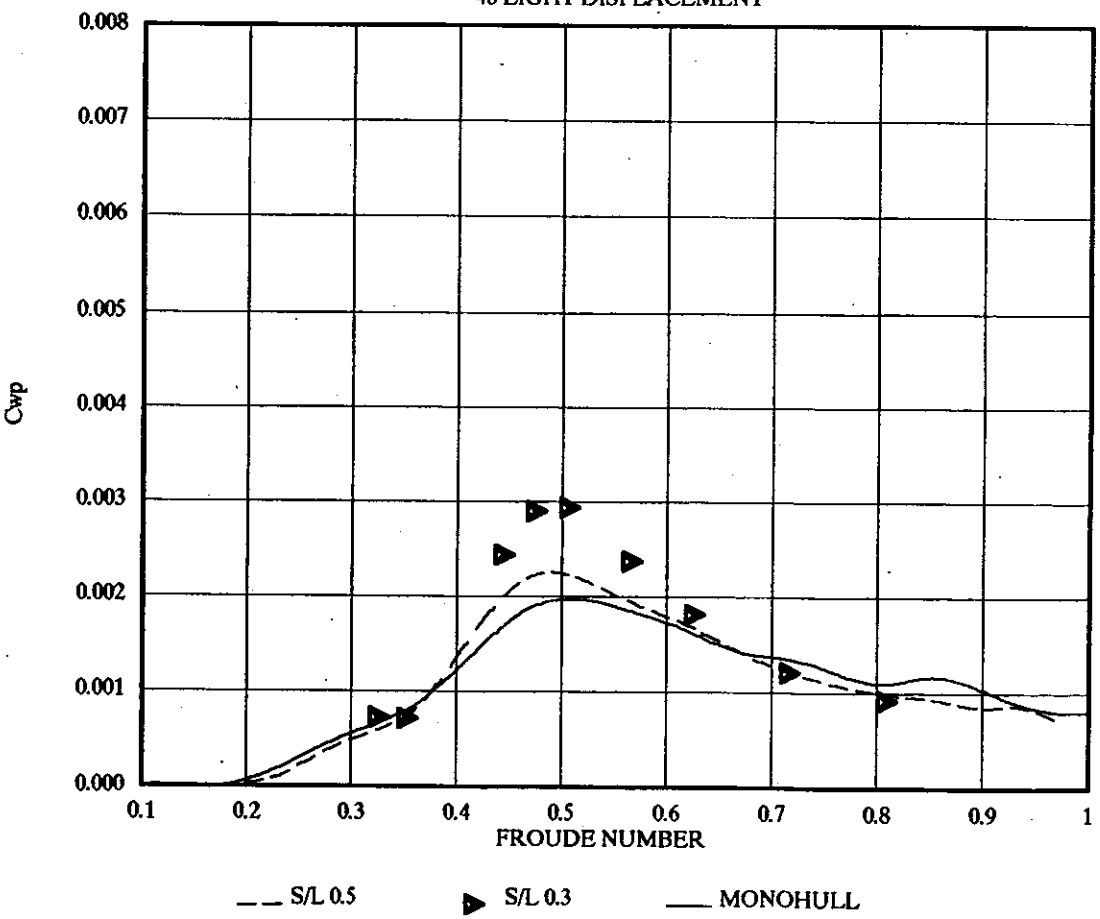

FIGURE 66

WAVE PATTERN RESISTANCE Cwp MONOHULL
5b, 5d, 5e

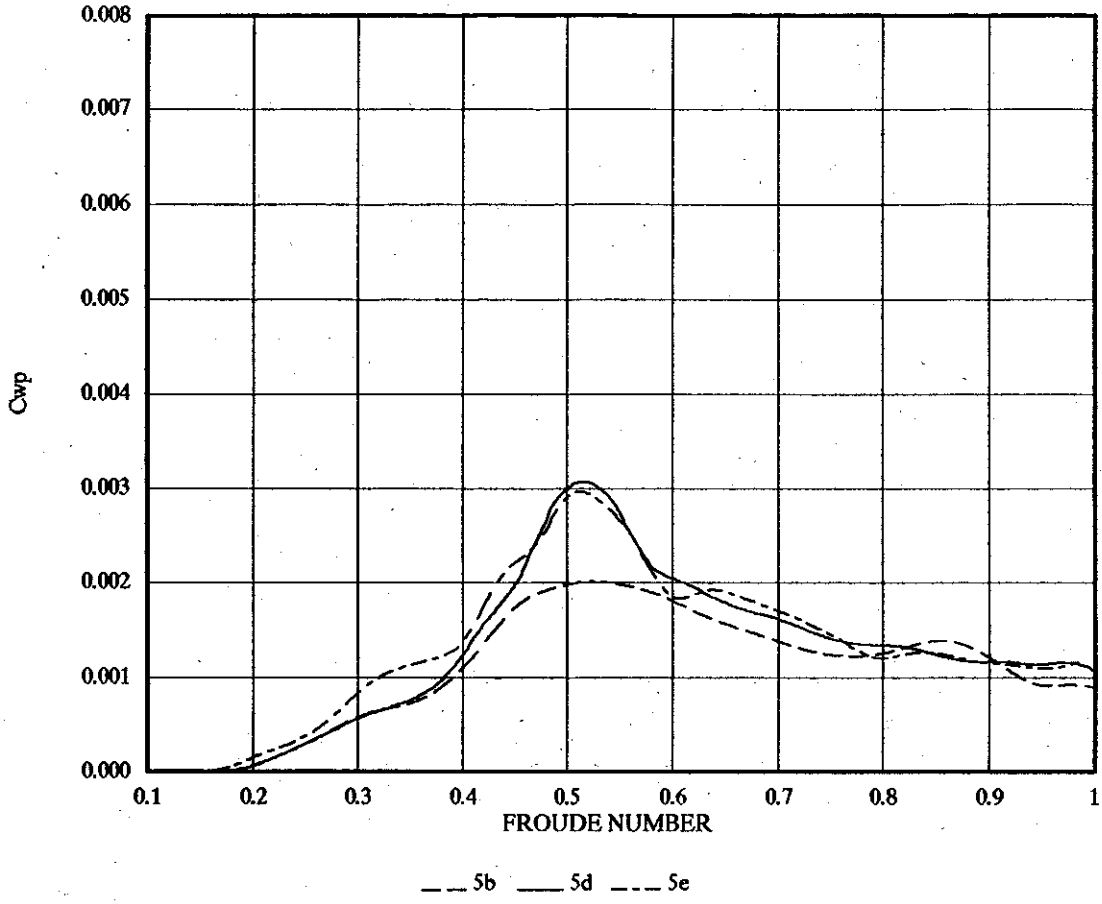

FIGURE 67

WAVE PATTERN RESISTANCE Cwp S/L 0.2
5b, 5d, 5e

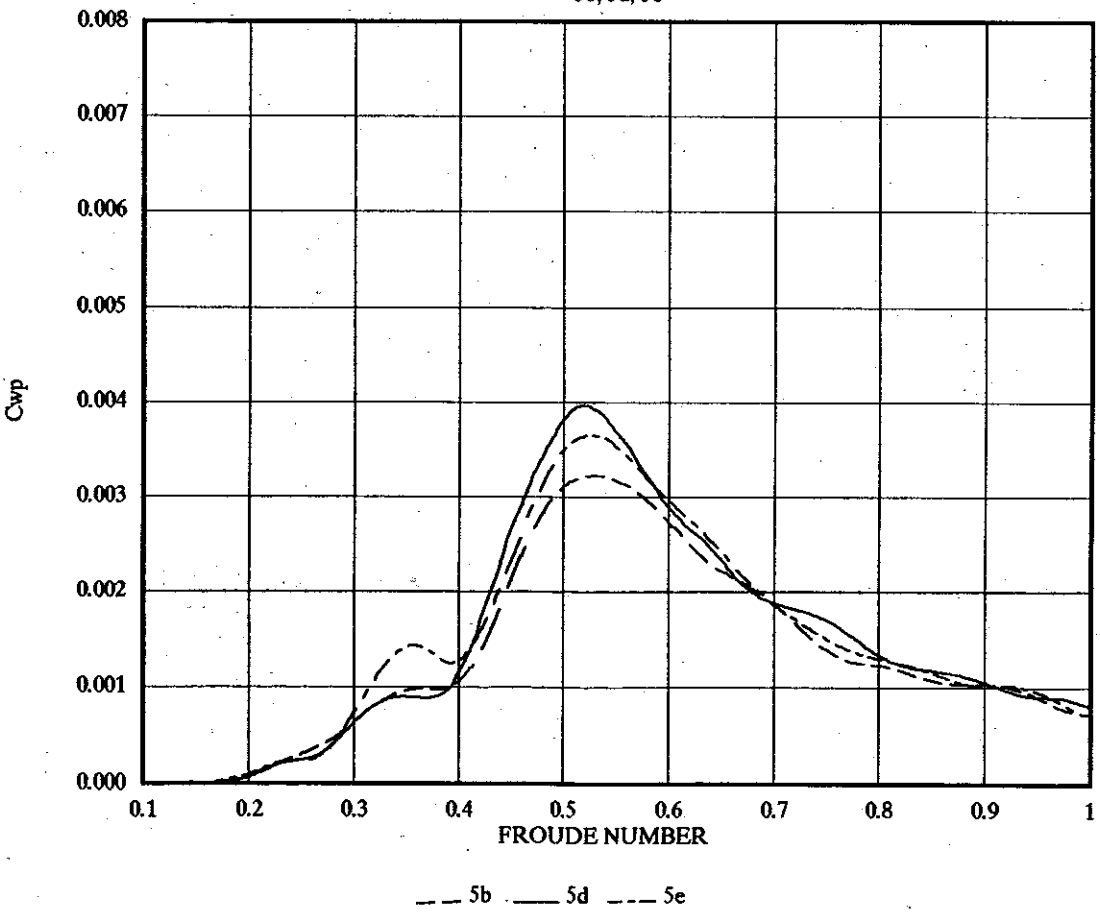

FIGURE 68

WAVE PATTERN RESISTANCE Cwp S/L 0.3
5b, 5d, 5e

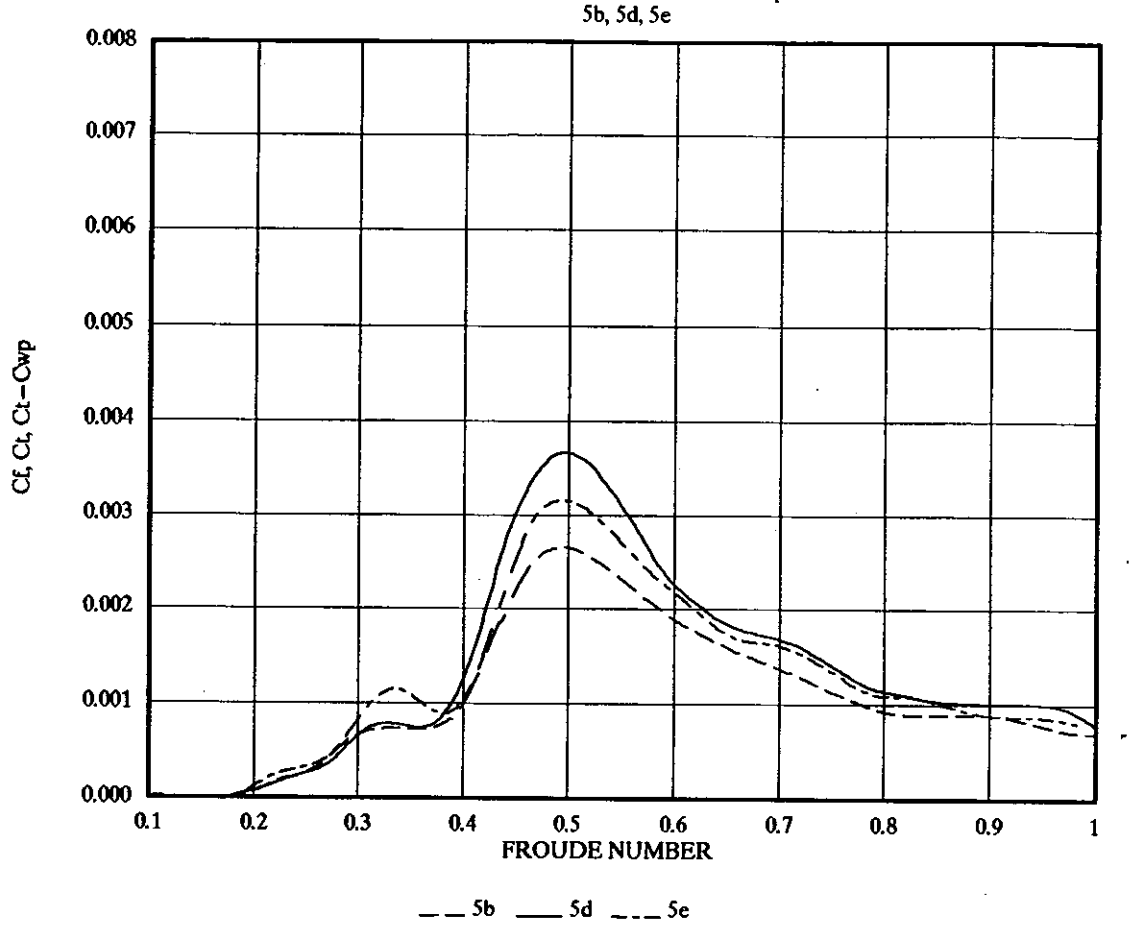

FIGURE 69

WAVE PATTERN RESISTANCE Cwp S/L 0.4
5d, 5e

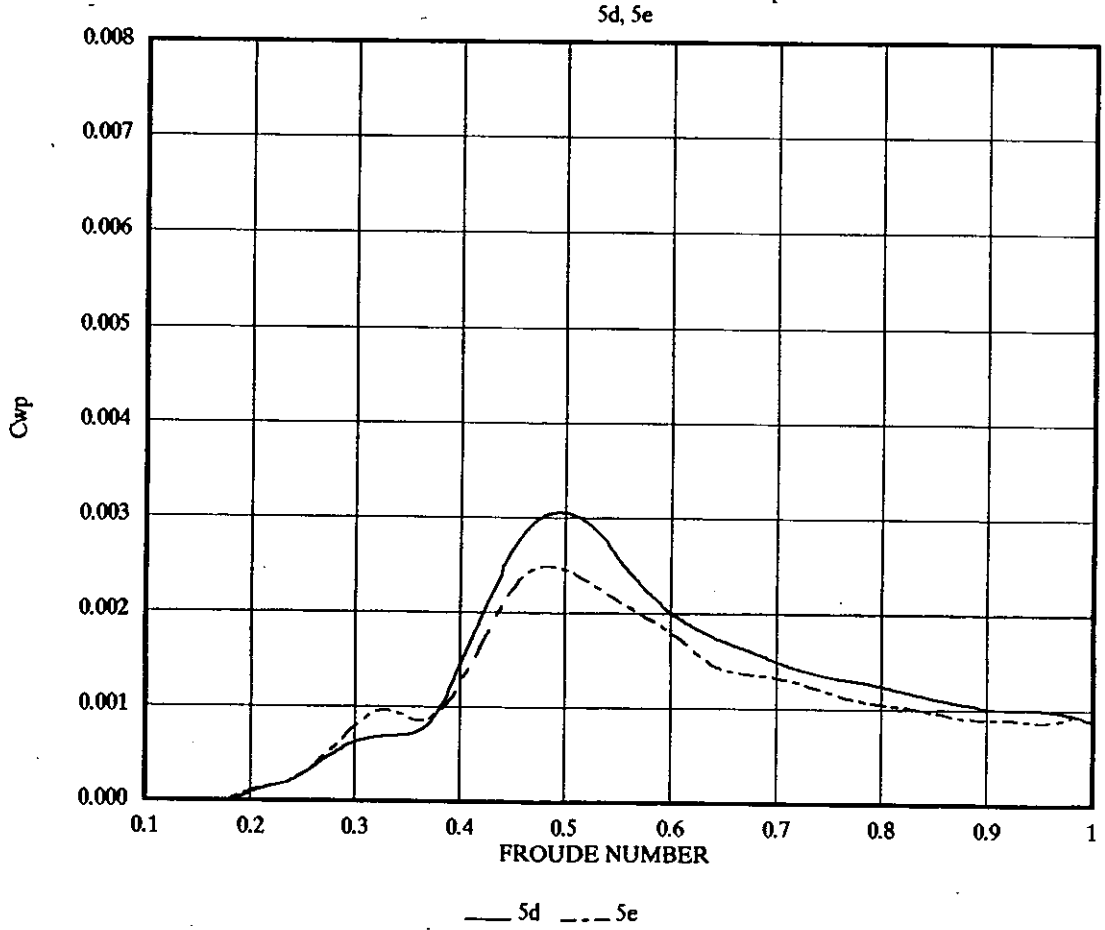

FIGURE 70

WAVE PATTERN RESISITANCE Cwp S/L 0.5
5b, 5d, 5e

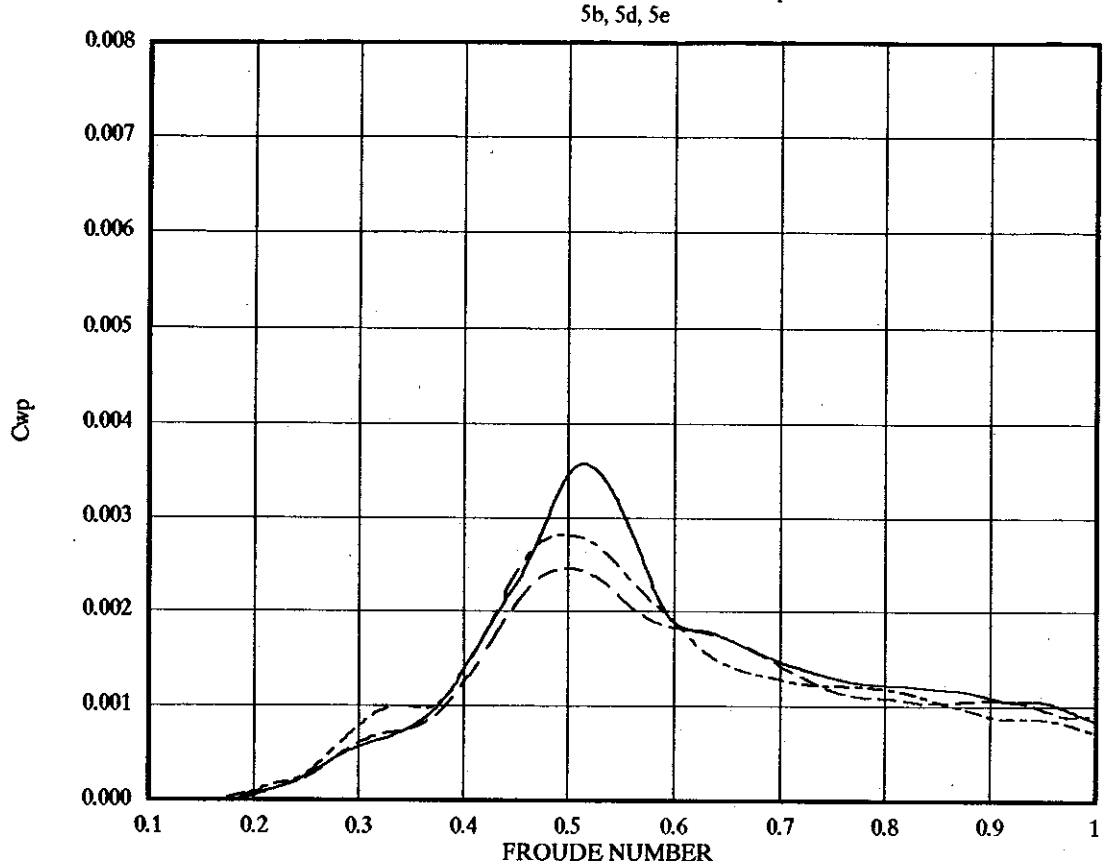

— — 5b ——— 5d — — — 5e

FIGURE 71

WAVE PATTERN RESISTANCE Cwp MONOHULL
4b, 4b LIGHT, 5b, 5d

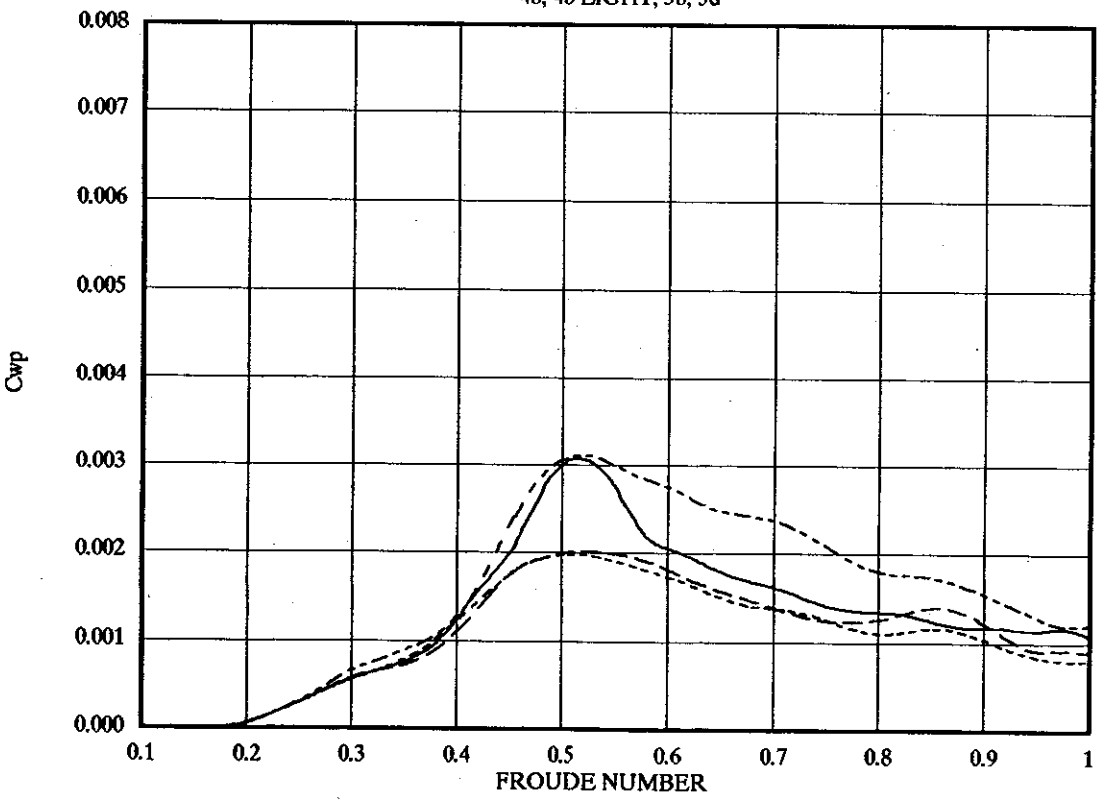

- - - - 4b LIGHT DISPLMNT. — — — 4b NORMAL DISPLMNT

— — 5b ——— 5d

FIGURE 72

WAVE PATTERN RESISTANCE Cwp S/L 0.3
4b, 4b LIGHT, 5b, 5d

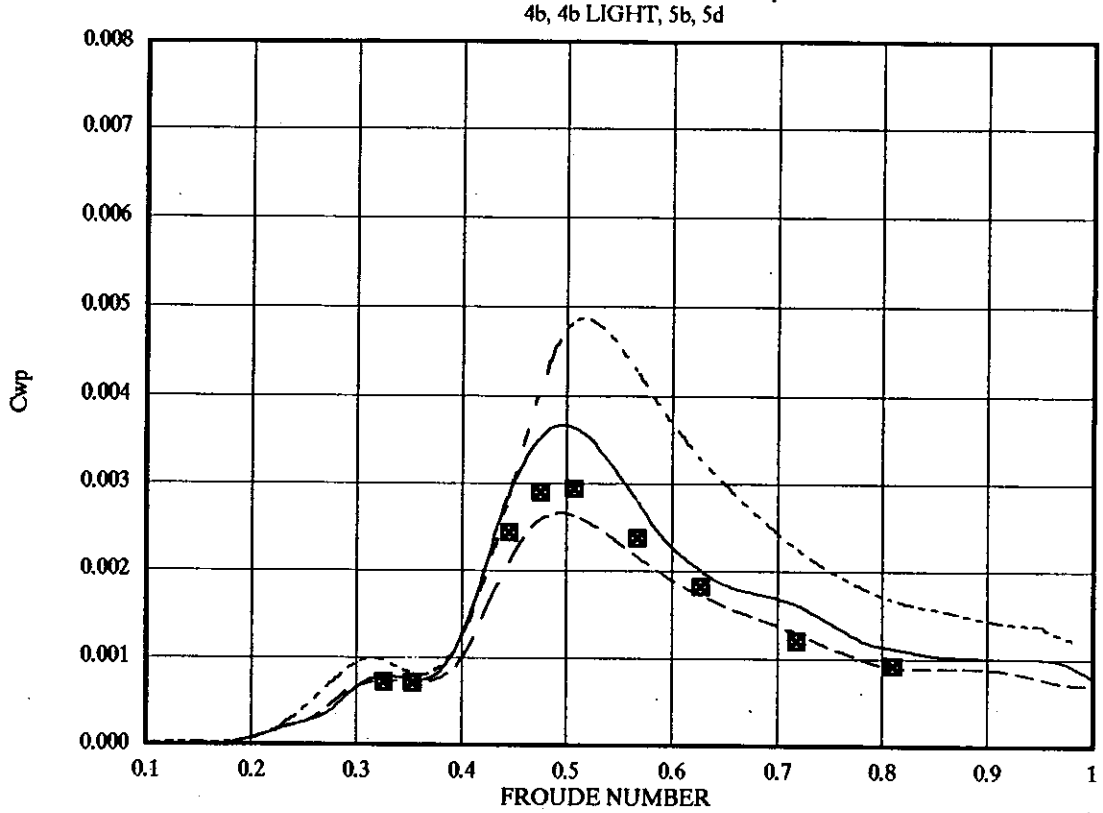

■ 4b LIGHT DISPLMNT. ---- 4b NORMAL DISPLMNT.

— — 5b ——— 5d

FIGURE 73

WAVE PATTERN RESISITANCE Cwp S/L 0.5
4b, 4b LIGHT, 5b, 5d

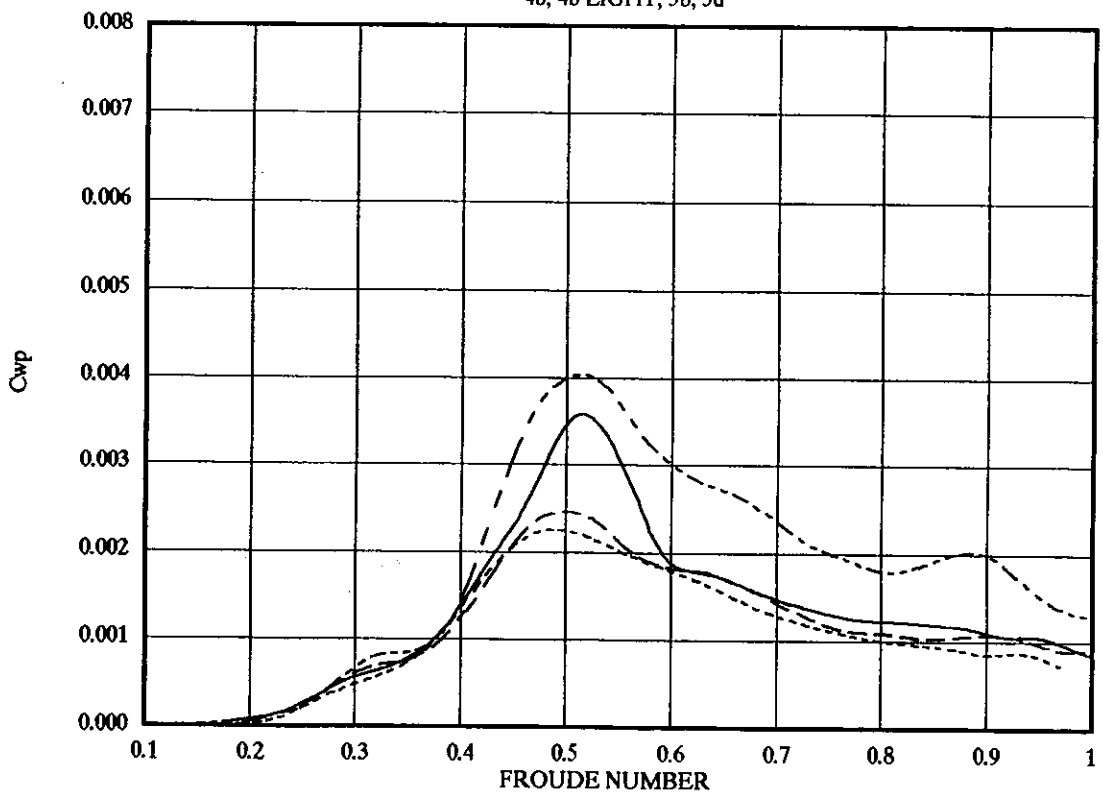

---- 4b LIGHT DISPLMNT. ---- 4b NORMAL DISPLMNT.

— — 5b ——— 5d

FIGURE 74 WAVE RESISTANCE Cw (BASED ON KwpCf)
5d

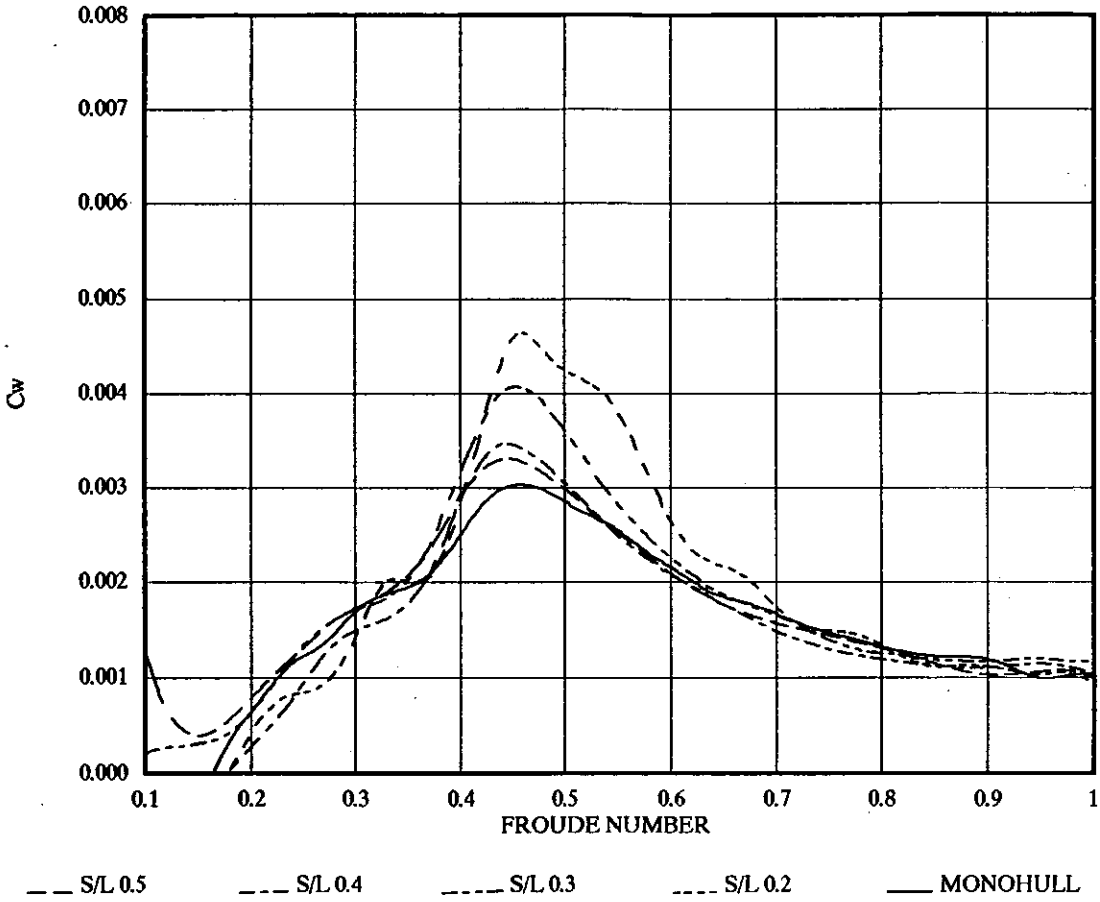

FIGURE 75 WAVE RESISTANCE Cw FOR 5b

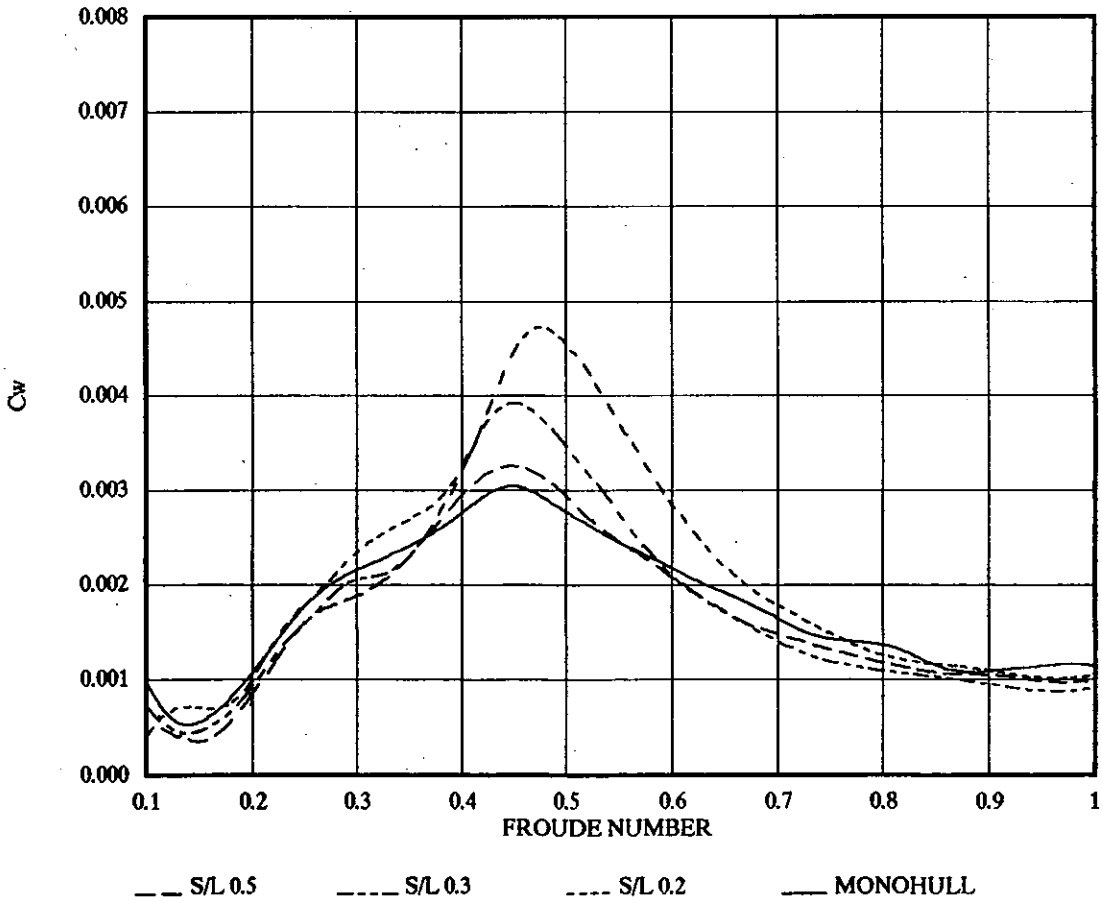

FIGURE 76

WAVE RESISTANCE Cw (BASED ON KwpCf)

5e

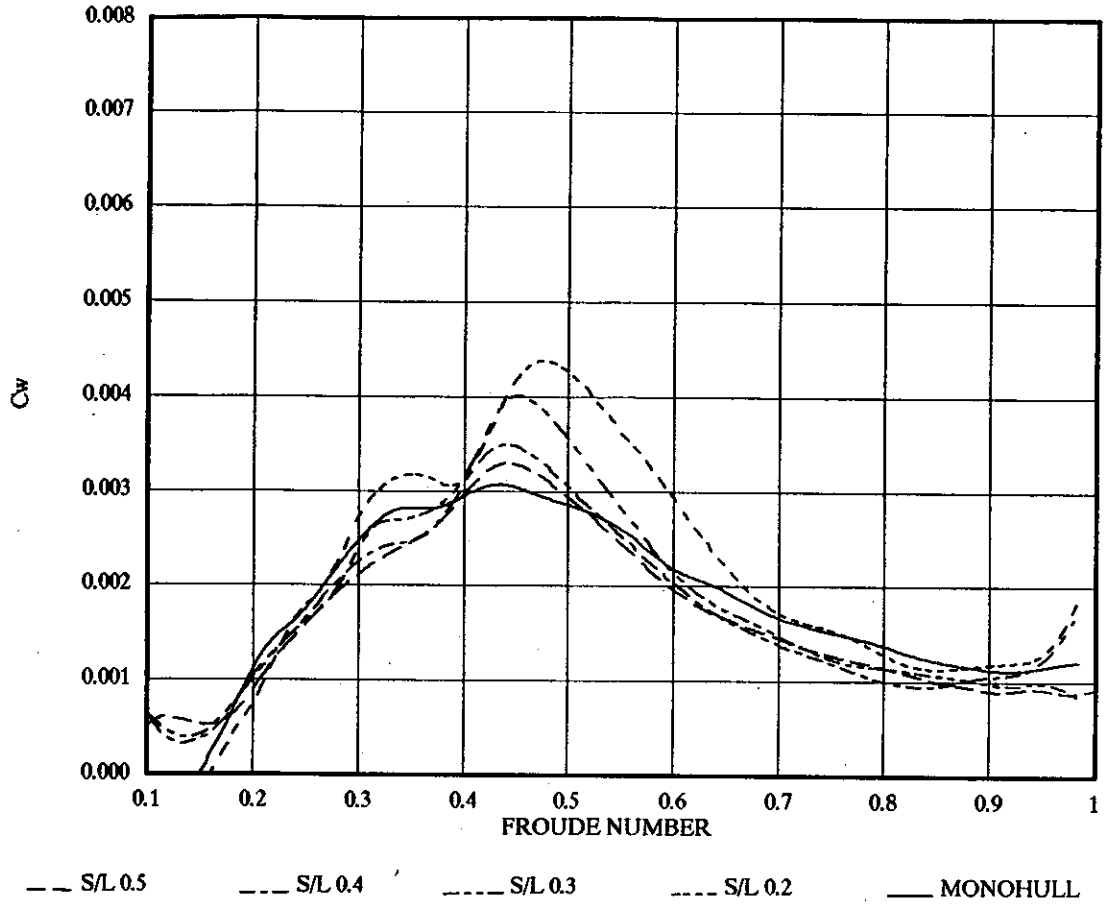

FIGURE 77

WAVE RESISTANCE Cw FOR MODEL 4b
LIGHT DISPLACEMENT

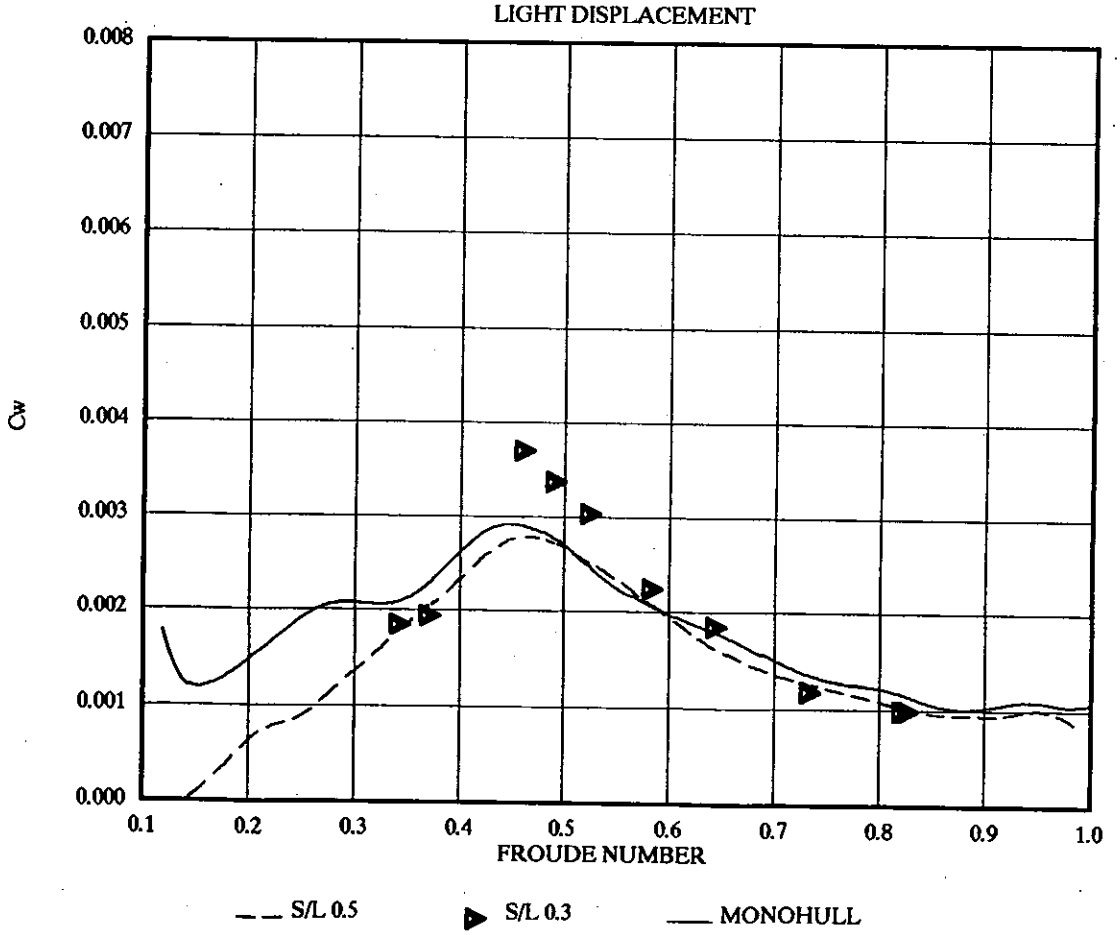

FIGURE 78 WAVE RESISTANCE Cw (BASED ON KwpCf) FOR MONOHULL
5b, 5d, 5e

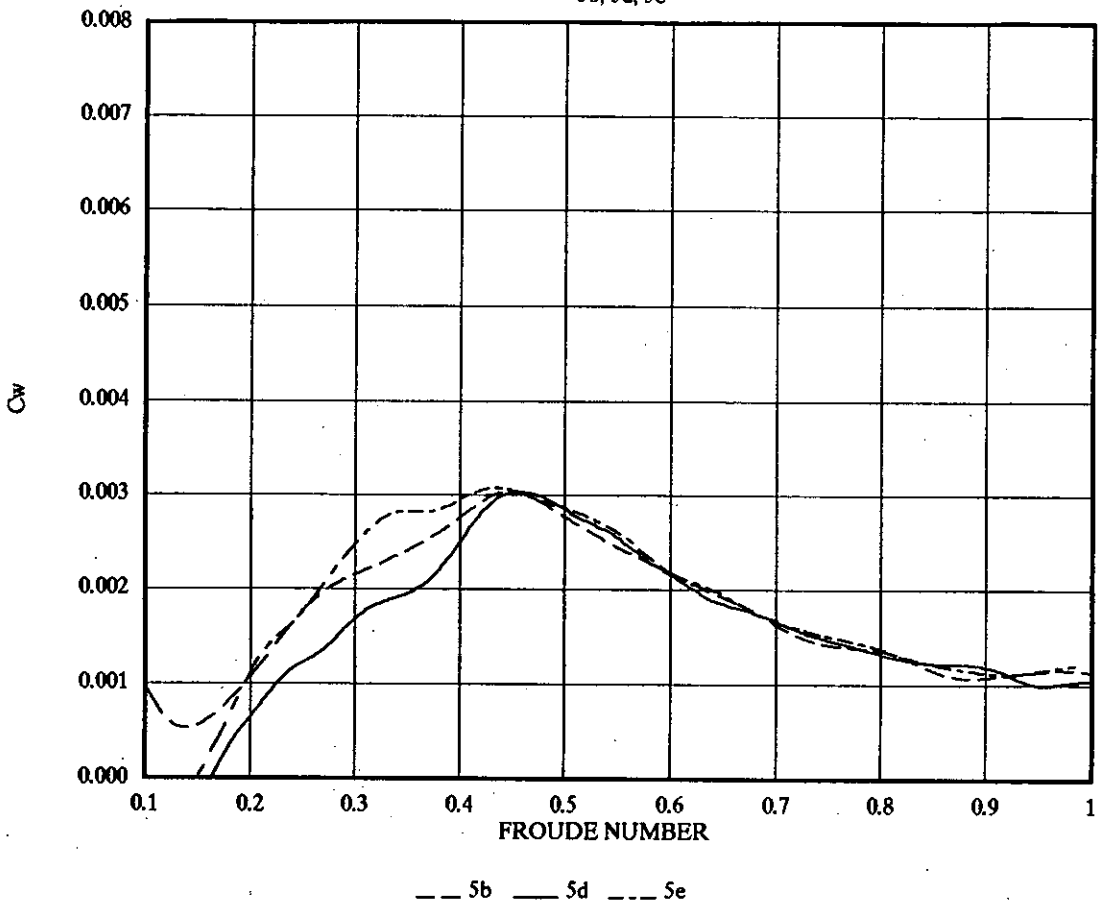

FIGURE 79 WAVE RESISTANCE (BASED ON KwpCf) FOR S/L 0.2
5b, 5d, 5e

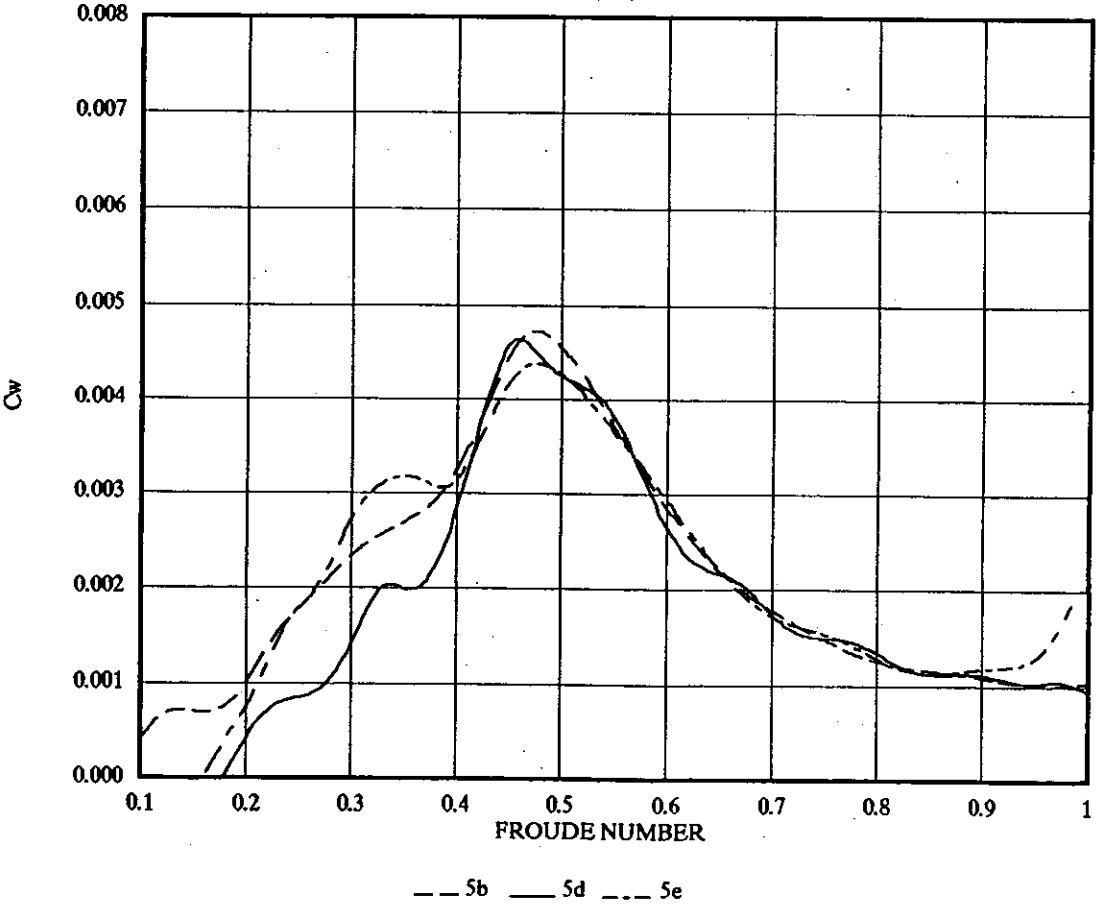

FIGURE 80 WAVE RESISTANCE Cw (BASED ON KwpCf) FOR S/L 0.3
5b, 5d, 5e

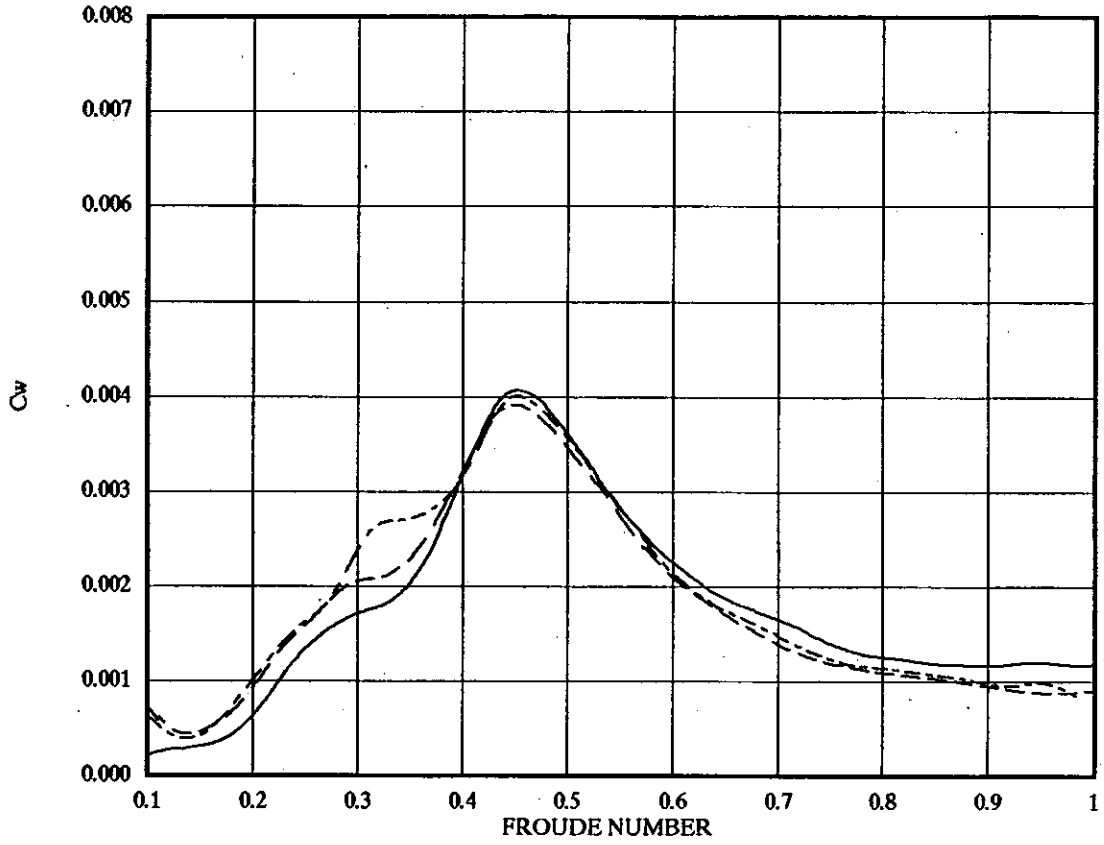

FIGURE 81 WAVE RESISTANCE Cw (BASED ON KwpCf) FOR SL 0.4
5d, 5e

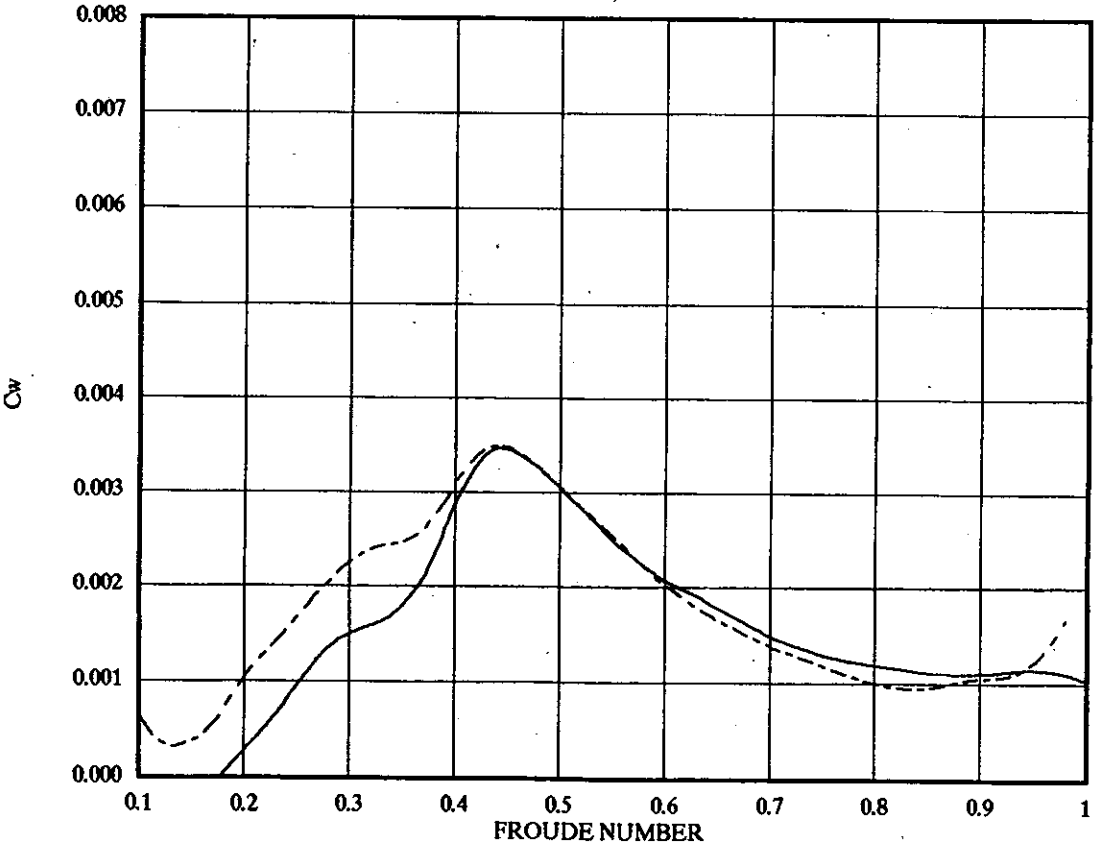

FIGURE 82 WAVE RESISTANCE Cw (BASED ON KwpCf) FOR S/L 0.5
5b, 5d, 5e

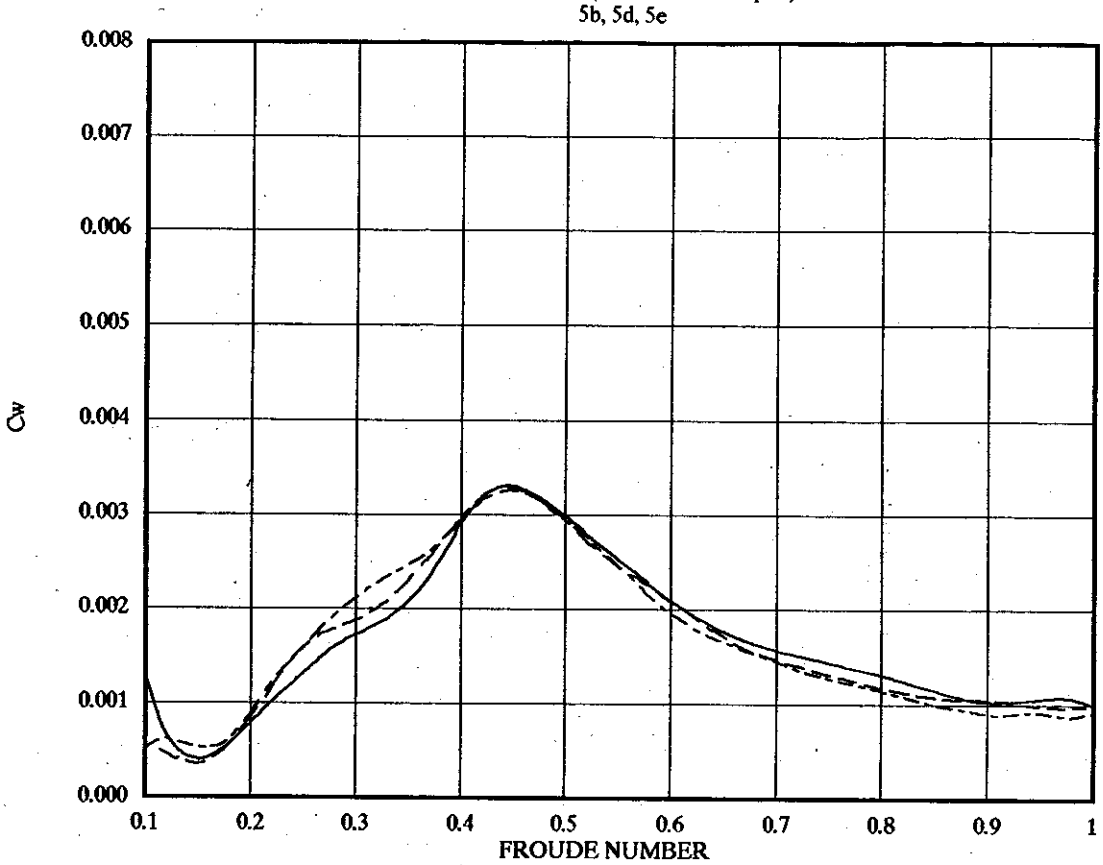

FIGURE 83 WAVE RESISTANCE Cw (BASED ON KwpCf) FOR MONOHULL
4b, 4b LIGHT, 5b, 5d

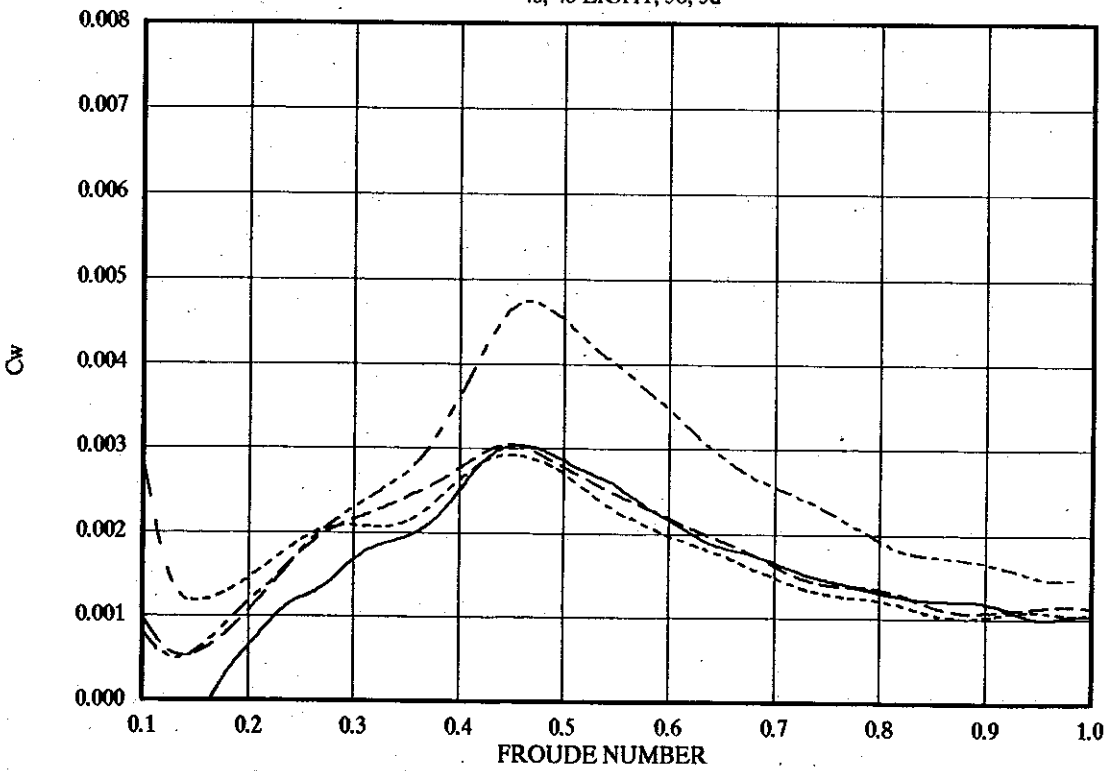

FIGURE 84 WAVE RESISTANCE Cw (BASED ON KwpCf) FOR S/L 0.3
4b, 4b LIGHT, 5b, 5d

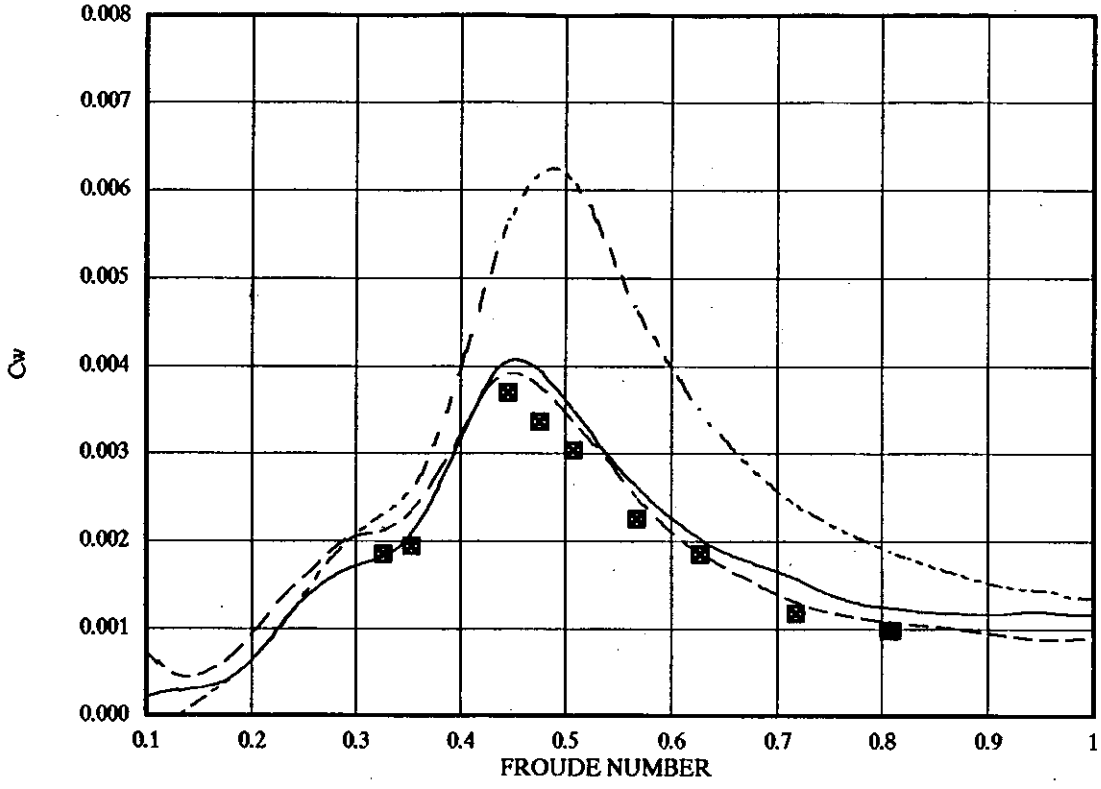

4b LIGHT DISPLMNT. 4b NORMAL DISPLMNT.

5b 5d

FIGURE 85 WAVE RESISTANCE Cw (BASED ON KwpCf) FOR S/L 0.5
4b, 4b LIGHT, 5b, 5d

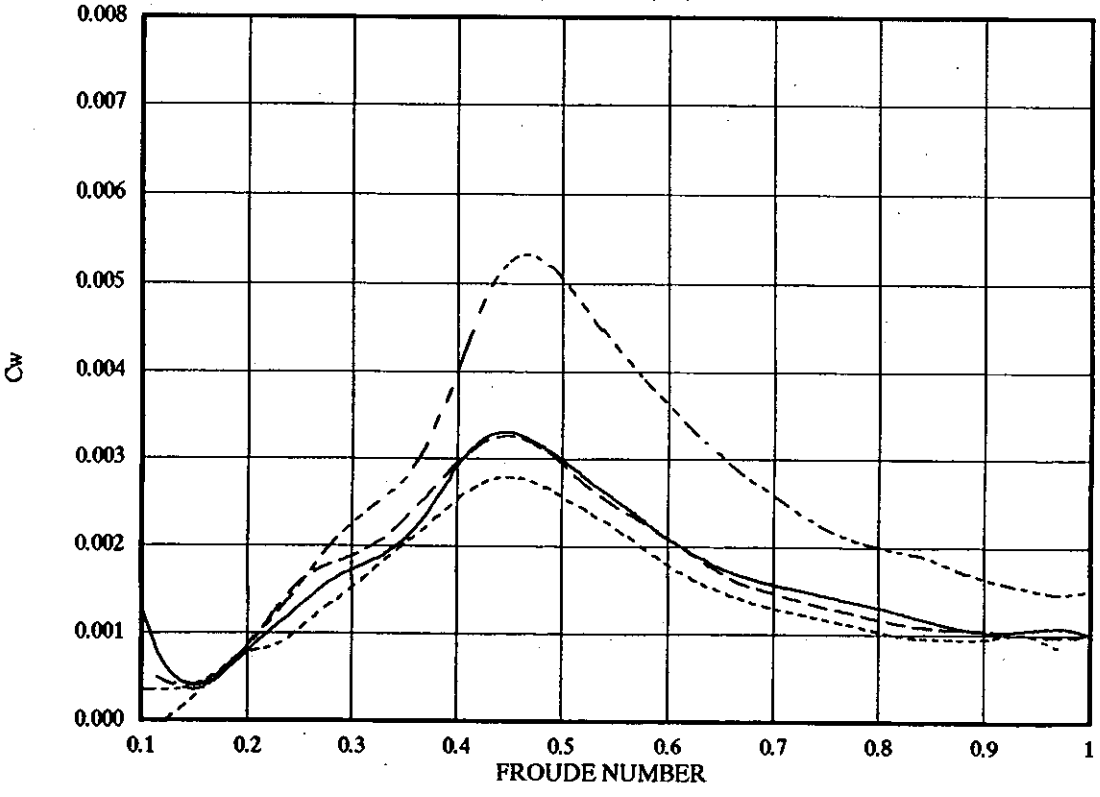

4b LIGHT DISPLMNT. 4b NORMAL DISPLMNT.

5b 5d

MODEL 5d TOTAL RESISTANCE AND WAVE PATTERN RESISTANCE										
	MONO		S/L 0.2		S/L 0.3		S/L 0.4		S/L 0.5	
Fn	Ct	Cwp	Ct	Cwp	Ct	Cwp	Ct	Cwp	Ct	Cwp
0.20	0.006467	0.000057	0.006751	0.000063	0.007096	0.000074	0.006826	0.000078	0.007475	0.000047
0.25	0.006767	0.000288	0.006875	0.000235	0.007497	0.000250	0.007198	0.000263	0.007689	0.000250
0.30	0.007027	0.000559	0.007239	0.000627	0.007642	0.000653	0.007503	0.000613	0.007865	0.000561
0.35	0.007126	0.000750	0.007620	0.000887	0.007780	0.000750	0.007606	0.000693	0.008022	0.000767
0.40	0.007543	0.001216	0.008292	0.001126	0.008776	0.001223	0.008555	0.001409	0.008691	0.001365
0.45	0.007945	0.001982	0.009935	0.002665	0.009528	0.003026	0.008998	0.002667	0.008955	0.002289
0.50	0.007664	0.002995	0.009483	0.003815	0.008960	0.003659	0.008476	0.003048	0.008509	0.003460
0.55	0.007284	0.002759	0.008925	0.003695	0.008067	0.003100	0.007835	0.002576	0.007961	0.003093
0.60	0.006814	0.002044	0.007697	0.002875	0.007423	0.002255	0.007315	0.002002	0.007439	0.001875
0.65	0.006424	0.001789	0.007147	0.002337	0.006957	0.001838	0.006924	0.001692	0.007031	0.001708
0.70	0.006184	0.001616	0.006635	0.001875	0.006662	0.001679	0.006572	0.001483	0.006761	0.001467
0.75	0.005926	0.001413	0.006335	0.001694	0.006340	0.001406	0.006309	0.001325	0.006561	0.001296
0.80	0.005719	0.001332	0.006122	0.001326	0.006139	0.001129	0.006146	0.001230	0.006368	0.001214
0.85	0.005572	0.001235	0.005855	0.001166	0.006015	0.001026	0.006016	0.001107	0.006153	0.001173
0.90	0.005495	0.001160	0.005794	0.001048	0.005946	0.000998	0.005955	0.001011	0.005979	0.001085
0.95	0.005256	0.001130	0.005663	0.000892	0.005932	0.000991	0.005945	0.000995	0.005964	0.001040

MODEL 5e TOTAL RESISTANCE AND WAVE PATTERN RESISTANCE										
	MONO		S/L 0.2		S/L 0.3		S/L 0.4		S/L 0.5	
Fn	Ct	Cwp	Ct	Cwp	Ct	Cwp	Ct	Cwp	Ct	Cwp
0.20	0.006669	0.000144	0.007167	0.000091	0.007697	0.000112	0.007818	0.000095	0.007677	0.000086
0.25	0.007043	0.000371	0.007904	0.000237	0.008001	0.000322	0.008121	0.000268	0.008057	0.000269
0.30	0.007570	0.000831	0.008627	0.000728	0.008541	0.000825	0.008482	0.000787	0.008351	0.000779
0.35	0.007757	0.001123	0.008883	0.001406	0.008668	0.001084	0.008502	0.000879	0.008496	0.000978
0.40	0.007746	0.001351	0.008699	0.001257	0.008942	0.001022	0.008946	0.001202	0.008833	0.001347
0.45	0.007734	0.002215	0.009605	0.002335	0.009664	0.002535	0.009214	0.002251	0.009020	0.002414
0.50	0.007454	0.002905	0.009574	0.003492	0.009077	0.003146	0.008653	0.002449	0.008559	0.002816
0.55	0.007111	0.002668	0.008860	0.003533	0.008264	0.002707	0.008047	0.002134	0.007963	0.002446
0.60	0.006612	0.001848	0.008061	0.002957	0.007486	0.002172	0.007447	0.001781	0.007378	0.001877
0.65	0.006304	0.001902	0.007265	0.002425	0.007010	0.001730	0.006977	0.001390	0.006984	0.001426
0.70	0.005960	0.001704	0.006696	0.001862	0.006669	0.001613	0.006645	0.001314	0.006710	0.001277
0.75	0.005754	0.001456	0.006451	0.001505	0.006352	0.001342	0.006380	0.001168	0.006463	0.001209
0.80	0.005562	0.001195	0.006125	0.001288	0.006198	0.001081	0.006131	0.001042	0.006268	0.001170
0.85	0.005355	0.001253	0.005926	0.001145	0.006066	0.001008	0.006024	0.000963	0.006068	0.001040
0.90	0.005228	0.001147	0.005925	0.001002	0.005925	0.000880	0.006071	0.000894	0.005917	0.000887
0.95	0.005214	0.001089	0.005992	0.000946	0.005886	0.000857	0.006191	0.000863	0.005885	0.000857

MODEL 5d SINKAGE AND TRIM										
	MONO		S/L 0.2		S/L 0.3		S/L 0.4		S/L 0.5	
Fn	SINK	TRIM	SINK	TRIM	SINK	TRIM	SINK	TRIM	SINK	TRIM
0.20	0.015	0.030	0.018	0.018	0.024	−0.021	0.016	−0.049	0.018	0.013
0.25	0.018	0.106	0.026	0.063	0.031	0.015	0.023	−0.008	0.026	0.046
0.30	0.024	0.173	0.038	0.093	0.040	0.034	0.031	−0.003	0.033	0.069
0.35	0.034	0.227	0.048	0.058	0.052	0.071	0.044	0.060	0.047	0.154
0.40	0.050	0.459	0.073	0.455	0.078	0.555	0.067	0.541	0.068	0.573
0.45	0.060	0.841	0.098	1.388	0.092	1.256	0.078	1.175	0.079	1.138
0.50	0.059	1.091	0.088	2.031	0.078	1.518	0.069	1.489	0.072	1.465
0.55	0.049	1.204	0.062	2.175	0.057	1.527	0.052	1.585	0.058	1.583
0.60	0.041	1.251	0.033	2.062	0.037	1.469	0.035	1.593	0.043	1.635
0.65	0.033	1.287	0.011	1.832	0.025	1.414	0.026	1.580	0.032	1.657
0.70	0.029	1.341	−0.002	1.653	0.020	1.391	0.021	1.596	0.030	1.684
0.75	0.028	1.371	−0.009	1.573	0.016	1.426	0.018	1.640	0.030	1.723
0.80	0.031	1.421	−0.013	1.517	0.013	1.467	0.018	1.684	0.028	1.770
0.85	0.032	1.501	−0.017	1.500	0.013	1.499	0.015	1.751	0.028	1.827
0.90	0.031	1.557	−0.020	1.507	0.013	1.552	0.011	1.810	0.025	1.885
0.95	0.032	1.602	−0.019	1.521	0.013	1.558	0.011	1.815	0.025	1.933

MODEL 5e SINKAGE AND TRIM										
	MONO		S/L 0.2		S/L 0.3		S/L 0.4		S/L 0.5	
Fn	SINK	TRIM	SINK	TRIM	SINK	TRIM	SINK	TRIM	SINK	TRIM
0.20	0.031	0.009	0.020	0.074	0.012	0.022	0.022	−0.021	0.010	0.015
0.25	0.036	0.040	0.027	0.080	0.018	0.055	0.029	0.015	0.017	0.061
0.30	0.040	0.082	0.038	0.171	0.033	0.095	0.036	0.038	0.025	0.088
0.35	0.049	0.121	0.050	0.214	0.048	0.117	0.047	0.084	0.037	0.178
0.40	0.062	0.274	0.070	0.420	0.069	0.478	0.068	0.432	0.055	0.489
0.45	0.074	0.621	0.094	1.204	0.084	1.142	0.081	0.934	0.067	0.892
0.50	0.074	0.887	0.089	1.786	0.076	1.489	0.072	1.173	0.063	1.088
0.55	0.066	1.009	0.065	1.941	0.056	1.502	0.054	1.233	0.051	1.155
0.60	0.057	1.067	0.038	1.870	0.040	1.432	0.041	1.235	0.035	1.199
0.65	0.048	1.088	0.015	1.714	0.027	1.368	0.031	1.197	0.023	1.213
0.70	0.044	1.102	0.002	1.584	0.015	1.336	0.027	1.198	0.019	1.227
0.75	0.043	1.130	−0.005	1.504	0.012	1.332	0.021	1.248	0.018	1.260
0.80	0.047	1.161	−0.010	1.460	0.012	1.348	0.020	1.288	0.018	1.328
0.85	0.051	1.209	−0.015	1.455	0.008	1.405	0.020	1.344	0.016	1.407
0.90	0.050	1.273	−0.020	1.466	0.009	1.454	0.016	1.379	0.012	1.487
0.95	0.050	1.292	−0.022	1.469	0.008	1.473	0.015	1.392	0.012	1.538

MODEL 5d RESIDUARY RESISTANCE Cr					
Fn	MONO	S/L 0.2	S/L 0.3	S/L 0.4	S/L 0.5
0.20	0.001870	0.002148	0.002882	0.002241	0.002502
0.25	0.002391	0.002506	0.003307	0.002807	0.003113
0.30	0.002819	0.003032	0.003658	0.003296	0.003435
0.35	0.003045	0.003542	0.003944	0.003528	0.003702
0.40	0.003551	0.004321	0.004720	0.004549	0.004766
0.45	0.004068	0.006059	0.005086	0.005121	0.005652
0.50	0.003880	0.005686	0.004729	0.004678	0.005162
0.55	0.003570	0.005228	0.004249	0.004106	0.004363
0.60	0.003149	0.004031	0.003773	0.003649	0.003758
0.65	0.002821	0.003537	0.003421	0.003314	0.003347
0.70	0.002633	0.003094	0.003208	0.003012	0.003111
0.75	0.002418	0.002824	0.003053	0.002802	0.002835
0.80	0.002248	0.002651	0.002897	0.002675	0.002668
0.85	0.002140	0.002426	0.002720	0.002584	0.002586
0.90	0.002099	0.002401	0.002585	0.002559	0.002551
0.95	0.001893	0.002301	0.002602	0.002583	0.002569

MODEL 5e RESIDUARY RESISTANCE Cr					
Fn	MONO	S/L 0.2	S/L 0.3	S/L 0.4	S/L 0.5
0.20	0.002059	0.002563	0.003101	0.003219	0.003078
0.25	0.002654	0.003520	0.003621	0.003735	0.003672
0.30	0.003363	0.004419	0.004334	0.004275	0.004137
0.35	0.003679	0.004805	0.004590	0.004424	0.004418
0.40	0.003769	0.004713	0.004972	0.004952	0.004862
0.45	0.003858	0.005729	0.005790	0.005337	0.005144
0.50	0.003656	0.005777	0.005304	0.004875	0.004761
0.55	0.003397	0.005132	0.004563	0.004338	0.004254
0.60	0.002947	0.004396	0.003821	0.003782	0.003713
0.65	0.002694	0.003655	0.003400	0.003367	0.003383
0.70	0.002409	0.003136	0.003121	0.003094	0.003159
0.75	0.002245	0.002944	0.002846	0.002874	0.002955
0.80	0.002098	0.002664	0.002727	0.002660	0.002797
0.85	0.001928	0.002496	0.002638	0.002592	0.002636
0.90	0.001832	0.002529	0.002534	0.002675	0.002524
0.95	0.001851	0.002630	0.002524	0.002829	0.002523